

# UNCLASSIFIED

<b>AD NUMBER</b>
ADB166585
<b>NEW LIMITATION CHANGE</b>
<b>TO</b> Approved for public release, distribution unlimited
<b>FROM</b> Distribution authorized to DoD only; Software Documentation; Proprietary Info.; Nov 90. Other requests shall be referred to WL/FIBG, Wright- Patterson AFB, OH 45433-6553. This document contains export-controlled technical data..
<b>AUTHORITY</b>
AFRL ltr., 14 Sep 99

THIS PAGE IS UNCLASSIFIED

AD-B166 585



✓ L(2)

WRDC-TR-90-3081

NONLINEAR RESPONSE AND FATIGUE OF  
SURFACE PANELS BY THE TIME DOMAIN  
MONTE CARLO APPROACH

Dr Rocky Richard Arnold  
Professor Rimas R. Vaicaitis

Anamet Laboratories, Inc.  
3400 Investment Blvd.  
Haywood, CA 94545-3811

DTIC  
ELECTE  
AUG 17 1992  
S A D



May 1992

Final Report for Period July 89 to January 90

PROPRIETARY INFORMATION

Distribution authorized to DOD components only; software documentation, Nov 90. Other requests for this document shall be referred to WL/FIBG, WPAFB, OH 45433-6553. Requests must include a Statement of Terms and Conditions--Release of Air Force-Owned or Developed Computer Software Packages. (See block 16 of SF 298).

This report contains proprietary information; see legend inside front cover.

WARNING - This document contains technical data whose export is restricted by the Arms Export Control Act (Title 22, U.S.C., Sec 2751, et seq.) or The Export Administration Act of 1979, as amended, Title 50, U.S.C., 2401, et seq. Violations of these export laws are subject to severe criminal penalties. Disseminate in accordance with the provisions of AFR 80-34. (Include this statement with any reproduced portion.)

DESTRUCTION NOTICE - Destroy by any method that will prevent disclosure of contents of reconstruction of the document.

92-22837



FLIGHT DYNAMICS DIRECTORATE  
WRIGHT LABORATORY  
AIR FORCE SYSTEMS COMMAND  
WRIGHT-PATTERSON AIR FORCE BASE, OHIO 45433-6553

416 955

143p

92 8 13 042

## NOTICE

When Government drawings, specifications, or other data are used for any purpose other than in connection with a definitely Government-related procurement, the United States Government incurs no responsibility or any obligation whatsoever. The fact that the government may have formulated or in any way supplied the said drawings, specifications, or other data, is not to be regarded by implication, or otherwise in any manner construed, as licensing the holder, or any other person or corporation; or as conveying any rights or permission to manufacture, use, or sell any patented invention that may in any way be related thereto.

## LICENSE RIGHTS LEGEND

Contract Nr. 33615-89-C-3210

Contractor or Subcontractor: Anamet Laboratories, Inc.

For a period of two (2) years after the delivery and acceptance of the last deliverable item under the above contract, this technical data shall be subject to the restrictions contained in the definition of "Limited Rights" in DFARS clause at 252.227-7013. After the two-year period, the data shall be subject to the restrictions contained in the definition of "Government Purpose License Rights" in DFARS clause 252.227-7013. The Government assumes no liability for unauthorized use or disclosure by others. This legend, together with the indications of the portions of the data which are subject to such limitations, shall be included on any reproduction hereof which contains any portions subject to such limitations and shall be honored only as long as the data continues to meet the definition on Government purpose license rights.

This technical report has been reviewed and is approved for publication.

  
KENNETH R. WENTZ, Aerospace Engineer  
Acoustic and Sonic Fatigue Group

  
RALPH M. SHIMOVETZ, Group Leader  
Acoustics and Sonic Fatigue Group

FOR THE COMMANDER

  
JEROME PEARSON, Chief  
Structural Dynamics Branch

Publication of this report does not constitute approval or disapproval of the ideas or findings. It is published in the interest of scientific and technical information exchange.

Copies of this report should not be returned unless return is required by security considerations, contractual obligations, or notice on a specific document.

REPORT DOCUMENTATION PAGE			Form Approved OMB No. 0704-0188	
Public reporting burden for this collection of information is estimated to average 1 hour per response, including the time for reviewing instructions, searching existing data sources, gathering and maintaining the data needed, and completing and reviewing the collection of information. Send comments regarding this burden estimate or any other aspect of this collection of information, including suggestions for reducing this burden, to Washington Headquarters Services, Directorate for Information Operations and Reports, 1215 Jefferson Davis Highway, Suite 1204, Arlington, VA 22202-4302, and to the Office of Management and Budget, Paperwork Reduction Project (0704-0188), Washington, DC 20503.				
1. AGENCY USE ONLY (Leave blank)		2. REPORT DATE 21 May 1992		3. REPORT TYPE AND DATES COVERED Final 13 JUL 89 - 13 Jan 90
4. TITLE AND SUBTITLE Nonlinear Response and Fatigue of Surface Panels by the Time Domain Monte Carlo Approach			5. FUNDING NUMBERS Program Element: 65502F Project Nr: 3005 Task: 40 WU: 64	
6. AUTHOR(S) Dr Rocky Richard Arnold Rimas R. Vaicaitis				
7. PERFORMING ORGANIZATION NAME(S) AND ADDRESS(ES) Anamet Laboratories, Inc 3400 Investment Blvd Hayward, CA 94545-3811			8. PERFORMING ORGANIZATION REPORT NUMBER  789.001	
9. SPONSORING/MONITORING AGENCY NAME(S) AND ADDRESS(ES) Flight Dynamics Directorate Wright Laboratory Structures Division Wright-Patterson AFB, OH 45433-6553			10. SPONSORING/MONITORING AGENCY REPORT NUMBER  WRDC-TR-90-3081	
11. SUPPLEMENTARY NOTES Cys of Statement of Terms and Conditions--Release of AF-Owned or Developed Computer Software Packages will be furnished upon request to WL/FIBG, WPAFB, OH. SBIR Phase I FINAL Report				
12a. DISTRIBUTION/AVAILABILITY STATEMENT Distribution auth to DoD Components only, Software documentation, Nov 90. Other requests for document, refer to WL/FIBG, WPAFB, OH 45433-6553. This report contains proprietary information (see legend inside front cover.)			12b. DISTRIBUTION CODE  F33615-89-C-3210 <b>PROPRIETARY INFORMATION</b>	
13. ABSTRACT (Maximum 200 words)  The objective of this Phase I research is to develop a computational procedure for predicting the life and reliability of metal and composite structural panels subjected to complex dynamic loads from acoustic, aerodynamic, and thermal environments. The proposed research uses a time domain Monte Carlo method to develop analytical equations of high accuracy and efficiency. The time domain Monte Carlo method will permit an examination of the effects of peak stresses and exceedances; subsequently, meaningful predictions of structural life (fatigue) can be made. Phase I research will be used to verify the Monte Carlo time domain analysis. The resulting computational procedure will be used to establish the feasibility of developing either a discretized (finite element) or numerical computer program to be completed during any Phase II effort. This research will lead to a new technology base for estimating the nonlinear response characteristics of a new generation of aircraft exposed to severe acoustic, aerodynamic, and thermal environments.				
14. SUBJECT TERMS  acoustic fatigue, sonic fatigue, time domain, Monte Carlo			15. NUMBER OF PAGES 146	
			16. PRICE CODE	
17. SECURITY CLASSIFICATION OF REPORT Unclassified	18. SECURITY CLASSIFICATION OF THIS PAGE Unclassified	19. SECURITY CLASSIFICATION OF ABSTRACT Unclassified	20. LIMITATION OF ABSTRACT DTIC Users	

February 13, 1990

## PREFACE

This is the final report for research conducted during the time period of July 13, 1989 through January 13, 1990 under Contract No. F33615-89-C-3210. All work completed under this contract was performed by Anamet Laboratories, Inc., 3400 Investment Blvd., Hayward, California 94545-3811 with Professor Rimas Vaicaitis of Columbia University as consultant. The work was accomplished for the Flight Dynamics Laboratory, Wright Research and Development Center, Aeronautical Systems Division (AFSC), United States Air Force, Wright-Patterson AFB, Ohio 45433-6553. The project officer was Mr. Kenneth R. Wentz, WRDC/FIBGD. The principal investigator for Anamet Laboratories was Dr. Rocky Richard Arnold. The report authors are Dr. Rocky Richard Arnold and Professor Rimas Vaicaitis.

Submitted by:



Rocky Richard Arnold, Ph.D.  
Principal Investigator

DTIC QUALITY INSPECTED 8

mh/025

Accession For	
NTIS CRA&I	<input checked="checked" type="checkbox"/>
DTIC TAB	<input checked="checked" type="checkbox"/>
Unannounced	<input type="checkbox"/>
Justification	
By	
Distribution /	
Availability Codes	
Dist	Avail and/or Special
E-4	SEB 57

## TABLE OF CONTENTS

<u>Section</u>	<u>Page</u>
I INTRODUCTION .....	1
II TECHNICAL DISCUSSION .....	4
A. SIMULATION OF RANDOM INPUT PRESSURES IN SPACE-TIME DOMAIN .....	4
1. Simulation of Stationary-Homogeneous Gaussian Random Pressure .....	5
2. Turbulent Boundary Layer Flow .....	9
3. Jet Engine Exhaust Noise .....	10
4. Uniform Distribution of Random Pressure .....	11
B. STRUCTURAL MODELING .....	11
C. PREDICTION OF RESPONSE IN SURFACE PANELS .....	14
1. The Power Spectral Density Method .....	15
2. The Time Domain Method .....	20
D. SONIC FATIGUE OF SURFACE PANELS .....	29
1. Linear Stress Response .....	31
2. Quasi-Nonlinear Single Degree of Freedom Stress Response .....	35
3. Nonlinear Stress Response .....	40
E. COMPUTER PROGRAM DESCRIPTION .....	41
III RESULTS .....	43
A. COMPARISONS BETWEEN THE TIME DOMAIN AND POWER SPECTRAL DENSITY METHODS (ISOTROPIC PLATES) .....	44
B. PREDICTION OF RESPONSE IN ORTHOTROPIC COMPOSITE PANELS USING THE TIME DOMAIN METHOD .....	51
IV CONCLUSIONS .....	57
REFERENCES .....	58
FIGURES .....	62
APPENDIX A - LISTING OF COMPUTER PROGRAM TDR .....	99

## LIST OF FIGURES

<u>Figure</u>	<u>Page</u>
1 A Rectangular Panel Exposed to Random Pressure .....	63
2 Computer Programs Used to Perform Time Domain Analysis and Predict Fatigue Life .....	64
3 Displacement Response Time Histories for Input Sound Pressure Levels of 80 dB and 120 dB .....	65
4 Displacement Response Time Histories for Input Sound Pressure Levels of 140 dB and 150 dB .....	66
5 The $\sigma_y$ Stress Response Time Histories for Sound Pressure Levels of 80 dB and 120 dB .....	67
6 The $\sigma_y$ Stress Response Time Histories for Input Sound Pressure Levels of 140 dB and 150 dB .....	68
7 Linear and Nonlinear Root-Mean-Square Displacement Response .....	69
8 Linear and Nonlinear Root-Mean-Square Stress Response .....	70
9 Spectral Density of Displacement Response for Input Sound Pressure Levels of 80 dB, 100 dB, and 120 dB .....	71
10 Spectral Densities of Stress $\sigma_y$ for Input Sound Pressure Levels of 80 dB, 100 dB, and 120 dB .....	72
11 Spectral Densities of Displacement and Stress $\sigma_y$ for Input Pressure Level of 140 dB .....	73
12 Probability Density and Peak Distribution Histograms of Displacement $w$ for 120 dB Input .....	74
13 Probability Density and Peak Distribution Histograms of Displacement $w$ for 150 dB Input .....	75
14 Probability Density and Peak Distribution Histograms of Normal Stress $\sigma_y$ for 120 dB Input ....	76
15 Probability Density and Peak Distribution Histograms of Normal Stress $\sigma_y$ for 150 dB Input ....	77
16 Threshold Up-crossing Rate for Stress $\sigma_y$ .....	78

# LIST OF FIGURES (Continued)

<u>Figure</u>		<u>Page</u>
17	Fatigue Damage for Different Input Pressure Levels .....	79
18	Typical Laminate Stress/Strain Distributions .....	80
19	Displacement Response Time History (150 dB Linear) .....	81
20	Displacement Response Time History (150 dB Nonlinear) .....	82
21	$\sigma_{yy}$ Stress Response Time History (150 dB Linear) ...	83
22	$\sigma_{yy}$ Stress Response Time History (150 dB Nonlinear) .....	84
23	Probability Density Histogram of Displacement (130 dB Nonlinear) .....	85
24	Probability Density Histogram of Displacement (150 dB Nonlinear) .....	86
25	Peak Distribution Histogram of Displacement (130 dB Nonlinear) .....	87
26	Peak Distribution Histogram of Displacement (150 dB Nonlinear) .....	88
27	Probability Density Histogram of $\sigma_{yy}$ (130 dB (Nonlinear) .....	89
28	Probability Density Histogram of $\sigma_{yy}$ (150 dB Nonlinear) .....	90
29	Peak Distribution Histogram of $\sigma_{yy}$ (130 dB Nonlinear) .....	91
30	Peak Distribution Histogram of $\sigma_{yy}$ (150 dB Nonlinear) .....	92
31	Up-Crossing Rate for $\sigma_{yy}$ for Various Sound Pressure Levels .....	93
32	RMS of $\sigma_{yy}$ as a Function of Lay-Up Angle .....	94



# LIST OF FIGURES (Concluded)

<u>Figure</u>		<u>Page</u>
33	Up-Crossing Rate for $\sigma_{yy}$ as a Function of Lay-Up Angle .....	95
34	Up-Crossing Rate for $\sigma_{xx}$ as a Function of Lay-Up Angle .....	96
35	Up-Crossing Rate for $\sigma_{yy}$ as a Function of Lay-Up Angle, $[+\theta/-\theta]_{x2}$ .....	97
36	RMS of $\sigma_{\parallel}$ , $\sigma_{\perp}$ as a Function of Lay-Up Angle, $[+\theta/-\theta]_{x2}$ .....	98

## LIST OF TABLES

<u>Table</u>		<u>Page</u>
1	Constants for Clamped-Plate Modes .....	19
2	Standard Deviation of $\sigma_{yy}$ Stress, Expected Number of Peaks and Fatigue Life .....	50

# I

## INTRODUCTION

Acoustic or sonic fatigue, the deterioration of material and structural strength from high frequency wide band noise, is an important factor in the structural design and safety of modern aircraft and aerospace structures. The need to understand how noise is generated and how structures respond to that noise is critical to the design of future aircraft such as the National Aerospace Plane (NASP) and various short take-off and landing aircraft (STOL). Advanced engine designs using propfans, presently noisier than conventional turbofans, add to the difficulty of properly designing structures without the support of an adequate experimental database.

The need for predictive techniques that are accurate and easy to use is of paramount importance to designers of present and future aircraft structures. Notwithstanding the uncertainties associated with acoustic load generation, stress prediction, adverse thermal environments, and the lack of fatigue damage prediction models for both metals and composite materials, it is important to have mathematical models that can represent the random nature of the noise environment to a degree that permits rational design to proceed. Of associated concern is that with increased noise levels, the structural panels can behave in a nonlinear fashion; thus, linear mathematical models may be inappropriate for use. Indeed, even if linear models were conservative in all respects, their use would only lead to designs which were inherently too heavy, thereby potentially provoking design modifications that are more costly and less optimal.

New materials such as polymer and metal matrix composites have shown themselves to be potentially useful in aircraft structures; however, the limited amount of data related to their performance in the presence of an acoustic environment is disturbing

to a designer. Thus, analytical techniques for predicting life and reliability when only a minimal amount of material property data is available are urgently needed.

The surface protection systems of aerospace and aircraft structures are usually constructed from discretely stiffened panels or stiffened shells. High cycle fatigue failures have occurred in these structures with the majority of fatigue cracks appearing in the near vicinity of the stiffening element or the stiffener itself (References 1-5). Proper dynamic interaction between the panel and various stiffening elements should be taken into account when calculating the response of the panels and of the stiffeners.

Extensive research has been carried out for linear and nonlinear analysis of a single bay panel (References 6-13). For discretely stiffened panels, most analytical work is based on linear theory. However, under intensive acoustic, aerodynamic, and thermal loadings, these panels vibrate in a nonlinear fashion and a nonlinear analysis is needed to predict deformations, stresses, and fatigue life. Different methods have been proposed to study random vibrations of nonlinear systems (References 14,15). Among the most widely used are the Fokker-Planck equation solution (References 16,17), perturbation method (References 18,19), stochastic linearization (References 20-22), and the time domain Monte Carlo approach (References 23-25). Exact solutions to the Fokker-Planck equations are available only for a few simple cases. The perturbation method is usually limited to one- or two-degrees-of-freedom systems and is valid only for weakly nonlinear cases. The stochastic linearization method, although suitable for problems with strong nonlinearities, may not yield meaningful results for complex nonlinear problems that might be encountered in flight structures. The time domain Monte Carlo approach can be used efficiently for response analysis of nonlinear structures subjected to random pressure fields. In this approach, the random pressure inputs are simulated first in time domain using simulation procedures of stationary and Gaussian

random process (Reference 23), then the resulting nonlinear equations of motion are solved in the time domain by numerical techniques (References 23-25).

When surface protection systems of a flight vehicle are exposed to high speed aerodynamic surface flow or engine exhaust hot gases, the surface temperatures could reach 3,000°F (Reference 26). The effects of those high thermal gradients are degradation of strength, stiffness, and fatigue life (References 8,27). In addition, structural-aerodynamic instabilities such as buckling, "oil canning," and "snap through" could be induced by the action of thermal, aerodynamic, and acoustic loads (References 5,8,12,13). These effects should be accounted for in the nonlinear response of structural panels.

The objective of the Phase I research documented herein was to develop a computational procedure for predicting the life and reliability of metal and composite structural panels subjected to complex dynamic loads from acoustic, aerodynamic, and thermal environments. Starting with existing work for the prediction of sonic fatigue in stiffened panels using the time domain method (Reference 28), this research has extended the model to include composite materials. Furthermore, the analytical procedure now includes programs to compute the time history response to random noise and statistical analysis to compute probability density and peak distribution histograms of the stresses, upcrossing rates, and expected fatigue damage.

## II

### TECHNICAL DISCUSSION

The basic approach used in the present research can be categorized into three distinct stages, each involving its own set of specialized formulations. The first stage (Section II A.) concerns a mathematical description and phenomenological representation of the acoustic pressures which act on surrounding structure (a panel in this work is used). The second important stage (Sections II B. and II C.) deals with the kinematic and structural response of the panel to the acoustic loading. In other words, what are the displacements and stresses? The third stage (Section II D.) requires an estimation of panel fatigue life based on panel structural response and the expected acoustic environment.

The relevant equations resulting from consideration of these three stages are contained in the computer code discussed in Section II E.

#### A. SIMULATION OF RANDOM INPUT PRESSURES IN SPACE-TIME DOMAIN

The random pressure acting on a thermal protection system of a supersonic/hypersonic aircraft or sub-orbital/orbital vehicle arises from engine exhaust noise, turbulent surface flow, oscillating shocks, and flow separations. In addition, there might be induced structure-borne dynamic loads due to engine and equipment vibrations and nonsteady aerodynamic loads due to high speed surface flow and vibrations of the thermal protection systems.

During a normal mission consisting of take-off, maneuvers, steady flight, and landing, the thermal protection systems will be exposed not only to long duration stationary pressure but also to short-burst intense nonstationary pressures. Furthermore, oscillating surface shocks and flow separations could create severe localized pressures which must be accounted for when predicting the fatigue life of a structural component.

In the Phase I work documented herein, the analysis of the random input pressure will be limited to stationary and Gaussian random pressures arising from engine exhaust noise and turbulent boundary layer flow. Examination of the nonstationary and non-Gaussian characteristics of surface pressures arising in regions of oscillating shocks, separated flows, and rapid changes in thrust requirements will be addressed during the Phase II activities.

#### 1. Simulation of Stationary-Homogeneous Gaussian Random Pressure

Consider a random pressure  $p(x,y,t)$  acting on the surface of a high speed flight vehicle. The pressure acting normal to the surface varies randomly in time and space along the surface coordinates  $x$  and  $y$ . The pressure  $p(x,y,t)$  is characterized by a cross-spectral density function  $S_p(\xi,\eta,\omega)$  where  $\xi = x_1 - x_2$  and  $\eta = y_1 - y_2$  are the spatial separations and  $\omega$  is frequency. The cross-spectral density  $S_p$  is obtained utilizing experimental data, and various empirical forms are available for jet noise (References 5,29), rocket noise (Reference 30), and turbulent boundary layer flow (References 7,9). The simplest form of the cross-spectral density is the truncated Gaussian white noise pressure uniformly distributed with spatial coordinates  $x$  and  $y$  and

$$S_p(\xi,\eta,\omega) = \begin{cases} S_0 & \text{if } 0 \leq \omega \leq \omega_u \\ 0 & \text{if } \omega < 0 \text{ or } \omega > \omega_u \end{cases} \quad (1)$$

where  $S_0$  is a given constant and  $\omega_u$  is the upper cut-off frequency.

The spectral density  $S_p(k_1,k_2,\omega)$  can be obtained in wave-number-frequency domain by taking the Fourier transformation of  $S_p(\xi,\eta,\omega)$  as

$$S_p(k_1, k_2, \omega) = \frac{1}{(2\pi)^2} \int_{-\infty}^{\infty} \int_{-\infty}^{\infty} S_p(\xi, \eta, \omega) e^{-ik_1\xi} e^{-ik_2\eta} d\xi d\eta \quad (2)$$

Then, the random pressure  $p(x, y, t)$  can be simulated by the series (Reference 23)

$$p(x, y, t) = \sqrt{2} \sum_{i=1}^{N_1} \sum_{j=1}^{N_2} \sum_{r=1}^{N_3} [S_p(k_{1i}, k_{2j}, \omega_r) \Delta k_1 \Delta k_2 \Delta \omega]^{\frac{1}{2}} \cos(k_{1i}x + k_{2j}y + \omega_r t + \phi_{ijr}) \quad (3)$$

where  $\phi_{ijr}$  are realized values of independent random phase angles uniformly distributed between 0 and  $2\pi$ . The values of the spectra are selected at

$$\begin{aligned} k_{1j} &= k_{1i} + i\Delta k_1 & i &= 1, 2, \dots, N_1 \\ k_{2j} &= k_{2i} + j\Delta k_2 & j &= 1, 2, \dots, N_2 \\ \omega_r &= \omega_i + r\Delta \omega & r &= 1, 2, \dots, N_3 \end{aligned} \quad (4)$$

where the wave number and frequency intervals are

$$\begin{aligned} \Delta k_1 &= (k_{1u} - k_{1l}) / N_1 \\ \Delta k_2 &= (k_{2u} - k_{2l}) / N_2 \\ \Delta \omega &= (\omega_u - \omega_l) / N_3 \end{aligned} \quad (5)$$

in which the subscripts  $u$  and  $l$  indicate the lower and the upper cut-off values of the wave number and frequency, respectively.



For a generation of random sample functions from Equation 3 with the spectral density function close to the one specified and a large number of spatial  $(x,y)$  and time  $(t)$  points,  $N_1$ ,  $N_2$ , and  $N_3$  must be large, and, as a consequence, a significant amount of computer time is required to achieve a simulation.

To reduce the computation costs and improve the efficiency of simulation, the Fast Fourier Transform (FFT) technique can be utilized (References 31,32). Rewriting Equation 3 in the form

$$p(x,y,t) = \text{Re} \left[ \sum_{i=0}^{M_1-1} \sum_{j=0}^{M_2-1} \sum_{r=0}^{M_3-1} A_{ijr} e^{i\phi_{ijr}} e^{i(k_{1i}x + k_{2j}y + \omega_r t)} \right] \quad (6)$$

and evaluating  $p(x,y,t)$  at

$$\begin{aligned} x &= m\Delta x, & m &= 0, 1, \dots, M_1 - 1 \\ y &= n\Delta y, & n &= 0, 1, \dots, M_2 - 1 \\ t &= q\Delta t, & q &= 0, 1, \dots, M_3 - 1 \end{aligned} \quad (7)$$

where "Re" indicates the real part of Equation 6 and

$$A_{ijr} = [2S_p(k_{1i}, k_{2j}, \omega_r) \Delta k_1 \Delta k_2 \Delta \omega]^{\frac{1}{2}}. \quad (8)$$

In Equations 6 and 7,

$$\begin{aligned} M_1 &= 2^{m_1} = v_1 N_1 > N_1 = 2^{n_1} \\ M_2 &= 2^{m_2} = v_2 N_2 > N_2 = 2^{n_2} \\ M_3 &= 2^{m_3} = v_3 N_3 > N_3 = 2^{n_3} \end{aligned} \quad (9)$$

and

$$\begin{aligned}\Delta x &= 2\pi/M_1 \Delta k_1 = 2\pi/v_1 k_{1u} \\ \Delta y &= 2\pi/M_2 \Delta k_2 = 2\pi/v_2 k_{2u} \\ \Delta t &= 2\pi/M_3 \Delta \omega = 2\pi/v_3 \omega_u\end{aligned}\tag{10}$$

with  $v_1 = 2^{m_1-n_1}$ ,  $v_2 = 2^{m_2-n_2}$ ,  $v_3 = 2^{m_3-n_3}$ , and  $m_1 > n_1$ ,  $m_2 > n_2$ ,  $m_3 > n_3$  all being positive integers. The use of the FFT technique can be applied to Equation 6 directly resulting in a drastic reduction of computer time.

A second difficulty arising from the simulation of a three dimensional random process, as shown in Equation 6, is the creation of a large number of complex numbers that must be stored in the computer for a standard FFT application. For example, if  $N_1 = N_2 = N_3 = 128$ ,  $v_1 = v_2 = v_3 = 4$ ,  $M_1 = M_2 = M_3 = 512$ , a three dimensional field of 512 by 512 by 512 complex numbers must be stored in order to perform a three dimensional FFT procedure. This storage requirement is significant even for large mainframe computers. Thus, simulations of random processes have been primarily applied to one dimensional and, in some cases, two dimensional uses. If a random pressure acting on a structural surface can be assumed to be uniformly distributed in space, Equation 6 reduces to a one dimensional simulation

$$P(t) = \text{Re} \left[ \sum_{r=0}^{M-1} A_r e^{i\phi_r} e^{i\omega_r t} \right]\tag{11}$$

where

$$A_r = [2S_p(\omega_r) \Delta \omega]^{\frac{1}{2}}\tag{12}$$

and  $S_p(\omega)$  is the power spectral density of random surface pressure. In order that random pressures can be simulated either from Equation 6 or Equation 11, the input spectral densities need to be prescribed.

## 2. Turbulent Boundary Layer Flow

Convective turbulent flow produces random pressure fluctuations that act on the surface protection system of all flight vehicles. A considerable amount of work, both theoretical and experimental, has been carried out on this subject with regard to panel response, panel flutter, and noise transmission (References 7,9,10,24). However, for high speed supersonic and hypersonic flow, the information that is available seems to be very limited, and a substantial amount of work will be needed to characterize random pressures for high speed flows. For the purpose of this work, the semi-empirical forms of the cross-spectral density corresponding to separated supersonic flow given in Reference 9 will be considered. For a homogeneous turbulent flow convecting in the x-direction over a structural surface, the cross-spectral density can be expressed as

$$S_p(\xi, \eta, \omega) = S(\omega) |R_x(\xi, 0, \omega)| |R_y(0, \eta, \omega)| e^{-i\omega\xi/U_c} \\ 0 \leq \omega < \infty \quad (13)$$

in which  $R(\xi, \eta, \omega)$ ,  $S(\omega)$ , and  $U_c$  are the correlation coefficient, surface pressure spectral density, and convection velocity, respectively. For separated supersonic flow, the empirical formulas from Reference 9 are

$$R_x(\xi, 0, \omega) = e^{-\alpha_1 |\xi|} \quad (14)$$

$$R_y(0, \eta, \omega) = e^{-\alpha_2 |\eta|} \quad (15)$$

$$S(\omega) = (\delta q_\infty^2 / U_\infty) e^{(-8.094 - 1.239\bar{\omega} - 0.295\bar{\omega}^2 - 0.090\bar{\omega}^3 - 0.014\bar{\omega}^4 - 0.001\bar{\omega}^5)} \quad (16)$$

where  $\bar{\omega} = \ln(\omega \delta / 2\pi U_\infty)$ ,  $\delta$ ,  $U_\infty$ , and  $q_\infty$  are boundary layer thickness, free stream velocity, and free stream dynamic pressure, respectively. The attenuation coefficients  $\alpha_1$  and  $\alpha_2$  indicate the degree of spatial correlation of random pressure  $p(x, y, t)$ . Similar forms of cross-spectral density are available for subsonic and attached supersonic flow (References 7, 9).

For a linear response analysis of surface panels using the power spectral density approach, Equation 13 can be used directly as an input parameter. This procedure is described in Section II C. 1. However, for the time-domain nonlinear response study simulated space-time histories are needed as presented in Equations 6 and 11. The required spectral density can be obtained by substituting Equation 13 into Equation 2 and performing Fourier transformation

$$S_p(k_1, k_2, \omega) = \frac{S(\omega) \alpha_1 \cdot \alpha_2}{\pi^2 [\alpha_1^2 + (\omega / U_\infty + k_1)^2] [\alpha_2^2 + k_2^2]} \quad (17)$$

For low supersonic flow at Mach number = 2,  $\delta = 0.91$  in.,  $\alpha_1 = 1.22$ ,  $\alpha_2 = 0.26$ , and  $U_\infty = 0.75 U_\infty$  (Reference 9).

### 3. Jet Engine Exhaust Noise

One of the primary causes of fatigue in many flight structures is a result of acoustic loads generated by near-field jet exhaust noise. Various empirical forms similar to those given in Equations 13-16 are available to characterize the random pressure due to jet exhaust noise. However, for supersonic-

hypersonic aircraft such as the NASP, detailed statistical information on the localized pressures does not seem to be available at the present time. Preliminary estimates indicate that the local noise levels will be very large, exceeding 180 decibels (Reference 26).

#### 4. Uniform Distribution of Random Pressure

Useful approximations can be obtained by assuming the input pressure to be uniformly distributed over the surface of a structural component. Then, the cross-spectral density can be approximated using band-limited Gaussian white noise conditions, such as the one given in Equation 1. The expression for  $S_0$  can be written as

$$S_0 = p_0^2 10^{SPL/10} \quad (18)$$

where  $p_0$  is the reference pressure,  $p_0 = 2.9 \times 10^{-9}$  psi ( $0.00002 N/m^2$ ), and SPL is the sound pressure level expressed in decibels.

#### B. STRUCTURAL MODELING

The governing equations of motion for an orthotropic composite are given by (Reference 33)

$$\begin{aligned} & D_{11} \frac{\partial^2 w}{\partial x^4} + 2(D_{12} + 2D_{66}) \frac{\partial^2 w}{\partial x^2 \partial y^2} + D_{22} \frac{\partial^2 w}{\partial y^4} + c\dot{w} + m_p \ddot{w} \\ & - \frac{\partial^2 F}{\partial y^2} \cdot \frac{\partial^2 w}{\partial x^2} - \frac{\partial^2 F}{\partial x^2} \cdot \frac{\partial^2 w}{\partial y^2} + 2 \frac{\partial^2 F}{\partial x \partial y} \cdot \frac{\partial^2 w}{\partial x \partial y} \\ & - N_x^b \frac{\partial^2 w}{\partial x^2} - N_y^b \frac{\partial^2 w}{\partial y^2} + \nabla^2 M_x^T + \nabla^2 M_y^T = P^r(x, y, t) \end{aligned} \quad (19)$$

$$\begin{aligned}
& \alpha_{22} \frac{1}{h} \frac{\partial^4 F}{\partial x^4} + (\alpha_{66} + 2\alpha_{12}) \frac{1}{h} \frac{\partial^4 F}{\partial x^2 \partial y^2} + \alpha_{11} \frac{1}{h} \frac{\partial^4 F}{\partial y^4} \\
& + \nabla^2 N_x^T + \nabla^2 N_y^T - \left( \frac{\partial^2 w}{\partial x \partial y} \right)^2 - \frac{\partial^2 w}{\partial x^2} \cdot \frac{\partial^2 w}{\partial y^2}
\end{aligned} \tag{20}$$

where  $D_{11}$ ,  $D_{12}$ ,  $D_{22}$ , and  $D_{66}$  are bending stiffnesses;  $\alpha_{11}$ ,  $\alpha_{12}$ ,  $\alpha_{22}$ , and  $\alpha_{66}$  are membrane compliances;  $N_x^b$  and  $N_y^b$  are the inplane loads applied at the boundaries;  $F$  is the Airy stress function;  $N_x^T$ ,  $N_y^T$ ,  $M_x^T$ , and  $M_y^T$  are the inplane and bending thermal load terms, respectively;  $P$  is the random input pressure;  $m_p$  is the mass per unit area;  $h$  is the plate thickness; and  $c$  is the damping coefficient.

The structural mechanics embodied in Equations 19 and 20 are a result of using von Karman's equations for large deflections (References 33-35) of elastic isotropic plates as modified by Ambartsumyan for orthotropic materials (Reference 33).

The terms  $N_x^T$ ,  $N_y^T$ ,  $M_x^T$ , and  $M_y^T$  are computed from

$$N_x^T = \frac{\alpha_{11}}{\alpha_{11}h} \int_{-h/2}^{h/2} T(x, y, z) dZ \tag{21}$$

$$N_y^T = \frac{\alpha_{22}}{\alpha_{22}h} \int_{-h/2}^{h/2} T(x, y, z) dZ \tag{22}$$

$$M_x^T = \frac{\alpha_{11}}{\alpha_{11}h} \int_{-h/2}^{h/2} T(x, y, z) Z dZ \tag{23}$$

$$M_y^T = \frac{\alpha_{22}}{\alpha_{22}h} \int_{-h/2}^{h/2} T(x, y, z) Z dZ \tag{24}$$

in which  $\alpha_{11}$  and  $\alpha_{22}$  are coefficients of thermal expansion and  $T$  is the temperature distribution in the panel.

The membrane inplane forces are given by

$$N_x = \frac{\partial^2 F}{\partial y^2} \quad (25)$$

$$N_y = \frac{\partial^2 F}{\partial x^2} \quad (26)$$

$$N_{xy} = -\frac{\partial^2 F}{\partial x \partial y} \quad (27)$$

such that inplane equilibrium requirements are identically satisfied. Equation 19 expresses the dynamic equilibrium in the direction normal to the panel, while Equation 20 is the compatibility condition for inplane strains.

The panel is assumed to be simply supported on all four edges. Exact boundary conditions for the Airy stress function  $F$  are very complicated and, for the present study, the inplane boundary conditions are satisfied on the average (References 10,35,36). Thus,

$$\int_0^b \int_0^a \frac{\partial u}{\partial x} dx dy = 0 \quad (28)$$

$$\int_0^a \int_0^b \frac{\partial v}{\partial y} dy dx = 0 \quad (29)$$

$$\bar{N}_{xy}|_{x=0,a} = 0 \quad (30)$$

$$\overline{N}_{yx}|_{y=0,b} = 0 \quad (31)$$

$$\overline{N}_{xy} = \frac{1}{b} \int_0^b N_{xy} dy \quad (32)$$

$$\overline{N}_{yx} = \frac{1}{a} \int_0^a N_{yx} dx \quad (33)$$

The terms  $u$  and  $v$  in Equations 28 and 29 are the inplane displacements which are expressed as

$$\frac{\partial u}{\partial x} = \left( \alpha_{11} \frac{\partial^2 F}{\partial^2 y} + \alpha_{12} \frac{\partial^2 F}{\partial^2 x} + N_x^T \right) - \frac{1}{2} \left( \frac{\partial w}{\partial x} \right)^2 \quad (34)$$

$$\frac{\partial v}{\partial y} = \left( \alpha_{12} \frac{\partial^2 F}{\partial^2 x} + \alpha_{22} \frac{\partial^2 F}{\partial^2 y} + N_y^T \right) - \frac{1}{2} \left( \frac{\partial w}{\partial y} \right)^2 \quad (35)$$

Equations 28 and 29 imply no inplane stretching of the panel edges in an average sense and they correspond to the inplane boundary conditions for immovable edges. Equations 30 and 31 specify that the average inplane shear forces are zero at the boundary.

### C. PREDICTION OF RESPONSE IN SURFACE PANELS

In order to assess the fatigue life and estimate the reliability of thermal surface protection systems, dynamic response in the form of deflection and stress is needed. For linear systems, response calculations can be obtained either in the time or frequency domains. The power spectral density (PSD) method is commonly used to obtain solutions for a frequency domain approach. For a time domain analysis, the simulation of random input pressure, as described in Section II A., and numerical integration procedures must be utilized. When the response is



nonlinear, a time domain Monte Carlo type method can be developed to obtain deflection and stress response solutions (References 11,24,25,28,36-42).

In the present study, the time domain analysis is verified for a linear case by a direct comparison of the response predictions to those obtained by the PSD procedure. Then, a detailed study of nonlinear response using a Monte Carlo time domain approach is developed.

In addition to the very high noise levels that will be acting on the surface of the NASP-type vehicles, the surface temperatures are expected to exceed 3,000°F (Reference 26). Such high temperatures will induce large thermal stresses and instabilities (buckling) of the surface panels. However, the thermal effects and inplane loads are not considered in Phase I work.

#### 1. The Power Spectral Density Method

Consider a rectangular panel, shown in Figure 1, exposed to a random pressure  $p(x,y,t)$ .

For a homogeneous panel, the governing equation of motion for small deformations can be written as

$$D_p \nabla^4 w + \beta \dot{w} + m_p \ddot{w} = p(x,y,t) \quad (36)$$

where

$$D_p \nabla^4 = D_{11} \partial^4 / \partial x^4 + 2(D_{12} + 2D_{66}) \partial^4 / \partial x^2 \partial y^2 + D_{22} \partial^4 / \partial y^4$$

$$D_{11} = E_{11} h^3 / 12 (1 - \nu_{12} \nu_{21})$$

$$D_{12} = \nu_{21} D_{11}$$

$$D_{22} = E_{22} h^3 / 12 (1 - \nu_{12} \nu_{21})$$

$$D_{66} = G_{12} h^3 / 12$$

in which  $E_{11}$ ,  $E_{22}$ ,  $G_{12}$ ,  $\nu$ ,  $\beta$ , and  $m_p$  are moduli of elasticity, Poisson's ratio, damping coefficient, and mass per unit area, respectively. The solution for panel deflection can be expressed as a superposition of orthogonal modes as

$$w(x, y, t) = \sum_{m=1}^{\infty} \sum_{n=1}^{\infty} q_{mn}(t) X_{mn}(x, y) \quad (37)$$

where  $q_{mn}$  are the generalized coordinates and  $X_{mn}$  are the modes. Taking the Fourier transformation of Equations 36 and 37 and utilizing orthogonality, it can be shown that

$$\bar{q}_{mn} = H_{mn} P_{mn} \quad (38)$$

where the frequency response function

$$H_{mn} = (\omega_{mn}^2 - \omega^2 + 2i\zeta_{mn}\omega_{mn}\omega)^{-1} \quad (39)$$

and the generalized random forces are

$$P_{mn} = \frac{1}{m_p} \int_0^a \int_0^b \bar{p}(x, y, \omega) X_{mn}(x, y) dx dy \quad (40)$$

in which a bar denotes a transformed quantity. The modal damping coefficients  $\zeta_{mn}$  and the natural frequencies of panel vibrations can be determined from

$$\zeta_{mn} = \zeta_0 (\omega_{11} / \omega_{mn})^\gamma \quad (41)$$

$$\omega_{mn}^2 = (D_p / M_p) \nabla^4 X_{mn} / X_{mn} \quad (42)$$

where  $\zeta_0$  is a modal damping coefficient (percent of critical damping) and  $\gamma$  is a parameter based on experimental data. For a stationary and Gaussian random pressure input  $p(x,y,t)$ , the deflection response spectral density can be determined from (Reference 43)

$$S_w(x,y,\omega) = \sum_{m=1}^{\infty} \sum_{r=1}^{\infty} \sum_{n=1}^{\infty} \sum_{l=1}^{\infty} H_{mn} H_{rl}^* S_{mnrl} X_{mn} X_{rl} \quad (43)$$

where

$$S_{mnrl} = \frac{1}{m_p^2} \int_0^a \int_0^a \int_0^b \int_0^b S_p(\xi, \eta, \omega) X_{mn}(x_1, y_1) X_{rl}(x_2, y_2) dx_1 dy_1 dx_2 dy_2 \quad (44)$$

where an asterisk indicates a conjugate quantity.

The orthonormal modes for a simply supported panel are

$$X_{mn}(x,y) = \frac{2}{\sqrt{ab}} \sin(m\pi x/a) \sin(n\pi y/b) \quad (45)$$

For a clamped-clamped panel, a rough approximation of the modes can be obtained by using clamped-clamped beam modes

$$X_{mn}(x,y) = X_m'(x) X_n'(y) \quad (46)$$

where

$$X_m'(x) = \frac{1}{A_m \sqrt{a}} \begin{cases} \cos \gamma_m \left( x/a - \frac{1}{2} \right) + \kappa_m \cosh \gamma_m \left( x/a - \frac{1}{2} \right) & m = \text{odd} \\ \sin \gamma_m \left( x/a - \frac{1}{2} \right) + \kappa_m \sinh \gamma_m \left( x/a - \frac{1}{2} \right) & m = \text{even} \end{cases} \quad (47)$$

The values of the constants  $A_m$ ,  $\gamma_m$ , and  $\kappa_m$  can be obtained from Table 1. Then, for a simply supported panel and uniformly distributed random pressure where  $S_p(\xi, \eta, \omega) = S(\omega)$ , the cross-spectral densities of generalized random forces are

$$S_{mnrl} = \frac{4S(\omega)ab}{m_p^2 \pi^4 mnr l} [1 - (-1)^m][1 - (-1)^n][1 - (-1)^r][1 - (-1)^l] \quad (48)$$

For a clamped-clamped panel

$$S_{mnrl} = \frac{16S(\omega)ab\alpha_m\alpha_n\alpha_r\alpha_l}{m_p^2 \gamma_m \gamma_n \gamma_r \gamma_l} [1 - (-1)^m][1 - (-1)^n][1 - (-1)^r][1 - (-1)^l] \quad (49)$$

Stresses in a thin panel undergoing linear deformation can be calculated from

TABLE 1  
CONSTANTS FOR CLAMPED-PLATE MODES

$m$	$\Lambda_m$	$\gamma_m$	$\kappa_m$	$\alpha_m$
1	0.7133	4.730040	0.132857	0.982
2	0.7068	7.853202	-0.0278749	1.000
3	0.7071	10.99560	-0.00579227	1.000
4	0.7071	14.137164	0.0012041	1.000
5	0.7071	17.278758	0.002503	1.000
>5	0.7071	$\gamma_m + (m-5)\pi$	$\frac{\sin \frac{\gamma_m}{2}}{\sinh \frac{\gamma_m}{2}}$	1.000

$$\sigma_x = -\frac{12D_{11}}{h^3} z (\partial^2 w / \partial x^2 + \nu_{12} \partial^2 w / \partial y^2) \quad (50)$$

$$\sigma_y = -\frac{12D_{22}}{h^3} z (\partial^2 w / \partial y^2 + \nu_{12} \partial^2 w / \partial x^2) \quad (51)$$

$$\tau_{xy} = -\frac{12D_{66}}{h^3} z \partial^2 w / \partial x \partial y \quad (52)$$

where  $\sigma_x$  and  $\sigma_y$  are the normal stresses and  $\tau_{xy}$  is the shear stress;  $z$  is the distance from the mid-plane of the panel. Taking the Fourier transformation of Equations 50-52, using Equation 37, it can be shown that the spectral densities of the stress components at the surface of a simply supported panel are

$$S_{\sigma_x}(x, y, \omega) = \left[ \frac{6D_{11}}{h^2} \right]^2 \sum_{m=1}^{\infty} \sum_{n=1}^{\infty} |H_{mn}|^2 [(m\pi/a)^2 + \nu_{12}(n\pi/b)^2]^2 \cdot S_{mn} X_{mn}^2 \quad (53)$$

$$S_{\sigma_y}(x, y, \omega) = \left[ \frac{6D_{22}}{h^2} \right]^2 \sum_{m=1}^{\infty} \sum_{n=1}^{\infty} |H_{mn}|^2 [(n\pi/b)^2 + \nu_{12}(m\pi/a)^2]^2 \cdot S_{mn} X_{mn}^2 \quad (54)$$

$$S_{\tau_{xy}}(x, y, \omega) = \left[ \frac{6D_{66}}{h^2} \right]^2 \sum_{m=1}^{\infty} \sum_{n=1}^{\infty} |H_{mn}|^2 (m\pi/a)^2 (n\pi/b)^2 [\partial^2 X_{mn} / \partial x \partial y]^2 \cdot S_{mn} \quad (55)$$

Equations 53-55 were obtained under a condition that the cross-modal terms can be neglected and the cross-spectral densities of the generalized random forces are determined from Equation 44 by setting  $m=r$  and  $n=l$ .

The root-mean-square (rms) values of displacement and stresses can be calculated from

$$rms = \left[ \int_0^{\infty} S_R(x, y, \omega) d\omega \right]^{\frac{1}{2}} \quad (56)$$

where  $S_R$  is the response spectral density given in Equation 43 for displacements and Equations 53-55 for stresses.

## 2. The Time Domain Method

To solve Equations 19 and 20, panel deflections are expanded in terms of panel modes:

$$w(x, y, t) = \sum_{m=1}^{\infty} \sum_{n=1}^{\infty} A_{mn}(t) \phi_{mn}(x, y) \quad (57)$$

in which  $A_{mn}$  are the modal amplitudes and  $\phi_{mn}$  are the natural modes corresponding to a linear panel. For a simply supported panel,  $\phi_{mn}$  may be written as

$$\phi_{mn}(x, y) = X_n(x) Y_n(y) \quad \begin{matrix} m = 1, 2, 3, \dots \\ n = 1, 2, 3, \dots \end{matrix} \quad (58)$$

where  $X_m = \sin(m\pi x/a)$  and  $Y_n = \sin(n\pi y/b)$ .

Substituting Equation 57 into Equation 20 yields:

$$\begin{aligned} & \alpha_{22} \frac{1}{h} \frac{\partial^4 F}{\partial x^4} + (\alpha_{44} + 2\alpha_{12}) \frac{1}{h} \frac{\partial^4 F}{\partial x^2 \partial y^2} + \alpha_{11} \frac{1}{h} \frac{\partial^4 F}{\partial y^4} + \nabla^2 N_x^T + \nabla^2 N_y^T \\ & - \frac{\pi^4}{4a^2 b^2} \sum_m \sum_n \sum_r \sum_s A_{mn} A_{rs} ms \\ & \cdot \left\{ (nr - ms) \left[ \cos \frac{(m+r)\pi x}{a} \cos \frac{(n+s)\pi y}{b} + \cos \frac{(m-r)\pi x}{a} \cos \frac{(n-s)\pi y}{b} \right] \right. \\ & \left. + (nr + ms) \left[ \cos \frac{(m+r)\pi x}{a} \cos \frac{(n-s)\pi y}{b} + \cos \frac{(m-r)\pi x}{a} \cos \frac{(n+s)\pi y}{b} \right] \right\} \quad (59) \end{aligned}$$

The solution for  $F$  consists of homogeneous  $F_h$ , and particular solution,  $F_p$ . The particular solution for  $F$  can readily be obtained from Equation 59 by following the procedures given in References 10 and 35:

$$\begin{aligned} F_p &= \frac{1}{4} \left( \frac{a}{b} \right)^2 \sum_m \sum_n \sum_r \sum_s A_{mn} A_{rs} ms (nr - ms) \\ & \cdot \left\{ \frac{\cos \frac{(m+r)\pi x}{a} \cos \frac{(n+s)\pi y}{b}}{T_{11}} + \frac{\cos \frac{(m-r)\pi x}{a} \cos \frac{(n-s)\pi y}{b}}{T_{12}} \right\} \\ & + \frac{1}{4} \left( \frac{a}{b} \right)^2 \sum_m \sum_n \sum_r \sum_s A_{mn} A_{rs} ms (nr + ms) \\ & \cdot \left\{ \frac{\cos \frac{(m+r)\pi x}{a} \cos \frac{(n-s)\pi y}{b}}{T_{21}} + \frac{\cos \frac{(m-r)\pi x}{a} \cos \frac{(n+s)\pi y}{b}}{T_{22}} \right\} \quad (60) \end{aligned}$$

where

$$\begin{aligned}
T_{11} &= \frac{a_{22}}{h}(m+r)^4 + \frac{a_{66} + 2a_{12}}{h} \cdot \frac{a^2}{b^2} \cdot (m+r)^2(n+s)^2 \\
&\quad + \frac{a_{11}}{h} \cdot \frac{a^4}{b^4} \cdot (n+s)^4 \\
T_{12} &= \frac{a_{22}}{h}(m-r)^4 + \frac{a_{66} + 2a_{12}}{h} \cdot \frac{a^2}{b^2} \cdot (m-r)^2(n-s)^2 \\
&\quad + \frac{a_{11}}{h} \cdot \frac{a^4}{b^4} \cdot (n-s)^4 \\
T_{21} &= \frac{a_{22}}{h}(m+r)^4 + \frac{a_{66} + 2a_{12}}{h} \cdot \frac{a^2}{b^2} \cdot (m+r)^2(n-s)^2 \\
&\quad + \frac{a_{11}}{h} \cdot \frac{a^4}{b^4} \cdot (n-s)^4 \\
T_{22} &= \frac{a_{22}}{h}(m-r)^4 + \frac{a_{66} + 2a_{12}}{h} \cdot \frac{a^2}{b^2} \cdot (m-r)^2(n+s)^2 \\
&\quad + \frac{a_{11}}{h} \cdot \frac{a^4}{b^4} \cdot (n+s)^4 \quad . \quad (61)
\end{aligned}$$

For the case of inplane boundary conditions that are satisfied on the average, the homogeneous solution can be written as

$$F_h = \frac{C_1 x^2}{2} + \frac{C_2 y^2}{2} - C_3 xy \quad (62)$$

where  $C_1$ ,  $C_2$ , and  $C_3$  are constants of integration that are to be determined from the boundary conditions specified in Equations 28-31. Using Equations 28-31 and 34 and 35, together with the expression for Airy stress function  $F$  and the solution for panel  $w$ , the constants of integration are



$$C_1 = \frac{\pi^2}{8} \sum_m \sum_n A_{mn}^2 \left( a_{22} \frac{m^2}{a^2} - a_{12} \frac{n^2}{b^2} \right) \quad (63)$$

$$C_2 = \frac{\pi^2}{8} \sum_m \sum_n A_{mn}^2 \left( -a_{12} \frac{m^2}{a^2} + a_{11} \frac{n^2}{b^2} \right) \quad (64)$$

$$C_3 = 0 \quad (65)$$

Having completely determined  $F$ , Equation 19 is solved using the Galerkin method by computing the integral average of Equation 19 weighted by each term of Equation 57. The natural frequencies of the panel obtained by the linear theory are imposed into Equation 19. Since  $\phi_{mn}$  are the natural modes of the panel, then

$$D_{11} \frac{\partial^4 \phi_{mn}}{\partial x^4} + 2(D_{12} + 2D_{66}) \frac{\partial^4 \phi_{mn}}{\partial x^2 \partial y^2} + D_{22} \frac{\partial^4 \phi_{mn}}{\partial y^4} = m_p \omega_{mn}^2 \phi_{mn} \quad (66)$$

in which  $\omega_{mn}$  are the natural frequencies of the undamped linear system. Substituting  $F = F_h + F_p$  and  $\omega$  as given in Equation 57 into Equation 19, and utilizing the Galerkin type procedure, the following system of nonlinear differential equations are obtained

$$\begin{aligned} \ddot{A}_{ij} + \frac{c}{M_{ij}} \dot{A}_{ij} + \omega_{ij}^2 A_{ij} + \frac{\pi^4 ab}{32 M_{ij}} \sum_s \sum_m \sum_k \sum_n A_{is} A_{mk} A_{ns} \\ \cdot \left[ \left( \frac{i}{a} \right)^2 \left( \frac{a_{22}}{a_{11} a_{22} - a_{12}^2} \cdot \frac{m^2}{a^2} - \frac{a_{12}}{a_{11} a_{22} - a_{12}^2} \cdot \frac{k^2}{b^2} \right) \right. \\ \left. + \left( \frac{j}{b} \right)^2 \left( -\frac{a_{12}}{a_{11} a_{22} - a_{12}^2} \cdot \frac{m^2}{a^2} + \frac{a_{11}}{a_{11} a_{22} - a_{12}^2} \cdot \frac{k^2}{b^2} \right) \right] \\ + \frac{\pi^4 \alpha}{64 b^3 M_{ij}} \sum_d \sum_s \sum_m \sum_n \sum_r \sum_t A_{ds} A_{mn} A_{rs} \cdot Z_{ijdemnrs} = Q_{ij}(t) \quad (67) \end{aligned}$$

where  $\omega_{ij}$  are the natural frequencies of a rectangular panel.

The generalized mass and the generalized random forces are

$$M_{ij} = m_p \int_0^a \int_0^b \phi_{ij}^2(x, y) dx dy \quad (68)$$

$$Q_{ij}(t) = \frac{1}{M_{ij}} \int_0^a \int_0^b p^r(x, y, t) \phi_{ij}(x, y) dx dy \quad (69)$$

The nonlinear stiffness coefficients  $Z_{lqdfmkrl}$  are given by

$$\begin{aligned} Z_{lqdfmkrl} = & (kr - ml)[F_{lqdfmkrl}(m + r, k + l) + \bar{F}_{lqdfmkrl}(m - r, k - l)] \\ & + (kr + ml)[F_{lqdfmkrl}(m - r, k + l) + F_{lqdfmkrl}(m + r, k - l)] \end{aligned} \quad (70)$$

where

$$\begin{aligned} F_{lqdfmkrl}(G, H) = & \left\{ 2GHdf[\beta(i + d, G) + \beta(i - d, G)] \left[ \beta(q + f, H) \right. \right. \\ & \left. \left. + \beta(q - f, H) \right] - (H^2d^2 + G^2f^2) \left[ \gamma(i + d, G) \right. \right. \\ & \left. \left. - \gamma(i - d, G) \right] \left[ \gamma(q + f, H) - \gamma(q - f, H) \right] \right\} / \bar{D}(G, H) \end{aligned}$$

where

$$\bar{D}(G, H) = \frac{a_{22}}{h} \cdot G^4 + \frac{a_{66} + 2a_{12}}{h} \cdot \frac{a^2}{b^2} \cdot G^2 H^2 + \frac{a_{11}}{h} \cdot \frac{a^4}{b^4} \cdot H^4$$

and

$$\bar{F}_{lqdfmkrl}(G, H) = \begin{cases} 0, & G = H = 0 \\ F_{lqdfmkrl}(G, H), & \text{otherwise} \end{cases}$$

$$\beta(j, k) = \begin{cases} 1, & j = k \neq 0 \\ -1, & j = -k \neq 0 \\ 0, & \text{otherwise} \end{cases}$$

$$\gamma(j, k) = \begin{cases} 2, & j = k = 0 \\ 1, & j = k \neq 0 \\ 0, & \text{otherwise} \end{cases}.$$

Before step-by-step numerical integration can be implemented for the coupled system of nonlinear differential equations given in Equation 67, the time histories of the generalized random forces  $Q_{ij}(t)$  are needed. This is achieved by first simulating the multidimensional random pressure  $p^r(x, y, t)$  in space-time domain and then evaluating Equation 69 numerically for each value of indices  $i, j$ . Following the procedures given in References 23 and 31, the stationary random pressure  $p^r(x, y, t)$  can be simulated as given in Equation 3.

An alternate procedure to generate the generalized random forces  $Q_{ij}(t)$  is to substitute Equation 3 into Equation 69 and evaluate all integrals in closed form. The generalized random forces are then simulated as multi-variate random processes (References 31, 32). If the pressure distribution is uniform over the panel surface, the simulation procedure reduces to a single variate and one dimensional random process.

The displacement and stress response time histories are developed for one realization of the random input pressure  $p^r(x, y, t)$ . These solutions would need to be repeated for a number of different realizations and then the response statistics calculated using ensemble averages in a Monte Carlo sense. However, by assuming the input pressure to be an ergodic random process, it is sufficient to obtain a solution for only one realization

and then use temporal averaging to calculate the required response statistics. Then, the mean and the rms values of the displacement can be determined from

$$\bar{w}(x,y) = \frac{1}{T} \int_0^T w(x,y,t) dt \quad (71)$$

$$w_{rms}(x,y) = \left\{ \frac{1}{T} \int_0^T w^2(x,y,t) dt \right\}^{\frac{1}{2}} \quad (72)$$

where  $T$  is the period of the simulated time history of input pressure. Similar expressions can be developed for panel stresses. The root-mean-square values calculated from Equations 56 and 72 should yield the same results.

$$\begin{aligned}
\sigma_x(x, y, z, t) = & \frac{\pi^2}{8} \sum_m \sum_n A_{mn}^2 \left( \frac{a_{22}}{a_{11}a_{22} - a_{12}^2} \cdot \frac{m^2}{a^2} - \frac{a^{12}}{a_{11}a_{22} - a_{12}^2} \cdot \frac{n^2}{b^2} \right) \\
& + \pi^2 z \sum_m \sum_n A_{mn} \sin \frac{m\pi x}{a} \sin \frac{n\pi y}{b} \left( \frac{a_{22}}{a_{11}a_{22} - a_{12}^2} \cdot \frac{m^2}{a^2} - \frac{a^{12}}{a_{11}a_{22} - a_{12}^2} \cdot \frac{n^2}{b^2} \right) \\
& - \frac{\pi^2}{4} \left( \frac{a}{b} \right)^2 \sum_m \sum_n \sum_r \sum_s A_{mn} A_{rs} ms(nr - ms) \\
& \cdot \left\{ \left( \frac{n+s}{b} \right)^2 \frac{\cos \frac{(m+r)\pi x}{a} \cos \frac{(n+s)\pi y}{b}}{T_{11}} \right. \\
& + \left. \left( \frac{n-s}{b} \right)^2 \frac{\cos \frac{(m-r)\pi x}{a} \cos \frac{(n-s)\pi y}{b}}{T_{12}} \right\} \\
& - \frac{\pi^2}{4} \left( \frac{a}{b} \right)^2 \sum_m \sum_n \sum_r \sum_s A_{mn} A_{rs} ms(nr + ms) \\
& \cdot \left\{ \left( \frac{n-s}{b} \right)^2 \frac{\cos \frac{(m+r)\pi x}{a} \cos \frac{(n-s)\pi y}{b}}{T_{21}} \right. \\
& + \left. \left( \frac{n+s}{b} \right)^2 \frac{\cos \frac{(m-r)\pi x}{a} \cos \frac{(n+s)\pi y}{b}}{T_{22}} \right\}
\end{aligned} \tag{73}$$

$$\begin{aligned}
\sigma_y(x, y, z, t) = & \frac{\pi^2}{8} \sum_m \sum_n A_{mn}^2 \left( \frac{a_{22}}{a_{11}a_{22} - a_{12}^2} \cdot \frac{n^2}{a^2} - \frac{a^{12}}{a_{11}a_{22} - a_{12}^2} \cdot \frac{m^2}{b^2} \right) \\
& + \pi^2 z \sum_m \sum_n A_{mn} \sin \frac{m\pi x}{a} \sin \frac{n\pi y}{b} \left( \frac{a_{22}}{a_{11}a_{22} - a_{12}^2} \cdot \frac{n^2}{a^2} - \frac{a^{12}}{a_{11}a_{22} - a_{12}^2} \cdot \frac{m^2}{b^2} \right) \\
& - \frac{\pi^2}{4} \left( \frac{a}{b} \right)^2 \sum_m \sum_n \sum_r \sum_s A_{mn} A_{rs} ms(nr - ms) \\
& \cdot \left\{ \left( \frac{m+r}{a} \right)^2 \frac{\cos \frac{(m+r)\pi x}{a} \cos \frac{(n+s)\pi y}{b}}{T_{11}} \right. \\
& + \left. \left( \frac{m-r}{a} \right)^2 \frac{\cos \frac{(m-r)\pi x}{a} \cos \frac{(n-s)\pi y}{b}}{T_{12}} \right\} \\
& - \frac{\pi^2}{4} \left( \frac{a}{b} \right)^2 \sum_m \sum_n \sum_r \sum_s A_{mn} A_{rs} ns(mr + ns) \\
& \cdot \left\{ \left( \frac{m-r}{a} \right)^2 \frac{\cos \frac{(m+r)\pi x}{a} \cos \frac{(n-s)\pi y}{b}}{T_{21}} \right. \\
& + \left. \left( \frac{m+r}{a} \right)^2 \frac{\cos \frac{(m-r)\pi x}{a} \cos \frac{(n+s)\pi y}{b}}{T_{22}} \right\}
\end{aligned} \tag{74}$$

$$\begin{aligned}
\tau_{xy}(x, y, z, t) = & \pi^2 z \sum_m \sum_n A_{mn} \sin \frac{m\pi x}{a} \sin \frac{n\pi y}{b} \left( \frac{a_{22}}{a_{11}a_{22} - a_{12}^2} \cdot \frac{m^2}{a^2} - \frac{a_{12}}{a_{11}a_{22} - a_{12}^2} \cdot \frac{n^2}{b^2} \right) \\
& - \frac{\pi^2}{4} \left( \frac{a}{b} \right)^2 \sum_m \sum_n \sum_r \sum_s A_{mn} A_{rs} ms(nr - ms) \\
& \cdot \left\{ \left( \frac{(m+r)(n+s)}{ab} \right) \frac{\cos \frac{(m+r)\pi x}{a} \cos \frac{(n+s)\pi y}{b}}{T_{11}} \right. \\
& \left. + \left( \frac{(m-r)(n-s)}{ab} \right) \frac{\cos \frac{(m-r)\pi x}{a} \cos \frac{(n-s)\pi y}{b}}{T_{12}} \right\} \\
& - \frac{\pi^2}{4} \left( \frac{a}{b} \right)^2 \sum_m \sum_n \sum_r \sum_s A_{mn} A_{rs} ms(nr + ms) \\
& \cdot \left\{ \left( \frac{(n-s)(m+r)}{ab} \right) \frac{\cos \frac{(m+r)\pi x}{a} \cos \frac{(n-s)\pi y}{b}}{T_{21}} \right. \\
& \left. + \left( \frac{(n+s)(m-r)}{ab} \right) \frac{\cos \frac{(m-r)\pi x}{a} \cos \frac{(n+s)\pi y}{b}}{T_{22}} \right\}
\end{aligned} \tag{75}$$

#### D. SONIC FATIGUE OF SURFACE PANELS

The key elements in predicting the fatigue life of a structural component to random loads are detailed stress load spectra at a critical point on the structure and reliable cumulative damage rules for random stress amplitudes. For a multidimensional stress state, the most damaging stress components must be known as well as the choice between the nominal stress and the actual load stress in complex geometries and connections. The load spectra is a function of mission requirements, flight conditions, and flight duration. The information on threshold crossings and peak exceedances is needed for the development of stress load spectra. In addition to this information, stress data in the form of S-N diagrams are required. Such data are usually obtained from coupon testing under constant amplitude loading and are approximated by the following equation

$$NS^\lambda = B$$

(76)

where  $S$  is a fixed stress amplitude for constant alternating load,  $N$  is the number of stress cycles until failure at the stress level  $S$ , and  $\lambda$  and  $B$  are material constants depending on the material.

Since stress response of surface panels is random, fatigue data from random tests should give the required information for life predictions. In this case, the stress response  $S$  is represented as the root-mean-square (rms) value and the number of cycles  $N$  correspond to cycles of a frequency at a dominant response peak. For a linear and narrow band Gaussian response, reasonable predictions of fatigue life can be expected using this approach. However, under severe acoustic and thermal environment, the stress response is nonlinear and non-Gaussian. Furthermore, for most practical applications, fatigue data under actual random inputs are rarely available for full scale structures or structural components. Most of the fatigue data digested into the S-N diagram form are for coupon specimens under constant amplitude loading. This information, together with the distribution of stress response peaks, can be utilized to construct a life prediction model for random stresses.

Consider that the number of fatigue cycles is equal to the number of positive stress peaks, or stress reversals, and that each damage occurs at each positive stress peak. Then, according to the Palmgren-Miner linear cumulative damage rule (Reference 44), the total cumulative damage can be written as

$$D = \sum_i n(S_i)/N(S_i) \quad (77)$$

where  $n$  is the number of stress peaks (cycles) experienced by the structure at stress level  $S_i$ , and  $N$  is the number of cycles at which failure occurs. Fatigue failure occurs when  $D$  reaches a value of unity. Substituting Equation 76 into Equation 77 gives



$$D = \frac{1}{B} \sum_i n(S_i) S_i^\lambda \quad (78)$$

To account for positive peaks that occur in the negative stress region and add to the cumulative damage, Equation 78 can be modified to

$$D = \frac{1}{B} \sum_i n(S_i) |S_i^\lambda| \quad (79)$$

Since stress response is a random quantity, the expected damage in the time interval  $\tau$  can be written as (Reference 43)

$$E[D(\tau)] = \frac{E[M_\tau] \tau}{B} \int_{-\infty}^{\infty} |S|^\lambda P_I(S) dS \quad (80)$$

where  $E[M_\tau]$  is the expected total number of positive stress peaks and  $P_I(S)$  is the probability density function of the peak magnitude of the random stress process. The expected total number of peaks can be estimated from (Reference 43)

$$E[M_\tau] = - \int_{-\infty}^{\infty} \int_{-\infty}^0 \ddot{s} P_{s\dot{s}\ddot{s}}(s, 0, \ddot{s}) d\ddot{s} ds \quad (81)$$

where  $P_{s\dot{s}\ddot{s}}$  is the joint probability density of  $S(t)$  (stress),  $\dot{S}(t)$  (stress velocity), and  $\ddot{S}(t)$  (stress acceleration).

### 1. Linear Stress Response

The response of a linear system to a Gaussian input is also Gaussian. For a stationary Gaussian random process, the

probability density  $P$ , and the joint densities  $P_{..}$ ,  $P_{...}$  are known. Then, the expected number of total peaks and the density of peaks can be evaluated in closed form (Reference 43)

$$E[M_T] = \frac{1}{2\pi} \sigma_{\dot{s}} / \sigma_s \quad (82)$$

$$P_I(s) = \frac{1}{\sigma_s} \left( \frac{1 - \alpha^2}{2\pi} \right)^{\frac{1}{2}} e^{\left( -\frac{s^2}{2\sigma_s^2(1 - \alpha^2)} \right)} + \frac{\alpha s}{2\sigma_s^2} \left\{ 1 + \operatorname{erf} \left( \frac{s}{\sigma_s \sqrt{2\alpha^{-2} - 2}} \right) \right\} e^{\left( -\frac{s^2}{2\sigma_s^2} \right)} \quad (83)$$

where  $\sigma_{..}$ ,  $\sigma_{\dot{s}}$ ,  $\sigma_s$  are standard deviations of  $S(t)$ ,  $\dot{S}(t)$ ,  $\ddot{S}(t)$  and the parameter  $\alpha$  is

$$\alpha = \sigma_{\ddot{s}}^2 / \sigma_{\dot{s}} \sigma_s \quad (84)$$

If the spectral density,  $S_s(\omega)$ , of the linear stress process  $S(t)$  is known,

$$\begin{aligned}
\sigma_s &= \left[ \int_{-\infty}^{\infty} S_s(\omega) d\omega \right]^{\frac{1}{2}} \\
\sigma_{\dot{s}} &= \left[ \int_{-\infty}^{\infty} \omega^2 S_s(\omega) d\omega \right]^{\frac{1}{2}} \\
\sigma_{\ddot{s}} &= \left[ \int_{-\infty}^{\infty} \omega^4 S_s(\omega) d\omega \right]^{\frac{1}{2}} .
\end{aligned} \tag{85}$$

The standard deviations  $\sigma_s$ ,  $\sigma_{\dot{s}}$ , and  $\sigma_{\ddot{s}}$  correspond to the principal (maximum) stress in the panel. Two limiting cases of peak distribution can be obtained for  $\alpha=1$  and  $\alpha=0$ . A value of  $\alpha=1$  corresponds to a narrow band process and the peak distribution reduces to the well known Rayleigh distribution while for very small  $\alpha$ . Equation 83 may be approximated by a Gaussian distribution.

For the case of narrow band stress response  $\alpha=1$ , the expected number of peaks per unit time reduces to

$$E[M_T] = E[N_+(0)] = \frac{1}{2\pi} \frac{\sigma_{\dot{s}}}{\sigma_s} \tag{86}$$

where  $E[N_+(0)]$  is the expected rate of upcrossing of stress process  $S(t)$  at zero threshold level. The distribution of stress peaks is that of Rayleigh distribution

$$P_I(s) = \frac{s}{\sigma_s^2} e^{(-s^2/2\sigma_s^2)} \quad 0 \leq s < \infty \tag{87}$$

The expected damage can be obtained in closed form from Equations 80, 86, and 87 as

$$E[D(\tau)] = E[N_+(0)] \cdot \frac{\tau(\sqrt{2}\sigma_s)^\lambda}{B} \Gamma\left(\frac{\lambda+2}{2}\right) \quad (88)$$

where

$$\Gamma(y) = 2 \int_0^\infty x^{2y-1} e^{-x^2} dx, \quad y > 0 \quad (89)$$

is the Gamma function. For a single degree of freedom response the expected upcrossing rate  $E[N_+(0)]$  can be replaced with the natural frequency  $f_0$  (cycles/sec) of the surface panel. For the cases where many modes participate, the single mode approximation is not valid and expected damage should be calculated using Equations 80, 81, and 83. In this case, it is difficult to obtain a closed form solution and a numerical procedure is used to evaluate the required integrals. The expected total damage in the interval from  $\tau=0$  to  $\tau=T$  (a selected time period) can be obtained from  $\int_0^T E[D(\tau)] d\tau$ . For a stationary random response process,  $E[D(T)] = TE[D(\tau)]$ .

As shown in Reference 39, the expected damage  $E[D(T)]$  does not change by much when plotted versus  $\Gamma[M_T]T$  for  $\alpha$  ranging from 0.25 to 1. However, for a wide band process ( $\alpha < 1$ ) the total number of stress peaks,  $E[M_T]$ , is much larger than for a narrow band process ( $\alpha = 1$ ). Thus, fatigue time to failure at  $E[D(T)] = 1$  will be shorter for a wide band response. For example, for an extreme case when  $\alpha$  is very small, distribution of peaks may be approximated by a Gaussian probability density

$$P_I(s) \approx \frac{1}{\sqrt{2\pi}\sigma_s} e^{(-s^2/2\sigma_s^2)} \quad -\infty < s < \infty \quad (90)$$

Then, from Equations 80 and 89

$$E[D(\tau)] = E[M_T] \frac{\tau(\sqrt{2}\sigma_s)^\lambda}{\sqrt{\pi}B} \Gamma\left(\frac{\lambda+1}{2}\right) \quad (91)$$

Since  $E[M_T]_w > E[N.(0)]_n$ ,  $(\sigma_s)_w > (\sigma_s)_n$ , where the subscripts  $w$  and  $n$  indicate wide band (many modes) and narrow band (single mode) stress response, the expected damage for a wide band response will be larger than for a narrow band response. However, except for these extreme cases the peak distribution of a stationary Gaussian random stress process is neither Rayleigh nor Gaussian.

## 2. Quasi-Nonlinear Single Degree of Freedom Stress Response

Approximate solutions for expected fatigue damage can be developed by assuming the nonlinear panel response to be dominated by a single mode, reducing the nonlinear equations of panel motions to a Duffing's type equation and using a linear stress-strain relationship. Such a procedure might not produce meaningful fatigue estimates of a realistic surface panel, but it could give preliminary guidelines on the effect of nonlinearities. If the inplane motions of a panel are constrained at the edges, the governing equation might be approximated by (Reference 45)

$$\begin{aligned} D\nabla^4 w - m_p \Lambda c^2 (\partial^2 w / \partial x^2 + \partial^2 w / \partial y^2) + c_1 \dot{w} \\ + m_p \ddot{w} = p(x, y, t) \end{aligned} \quad (92)$$

where

$$\Lambda = \frac{1}{2ab} \int_0^a \int_0^b [(\partial w / \partial x)^2 + (\partial w / \partial y)^2] dx dy \quad (93)$$

and  $c$  is the wave speed

$$c^2 = \frac{E}{\rho(1 - \nu^2)} \quad (94)$$

where  $\rho$  is the material density and  $\nu$  is the Poisson's ratio. For simple support boundary conditions and single mode approximation

$$w(x, y, t) = q(t) \sin(\pi x / a) \sin(\pi y / b) \quad (95)$$

Substituting Equation 95 into Equations 92 and 94, and utilizing orthogonality gives

$$\ddot{q} + 2\zeta_0 \omega_{11} \dot{q} + \omega_{11}^2 (q + \gamma q^3) = P(t) \quad (96)$$

where

$$P(t) = \frac{4}{m_p ab} \int_0^a \int_0^b p(x, y, t) \sin \frac{\pi x}{a} \sin \frac{\pi y}{b} dx dy \quad (97)$$

$$\gamma = 3/2 h^2 \quad (98)$$

For a uniform noise pressure distribution over the panel surface,

$$P(t) = \frac{16}{m_p \pi^2} p(t) \quad (99)$$

Stresses in the panel (linear stress-strain assumption) can be calculated from Equations 50-52 in terms of the generalized coordinate  $q(t)$ . At  $x = \pm h/2$  and the middle of the panel ( $x = a/2$ ,  $y = b/2$ ),  $\tau_{xy} = 0$  and the principal stress is the larger of  $\sigma_x$  and  $\sigma_y$ . Then, the principal stress  $S(t)$  can be related to  $q(t)$  as

$$S(t) = Aq(t) \quad (100)$$

where

$$A = \frac{Eh}{2(1-\nu^2)} [(\pi/a)^2 + \nu(\pi/b)^2] \quad \sigma_x > \sigma_y$$

$$A = \frac{Eh}{2(1-\nu^2)} [(\pi/b)^2 + \nu(\pi/a)^2] \quad \sigma_y > \sigma_x \quad (101)$$

It should be noted that Equation 100 is a crude linear approximation to relate stress and nonlinear displacement. Then, Equation 96 can be written as

$$\ddot{S} + 2\zeta_0\omega_{11}\dot{S} + \omega_{11}^2[S + \epsilon S^3] = W(t) \quad (102)$$

where  $W(t)$  is assumed to be a Gaussian white noise in which

$$W(t) = \frac{16A}{m_p\pi^2}p(t) \quad \text{and} \quad \epsilon = \frac{\gamma}{A^2} \quad (103)$$

The approximate solution for probability density of peak magnitude was obtained in Reference 43

$$P_I(S) = \frac{2\xi_0\omega_{11}^3}{\pi k} (S + \epsilon S^3) e^{\left\{ -\frac{2\xi_0\omega_{11}^3}{\pi k} [S^2/2 + \epsilon S^4/4] \right\}} \quad (104)$$

and

$$k = \left( \frac{16A}{m_p \pi^2} \right)^2 S_w \quad (105)$$

where  $S_w$  is the spectral density level of the Gaussian white noise approximation. Since the standard deviation of linear stress response is

$$\sigma_s = [\pi k / (2\xi_0\omega_{11}^3)]^{\frac{1}{2}} = \frac{16A}{m_p \pi^2} \left[ \frac{S_w \pi}{2\xi_0\omega_{11}^3} \right]^{\frac{1}{2}}, \quad (106)$$

Equation 104 can be written as

$$P_I(S) = \frac{1}{\sigma_s^2} (S + \epsilon S^3) e^{\left\{ -\frac{S^2}{2\sigma_s^2} - \epsilon \frac{S^4}{2\sigma_s^2} \right\}} \quad 0 \leq S < \infty \quad (107)$$

Substituting Equation 107 into Equation 80, the expected damage for the simplified nonlinear system can be determined from

$$E[D(\tau)] = \frac{E[M_T]\tau}{B\sigma_s^2} \int_0^\infty (S^{\lambda+1} + \epsilon S^{\lambda+3}) e^{\left\{ -\frac{S^2}{2\sigma_s^2} - \epsilon \frac{S^4}{2\sigma_s^2} \right\}} dS \quad (108)$$

The expected number of total peaks per unit time for a narrow band approximation can be computed from (Reference 43)

$$E[M_T] \approx C\omega_{11}^2 \sigma_s^2 \quad (109)$$



where the constant  $C$  can be evaluated from the normalization condition

$$\int_{-\infty}^{\infty} \int_{-\infty}^{\infty} P_{ss}(s, \dot{s}) ds d\dot{s} = 1 \quad (110)$$

where  $P_{ss}$  is the joint density function of the nonlinear stress  $s$  and stress velocity  $\dot{s}$

$$P_{ss}(s, \dot{s}) = Ce^{\left\{ -\frac{1}{\sigma_s^2 \omega_{11}^2} \left[ \frac{\dot{s}^2}{2} + \omega_{11}^2 \left( \frac{s^2}{2} + \frac{\epsilon s^4}{4} \right) \right] \right\}} \quad (111)$$

Substituting Equation 111 into Equation 110 and integrating (Reference 43)

$$C = \frac{\sqrt{\epsilon}}{\sqrt{\pi} \sigma_s \omega_{11}} e^{\left[ -\frac{1}{(\sigma_s \omega_{11})^2} \right] / K_{\frac{1}{4}} \left( \frac{1}{\sigma_s \omega_{11}^2} \right)} \quad (112)$$

where  $K_{\nu}$  is Bessel's function of the second kind with imaginary arguments. To the first order in  $\epsilon$ , the equation can be approximated as

$$C \approx \frac{1}{2\pi \omega_{11} \sigma_s^2} / \left( 1 - \epsilon \frac{3}{4} \sigma_s^2 \right) \quad (113)$$

Thus,

$$E[M_T] \approx \frac{\omega_{11}}{2\pi \left( 1 - \epsilon \frac{3}{4} \sigma_s^2 \right)} \quad (114)$$

For linear response  $\epsilon=0$ , and  $E[M_T] = E[N.(0)] = \omega_{11}/2\pi$ .

To evaluate the expected damage from Equation 108, numerical integration procedures can be utilized. The Equations 108 and 109 correspond to nonlinear deflections of the panel with linear stress-strain relationships assumed. If the stress-strain relationship is nonlinear such as

$$S = D_1 x + \sum_{n=2} D_n x^n, \quad (115)$$

where  $D_n$  are proportionality constants, difficulties would arise in obtaining the joint density function  $P_{..}$  and the peak density function  $P_I(s)$ . For  $n=2$ , closed form solutions were obtained for  $P_{..}$ ,  $E[M_T]$  and  $P_I(s)$  in Reference 43.

The procedure presented in this section can be applied to estimate the fatigue life of simple narrow band single-degree-of-freedom systems. The linear and the nonlinear response of surface protection systems to exhaust noise and supersonic-hypersonic turbulent flow will be composed of many modes, and simplified models presented could lead to erroneous fatigue life estimates. However, these procedures could serve as useful guidelines for the more realistic fatigue life estimates of multimodal nonlinear systems.

### 3. Nonlinear Stress Response

For a nonlinear random stress response, the amplitude distribution is non-Gaussian. Furthermore, the spectral density of stress response exhibits a wide band characteristic indicating that a large number of modes could be contributing to the response process. An improved damage model for nonlinear stress can be constructed by computing the histograms of stress peak distribution directly from stress response time histories and then using Equation 80 to predict fatigue damage. The total number of peaks per unit time  $E[M_T]$  also can be evaluated numerically.

ically from the response time history. Such a procedure has been used in References 38-42 to determine fatigue life of stiffened titanium panels at room and elevated temperatures.

The histograms of peak distribution and the total number of peaks could account for the stress overloads, pressurization loads, persistent stress reversals due to snap-through, oil canning, etc. However, the fatigue relationship given in Equation 76 corresponds to either a constant amplitude stress or a root-mean-square stress of a stationary process. Furthermore, the linear damage superposition from Equation 77 might not be valid for the severe loading conditions to be encountered by the surface protection systems. For metal materials and low cycle fatigue, significant improvements have been made in predicting the life of a structure by utilizing fracture mechanics and time domain stress solutions (Reference 46). However, for high cycle fatigue, the crack propagation stage might be relatively short as compared to crack initiation, and the time domain crack growth solution might not be meaningful in assessing the life of a structure. Additionally, for composite materials no reliable theory seems to exist for predicting crack growth as a function of random stress response.

#### **E. COMPUTER PROGRAM DESCRIPTION**

The primary objective of this research has been to demonstrate that the use of a Monte Carlo simulation of a random process can be integrated into dynamical equations of motion to produce a time domain response predictive approach to understanding the fatigue of panels exposed to acoustic and sonic noise. The theoretical equations of the time domain approach presented in Section II C. 1. have been programmed using FORTRAN, and the resulting computational procedure is called TDR (Time Domain Response). In this section, a brief explanation of TDR will be presented. Appendix A of this report contains a FORTRAN listing.

TDR is written to handle the time domain response analysis of a simply supported rectangular panel subjected to uniform random pressure. Once TDR has been successfully executed, an output file (FOR001.DAT) is created which contains the time response history of displacements and stresses. That file becomes input to another program, PDF, which calculates the probability density functions of displacement and stresses and up-crossing rates. A schematic of these programs and their relationship to each other is provided in Figure 2. The files created by PDF can be read by various graphical display devices to produce plots of statistical quantities of interest. The fatigue life of a panel is computed with the computer program DAMAGE1 which uses as input the output file FOR008.DAT from PDF.

### III

#### RESULTS

Earlier sections of this report have discussed noise sources, their interaction with structure, especially light-weight panels, and methods for determining structural response under acoustic and sonic noise inputs. The primary objective of the present research is to use Monte Carlo simulation techniques to model random noise in such a manner that the response of a panel can be examined in the time domain. The validity of the time domain approach is verified by comparison to existing methods and/or experimental data. In the present research the lack of experimental data necessitates the former manner of verification.

Since existing methods of sonic fatigue prediction rely upon linear strain-displacement relations, the theoretical derivations in the time domain presented earlier were reduced to equivalent linear analysis. The results from the linearized time domain method is then directly comparable to the power spectral density approach. The results of that comparison are provided in Section III A. which is concerned with isotropic plates.

A significant advantage of the time domain method presented herein is that it can be extended to the regions involving both nonlinear kinematic and nonlinear material behavior. For purposes of this research, nonlinear kinematic relations were used to model the strain-displacement behavior of the flat panel. The nonlinear strain-displacement relations allow the modeling of inplane stretching in the panel--a phenomenon which is extremely critical to the prediction of fatigue in panels exposed to high levels of acoustic noise. Demonstrations of the importance of this modeling assumption are provided for both isotropic and orthotropic composite panels in the sections to follow.

The extension of the isotropic derivations to the composite idealization is important and underscores the versatility and adaptability of the time domain method. While not addressed in this research, the role of transverse shear and material nonlinearity in the matrix material is an important behavior which will be examined in future Phase II work.

The results presented herein are comprised of time response histories of displacement and stress, probability density and peak distribution histograms, up-crossing rates, and predictions of sonic fatigue life for both isotropic and orthotropic composite panels.

#### A. COMPARISONS BETWEEN THE TIME DOMAIN AND POWER SPECTRAL DENSITY METHODS (ISOTROPIC PLATES)

As an example of the veracity of the time domain approach, the nonlinear response and fatigue life of a simply supported panel made from 6Al-4V titanium material is predicted. The panel shown in Figure 1 is assumed to be exposed to a uniformly distributed stationary Gaussian random pressure for which the truncated spectral density is given in Equation 18. All the analyses presented here are obtained for lower and upper cut-off frequencies of 0 Hz and 500 Hz, respectively. The selected frequency bandwidth was  $\Delta\omega = 2\pi$  rad/sec (1 cycle/sec) with the input levels of the random pressure prescribed in decibels. For example, a uniformly distributed white noise spectral density of 140 dB over a frequency range 0-500 Hz corresponds to an overall sound pressure level of 167 dB. If the upper cut-off frequency is increased to 1,000 Hz, the overall sound pressure level would increase to 170 dB.

The random input pressure  $p(t)$  was simulated from Equation 11 with  $M_s = 4,096$ ,  $N_s = 512$ , and  $\Delta t = 0.00025$  second. Thus, the length of the simulated process is  $0.00025 \text{ second} \times 4,096 = 1.024$  second. The fundamental frequency of the metallic panel selected for this study is about 100 Hz and the fundamental period is 0.01 second. Thus, the simulated process covers about 102 natural

periods of the panel. It has been shown in previous studies, that for a stationary response, reasonable statistical properties can be obtained from a time history which extends for about 100 natural periods of the structure.

The numerical results were obtained for a panel with the following geometric and material properties:  $a = 20$  inches,  $b = 8.2$  inches,  $h = 0.06$  inches,  $E = 16.0 \times 10^6$  psi,  $\nu = 0.34$ ,  $m_p = \rho_p h$ ,  $\rho_p = 0.000414$  lb<sub>f</sub>-sec<sup>2</sup>/in<sup>4</sup>. The modal damping coefficients were obtained from Equation 41 with  $\gamma = 1$  and  $\xi_0 = 0.02$ . The numerical calculations were obtained for three modes in the  $x$  direction ( $m=1,2,3$ ) and one mode in the  $y$  direction ( $n=1$ ). It should be noted that for a uniform input pressure distribution only the odd modes contribute to panel response. The modal frequencies of the simply supported panel are  $\omega_{11} = 620$  rad/sec (98.7 Hz) and  $\omega_{21} = 1,333$  rad/sec (212.2 Hz).

When the panel response is calculated in time domain, the spectral densities of displacement or stress process  $Z(x^*, y^*, t)$ , where  $x^*$  and  $y^*$  are the selected spatial points on the panel, can be obtained utilizing the Fast Fourier Transform (FFT) technique (Reference 32). The finite transform of  $Z(x^*, y^*, t_n)$  at discrete frequencies  $\omega_k$  can be written as (Reference 32)

$$\bar{Z}(x^*, y^*, \omega_k) = \frac{\bar{Z}(x^*, y^*, T_t)}{\Delta t} = \sum_{n=0}^{M-1} Z(x^*, y^*, t_n) e^{-i2\pi kn/M} \quad (116)$$

$$k = 1, 2, \dots, M$$

in which  $T_t$  is the total duration of the response random process and  $t_n = n\Delta t$  with  $\Delta t$  being the time interval. Then, the FFT numerical estimate of the response spectral density is

$$S_Z(x^*, y^*, \omega_k) = \frac{2\Delta t}{M} |\bar{Z}(x^*, y^*, \omega_k)|^2 \quad (117)$$

The numerical results presented in this section correspond to the center of the panel, i.e.,  $x' = 10$  inches and  $y' = 4.1$  inches. Stresses are calculated at  $z = h/2$  (top surface of the panel).

The displacement response time histories at different levels of input sound pressure are shown in Figures 3 and 4. For an 80 dB (overall = 107 dB) pressure input, panel response is linear and the largest peaks reach about 0.01 inches. At 120 dB and higher levels of input pressure, panel response is nonlinear with peaks reaching about 0.26 inch for 150 dB (overall = 177 dB) input. As can be observed from these results, the character of the random response process changes with the increasing degree of nonlinearity. It should be noted that the mean value of displacement response is zero for the linear and the nonlinear cases.

The  $\sigma_{yy}$  stress response time histories are presented in Figures 5 and 6 for several different levels of input pressure. For the geometric conditions chosen for these numerical examples, the shearing stress  $\tau_{xy} = 0$  and the normal  $\sigma_{xx}$  stress is about one half the value of the  $\sigma_y$  stress. Thus,  $\sigma_{yy}$  is the principal stress.

For an 80 dB sound pressure input, panel response is linear and the time history of stress response is similar to the displacement response. However, as the input levels increase and the panel exhibits nonlinear vibrations, the stress response changes to a wide band process. Furthermore, the mean value is not zero and it increases with the increasing sound pressure input level. The mean values of stress response corresponding to input levels 80 dB, 120 dB, 140 dB, and 150 dB are, respectively, 0.04 psi, 431 psi, 5,418 psi, and 10,080 psi. The mean stress is caused by the inplane stretching of the nonlinear panel.

The nonlinear transformation between stress and displacement (Equations 73,74,75) contains quadratic terms of the displacement component  $w$ . With the increasing degree of nonlinearity, these quadratic terms tend to dominate the stress-displacement transformation process. These effects are clearly evident in Figures



5 and 6. For the sound pressure input of 150 dB (177 dB overall), the stress peaks reach 67,000 psi. It should be noted that even these high stress values are below the yield strength (120,000 psi) of the titanium material.

The root-mean-square (rms) displacement and normal stresses are plotted in Figures 7 and 8 versus the rms of the input pressure. The linear response predictions were obtained by the power spectral density (PSD) and the time domain methods. In the time domain approach, the governing equations of motion and the stress-displacement relationships were reduced to those of a linear problem. However, the simulation of the random input pressure and the solution procedure of the governing linearized equations were identical to that of the nonlinear case. As can be observed from these results, the agreement between the PSD method and the time domain approach is very good. For example, at an input level of 140 dB (167 dB overall) the rms displacements and stresses are:  $w_{rms} = 0.314$  inch, 0.306 inch;  $\sigma_{xx} = 14,300$  psi, 13,900 psi;  $\sigma_{yy} = 26,760$  psi, 26,020 psi (PSD, time domain).

It should be noted that these linear response predictions overestimate the actual nonlinear response by a large amount. This can be seen from the results shown in Figures 7 and 8. For the input levels exceeding about 110 dB (137 dB overall), nonlinear analysis is required for displacement and stress response predictions. This input limit corresponds only for the simply supported 20 inch by 8.2 inch by 0.06 inch titanium panel exposed to uniform random noise pressure. For stiffer panels this limiting input pressure value would increase while for less stiff panels it would decrease.

The response spectral densities for deflection and normal stress  $\sigma_{yy}$  are shown in Figures 9-11. At low input levels (80 dB and 100 dB) where response is linear, distinct peaks can be seen at the modal frequencies of 98.7 Hz and 212.2 Hz. Furthermore, similar characteristics can be seen between the spectral densities of displacement and stress. As the input pressure

increases, the distinct peaks that are characteristic of linear vibrations tend to flatten and shift towards higher frequencies. For an input level of 140 dB, the distinct peaks are no more evident and the response spectra tends to exhibit the characteristics of a wide band random process. In addition, the shape of the displacement and stress spectral densities is different. The spectral densities shown in these figures are the unsmoothed outputs of the FFT of the response time history corresponding to one solution realization.

When the random process possesses wide band characteristics, large fluctuations of the FFT output are typical. To improve the FFT inverse calculations, a larger number of simulated points and smaller time steps should be taken. In addition, the response spectral densities should be calculated for several realizations of the random input pressure. These spectral densities are then averaged to obtain the response spectral density.

Displacement or stress response probability density histograms, peak distributions, total number of peaks per unit time, and threshold crossing rates can be obtained from the response time histories. Figures 12 and 13 show the probability density and peak distribution histograms for the nonlinear displacement response. For comparison, a Gaussian density function is given with each probability density histogram and a Rayleigh distribution with each histogram of peak distribution. As can be observed from these results, the nonlinear response is no longer Gaussian and the peak distribution does not follow the Rayleigh distribution.

Similar results are presented in Figures 14 and 15 for normal stress component  $\sigma_{yy}$ . For the nonlinear stress process, large differences can be seen between the response histograms and the theoretical probability and peak distributions. These large differences are produced by the nonlinear relationship between stress and displacement. Thus, the various approximate theories which predict the nonlinear displacement response but use a

linear stress-displacement relationship to obtain stresses do not give a meaningful procedure to obtain nonlinear stresses for sonic fatigue analysis.

From the results presented in Figures 13 and 15, it can be seen that for a highly nonlinear response the stress process contains a large number of peaks above the  $2\sigma$  ( $\sigma$  = standard deviation) range. However, the histogram of displacement peak distribution does not show any peaks above the  $2.2\sigma$  range. Here the peaks seem to be concentrated at about the  $1.5\sigma$  value. Since fatigue life is very sensitive to the magnitude of stress ranges, erroneous fatigue life predictions will be obtained if the form of the stress peak distribution is assumed to be the same as the displacement peak distribution. In addition, the nonlinear stress process contains a mean value while the mean is zero for a nonlinear displacement response.

The threshold up-crossing rates for the  $\sigma_{yy}$  stress process are given in Figure 16 for several levels of input pressure. For a linear stress response at 80 dB input, the threshold up-crossing rate closely approximates a theoretical Gaussian prediction. As the input pressure increases and stress response becomes more nonlinear, the up-crossing rates increase.

The expected fatigue damage has been predicted utilizing Equation 78. The expected total number of peaks  $E[M_T]$  were estimated directly from the stress response time histories. The values for  $E[M_T]$  are 150, 228, 556, and 748 peaks/second for 120, 130, 140, and 150 dB sound pressure inputs, respectively. The integral in Equation 78 was evaluated numerically. The distribution of stress peaks  $P_i(s)$  is the histogram of the peak distribution corresponding to the principal stress  $\sigma_{yy}$  (Figures 14 and 15).

To illustrate the fatigue damage estimation procedure, typical parameters were chosen from experimental data for the titanium material under room temperature. These parameters correspond to tests at constant stress amplitude and stress ratio  $R = -1$ . The stress ratio  $R$  is defined as  $R = \sigma_{min} / \sigma_{max}$  in which  $\sigma_{min}$

is the minimum stress and  $\sigma_{\max}$  is the maximum stress. A stress ratio  $R = -1$  corresponds to a zero mean value. The experimental parameters chosen in this study are  $\lambda = 6.0$  and  $B = 1.518 \times 10^6$ . When using these parameters, the stress amplitude is in units of ksi. To account for stress concentrations, size effects, and manufacturing imperfections, a fatigue reduction factor  $K_f$  should be introduced. However, for the simple panel chosen in this study no fatigue reduction factor was introduced.

The expected fatigue damage is plotted in Figure 17 versus the product of  $E[M_T]\tau$ . A value of  $E[D(\tau)] = 0.1$  corresponds to 10 percent damage and  $E[D(\tau)] = 1$  a 100 percent damage or total failure of the structure. By selecting  $E[D(\tau)] = 1$  and the calculated value of the total number of peaks  $E[M_T]$ , the time to failure can be obtained from Figure 17. These results are given in Table 2.

TABLE 2  
STANDARD DEVIATION OF  $\sigma_{yy}$  STRESS,  
EXPECTED NUMBER OF PEAKS AND FATIGUE LIFE

Input Sound Pressure, dB	Number of Peaks/Second		Standard Deviation, psi		Fatigue Life, Hours	
	Linear	Nonlinear	Linear	Nonlinear	Linear	Nonlinear
120 (147)	124	150	2,676	2,298	$2.39 \times 10^6$	938,888
130 (157)	124	228	8,462	3,697	2,393	15,578
140 (167)	124	556	26,760	9,260	2.393	18.7
150 (177)	124	748	84,622	14,100	---	1.0

( ) = Overall levels

When the stress response analysis is performed using a linear plate theory, the stresses can be calculated by the PSD method and the expected fatigue damage estimated from Equation 86. The results based on linear theory are also presented in Table 2. These results indicate that for input levels above 120 dB (147 dB overall) the linear theory over estimates stress and under esti-

mates fatigue life of surface panels. For sound pressure inputs of 120 dB or lower, the titanium panel would not fail by fatigue. The fatigue life estimates presented in this report should be viewed as preliminary merely to illustrate the procedure of the time domain analysis.

#### **B. PREDICTION OF RESPONSE IN ORTHOTROPIC COMPOSITE PANELS USING THE TIME DOMAIN METHOD**

In this section, representative examples of the predictive capabilities of the time domain approach for application to orthotropic panels is presented. For the most part, the examples provided are analogous to those shown for the isotropic panel of Section III A. However, examples showing the effects of variation in lay-up angle have been included to demonstrate the design/analysis capabilities of the time domain approach.

A subtle but important distinction between an orthotropic and laminated composite material should be noted; namely, for purposes of this Phase I research, the orthotropic derivation implicitly assumes that the entire plate is composed of a single material possessing orthotropic properties, as contrasted to a laminated panel wherein orthotropic properties generally vary throughout the thickness. This assumption presents no problem with respect to the calculation of displacement response time histories and statistics since the constitutive properties of the chosen orthotropic material ( $A_{11}$ ,  $A_{12}$ ,  $A_{22}$ ,  $A_{66}$ ,  $D_{11}$ ,  $D_{12}$ ,  $D_{22}$ , and  $D_{66}$ ) have been obtained from the equations used to obtain constitutive properties of a laminated composite structure.

Derivation of stresses within an orthotropic or laminated composite panel are different, however. An orthotropic material has a membrane stress field which is constant through the thickness. The bending stresses vary linearly through the thickness with the stress being zero at the location of the neutral axis. Thus, for an orthotropic material, the total stress is simply a function of the through-thickness coordinate of the panel. For a laminated composite material, the stress is a function of the

material properties of the particular lamina. Since, in general, lamina lay-up angles vary throughout the thickness, a laminated composite requires stress-displacement relations which depend both upon the through-thickness location of the lamina and the constitutive properties of the lamina.

Figure 18 shows an example of the stress and strain distribution through the thickness of a laminated composite. Note that the membrane strain field is constant in value and the bending strains vary linearly with through-thickness position. The stresses vary according to the lamina constitutive properties and are neither constant nor linear. The stress distribution for an orthotropic material would be similar to the strain distributions shown in Figure 18, i.e., membrane stress is constant and the bending stress is linear through the thickness.

For this research, the simpler orthotropic stress-displacement relations have been used inasmuch as demonstration of the feasibility of the time domain approach was the primary objective. During Phase II the relations for a laminated composite material will be implemented.

The panel shown in Figure 1 represented the basic configuration used for the orthotropic analysis shown herein. As before, the lower and upper cut-off frequencies are 0 and 500 Hz, respectively. The duration of the simulated process is 1.024 sec. The first laminated composite example is composed of the lay-up  $[0/+45/-45/90]$ , for a total of eight layers and an overall thickness of 0.0416 inches. Each layer is made from A-S/3501 Graphite/Epoxy. The basic lamina constitutive properties are obtained from the 0-degree lamina elastic properties, i.e.,

$$E_1 = 18.6E+06$$

$$E_2 = 2.0E+06$$

$$G_{12} = 0.8E+06$$

$$\nu_{12} = 0.31$$

The numerical results were obtained for a panel with overall dimensions of  $a = 20.0$  inches,  $b = 8.2$  inches,  $\rho_p = 0.0001302$  lb<sub>f</sub>-sec<sup>2</sup>/in<sup>4</sup>. The material damping factor was  $\zeta_o = 0.05$ . The calculated modal frequencies were

$$f_{11} = 133 \text{ cycles/sec}$$

$$f_{12} = 466 \text{ cycles/sec}$$

$$f_{13} = 1,021 \text{ cycles/sec}$$

$$f_{21} = 200 \text{ cycles/sec}$$

$$f_{22} = 533 \text{ cycles/sec}$$

$$f_{23} = 1,088 \text{ cycles/sec}$$

$$f_{31} = 313 \text{ cycles/sec}$$

$$f_{32} = 644 \text{ cycles/sec}$$

$$f_{33} = 1,199 \text{ cycles/sec}$$

As an example of the importance of the assumption of linearity or nonlinearity with respect to the strain-displacement relations, Figures 19 and 20 show the effect of the two assumptions. Figure 19, the linear response, shows a maximum displacement of almost 4 inches, whereas the nonlinear response provides only 0.3 inches approximately. The difference is dramatic with the nonlinear response obviously the more realistic.

In the response histories shown, the limitations in the graphical display device allowed only 240 discrete points of displacement and time to be plotted. Thus, a separate program was written to take the time history produced by TDR, containing 4,096 discrete points, and reduce it to the first 240 minimum and maximum points. As a result, the time histories shown appear slightly different than those prepared for the isotropic panel.

In comparing Figures 19 and 20, it is also observed that there are apparently more variations between high and low values for the nonlinear response because 240 points of minimum/maximum appear in just 0.24 seconds for the nonlinear case as contrasted

to about 0.63 seconds for the linear case. The indication that a nonlinear response produces more changes in stress direction could have important implications in the determination of panel fatigue life and is one more reason why the nonlinear assumption is preferred over that of linear.

The time histories of the lateral component of stress,  $\sigma_{yy}$ , for both the linear and nonlinear cases are shown in Figures 21 and 22, respectively. As with the displacement response, the linear prediction provides unrealistic values, whereas the nonlinear assumption results in the calculation of stress values that are comparable to the actual expected response of the panel. Note also that the mean value for the nonlinear assumption is not zero. Clearly, the use of linear strain-displacement relations is not warranted for applications involving high levels of acoustic loading.

Displacement and stress response probability density histograms, peak distributions, total number of peaks per unit time, and threshold crossing rates can be obtained from the response time histories. Figures 23 and 24 show the probability density histograms for two different sound pressure levels (130 and 150 dB) using nonlinear strain-displacement relations. For comparison, a Gaussian density function is given with each probability density histogram. The nonlinear response is no longer Gaussian.

Figures 25 and 26 show the peak distribution histogram for the nonlinear strain-displacement relations compared to a Rayleigh distribution. The nonlinear prediction does not follow the Rayleigh distribution.

Similar histograms of probability density and peak distribution for the lateral stress component,  $\sigma_{yy}$ , are shown in Figures 27-30. As for the isotropic panel, large differences between the response histograms and the theoretical probability and peak distributions can be seen. These large differences are produced by the nonlinear relationship between stress and displacement and are additional confirmation that the assumption of linearity in



strain-displacement relations is not appropriate for the prediction of stress response in panels subject to high levels of acoustic noise.

Figure 31 shows up-crossings per second for  $\sigma_{yy}$  for various levels of sound pressure level. For the lower sound pressure level (i.e., 110 dB) the response is mostly linear; however, for higher levels of input the response is increasingly nonlinear and the up-crossing rate increases markedly.

When the basic lay-up just used is varied slightly, it is possible to alter the response of the panel. As an example, Figure 32 shows the  $\sigma_{yy}$  RMS response of the panel for 150 dB input when the lay-up angle of the interior plies are varied from 0 through 90 degrees. At approximately 30 degrees the RMS response is at a minimum. Figure 33 shows how the up-crossing rate varies with lay-up angle--apparently, the up-crossing rate is not strongly dependent on the lay-up angle for this particular laminated composite example.

As a final example of the usage of the time domain approach, another laminate construction is examined. Figures 34 and 35 show the up-crossing rate for stress components  $\sigma_{xx}$  and  $\sigma_{yy}$  for a  $[+\theta/-\theta]_{x2}$  laminate. The effect of lay-up angle on response is of importance in these examples. A designer, knowing that the lay-up angle would have an effect on panel response, could potentially alter the design in such a manner that the RMS stresses and up-crossing rates would be reduced and fatigue life increased.

Figure 35 shows the RMS stresses for fiber directed and transverse stresses as a function of the lay-up angle. The fiber direction stresses are relatively low in this example, approximately 15,000 psi, when compared to a nominal allowable of 180,000 psi. However, in the transverse to fiber direction the stress level peaks at about 6,300 psi, which is very close to the static stress allowable for the matrix material. In an actual

design situation, the panel would need sizing to ensure that the anticipated stress level is below the allowable fatigue stress level for the matrix material.

Prediction of fatigue life in composite materials is not possible at this time because of limitations in the theoretical understanding of fatigue in composites and the lack of material property data. As a consequence, predictions of sonic fatigue life for a composite panel have not been produced. However, the statistical approach documented for metal panels and the techniques used to produce predictions based on time domain response analysis are valid and can be utilized when polymer-based composite technology advances. Phase II work will develop the time domain response methods for laminated composite materials to the maximum extent possible. Also, Phase II work will concentrate on the appropriate theoretical relationship to be used to predict composite fatigue. The ability to predict acoustically generated stresses combined with an approach for predicting fatigue of composite materials will allow an analyst the ability to use the time domain approach to predict the sonic fatigue life of structural panels.

## IV

### CONCLUSIONS

A simple rectangular panel was selected to demonstrate the applicability of time domain analysis to predict nonlinear response and fatigue life of metal and composite panels. It is shown that the linear theory overestimates deflection and stress response by a large amount, resulting in a predicted shorter fatigue life. If one were to use linear theory as a design tool, then properly designed panels would be relatively stiffer and heavier than required. A non-optimal, weight-inefficient structure would result.

The nonlinear response, as predicted by the Monte Carlo time domain approach, is non-Gaussian and peaks do not follow a Rayleigh distribution. With a nonlinear relationship between stress and displacement, both the probability density function and the peak distribution of displacement response process are significantly different from those of the linear stress response.

The number of stress peaks per unit time and the up-crossing rates increase with the increase of input sound pressure levels as would be expected; however, the nonlinear stress response has a mean value while the mean value for the nonlinear displacement response is zero.

The spectral densities of the nonlinear response show a widening of response peaks and a shift towards higher frequencies as the input levels increase and the nonlinearity effects become more dominant.

The time domain analysis presented in this study indicates that for anticipated sound pressure levels acting on present and future aircraft structures, the various simplified linear theories used to predict stress response and fatigue life would not produce realistic structural panel configurations. The rather dramatic differences between linear and nonlinear predictions is significant and, thus, is a reminder that structures exposed to acoustic noise must be carefully designed.

## REFERENCES

1. Jacobson, M. J., "Advanced Composite Joints: Design and Acoustic Fatigue Characteristics," AFFDL-TR-71-126, Air Force Flight Dynamics Laboratory, Wright-Patterson Air Force Base, Ohio, 1972.
2. Holehouse, I., "Sonic Fatigue Design Techniques for Advanced Composite Aircraft Structures," AFWAL-TR-80-3019, Air Force Wright Aeronautical Laboratories, Wright-Patterson Air Force Base, Ohio, April 1980.
3. Soovere, J., "Effect of Acoustic, Thermal and Shear Loading on Flat Integrally Stiffened Graphite/Epoxy Fuselage Panels," NADC-78169-60, 1982.
4. Soovere, J., "Dynamic Response and Acoustic Fatigue of Stiffened Composite Structures," The Second International Conference on Recent Advances in Structural Dynamics, Southampton, England, 1984.
5. Rudder, F. F., Jr. and Plumblee, H. E., Jr., "Sonic Fatigue Design Guide for Military Aircraft," AFFDL-TR-74-112, Air Force Flight Dynamics Laboratory, Wright-Patterson Air Force Base, Ohio, May 1975.
6. Powell, A., "On the Fatigue Failure of Structures due to Vibration Excited by Random Pressure Fields," *Journal of the Acoustic Society of America*, Vol. 30, 1958, pp. 1130-1135.
7. Maestrello, L., "Radiation from and Panel Response to a Supersonic Turbulent Boundary Layer," *Journal of Sound and Vibration*, Vol. 10, No. 2, 1969, pp. 261-295.
8. Jacobson, M. J. and Maurer, O. F., "Oil Canning of Metallic Panels in Thermal-Acoustic Environments," AIAA 6th Aircraft Design, Flight Test and Operation Meeting, AIAA Paper No. 74-982, Los Angeles, California, August 12-14, 1974.
9. Coe, C. F. and Chyu, W. J., "Pressure Fluctuation Inputs and Response of Panels Underlying Attached and Separated Supersonic Turbulent Boundary Layers," NASA TM X-62, 189, 1972.
10. Dowell, E. H., "Transmission of Noise from a Turbulent Boundary Layer Through a Flexible Plate into a Closed Cavity," *Journal of the Acoustic Society of America*, Vol. 46, No. 1, July 1969, pp. 238-252.

11. Vaicaitis, R., Jan, C. M., and Shinozuka, M., "Nonlinear Panel Response and Noise Transmissions from a Turbulent Boundary Layer by Monte Carlo Approach," AIAA Paper No. 72-199, AIAA 10th Aerospace Science Meeting, San Diego, California, January 17-19, 1972.
12. Ng, C. F., "The Influence of Snap-through Motion on the Random Response of Curved Panels to Intense Acoustic Excitation," Proceedings of the Third International Conference on Recent Advances in Structural Dynamics, AFWAL-TR-88-3034, July 1988.
13. Maekawa, F., "On the Sonic Fatigue Life Estimation of Skin Structures at Room and Elevated Temperatures," *Journal of Sound and Vibration*, 80(1), 1982, pp. 41-59.
14. Crandall, S. H. and Zhu, W. Q., "Random Vibration: A Survey of Recent Developments," *Journal of Applied Mechanics*, ASME, Vol. 50, December 1983, pp. 953-962.
15. To, C. W. S., "The Response of Nonlinear Structures to Random Excitation," *The Shock and Vibration Digest*, Vol. 16, No. 4, April 1984, pp. 13-33.
16. Caughey, T. K., "Derivation and Application of the Fokker-Planck Equation to Discrete Nonlinear Dynamic Systems Subjected to White Random Excitation," *Journal of the Acoustical Society of America*, Vol. 35, November 1963, pp. 1683-1692.
17. Iwan, W. D. "Application of Nonlinear Analysis Techniques," *Applied Mechanics in Earthquake Engineering*, Edited by W. D. Iwan, ASME AMD-Vol. 8, 1974, pp. 135-161.
18. Crandall, S. H., "Perturbation Techniques for Random Vibration of Nonlinear Systems," *Journal of the Acoustic Society of America*, Vol. 35, November 1963, pp. 1700-1705.
19. Anand, G. V. and Richard, K., "Nonlinear Response of String to Random Excitation," *International Journal of Nonlinear Mechanics*, Vol. 9, 1974, pp. 251-260.
20. Iwan, W. D. and Yang, I. M., "Statistical Linearization for Nonlinear Structure," *Journal of Engineering Mechanics Division*, ASCE, Vol. 97, No. EM6, 1971, pp. 1609-1623.
21. Spanos, P-T. D., "Formulation of Stochastic Linearization for Symmetric or Asymmetric M. D. O. F. Nonlinear Systems," *Journal of Applied Mechanics*, ASME, Vol. 47, 1980, pp. 209-211.

22. Spanos, P-T. D., "Stochastic Linearization in Structural Dynamics," *Applied Mechanics Review*, Vol. 34, No. 1, January 1981, pp. 1-8.
23. Shinozuka, M., "Monte Carlo Solution of Structural Dynamics," *International Journal of Computers and Structure*, Vol. 2, 192, pp. 855-874.
24. Vaicaitis, R., Dowell, E. H., and Ventres, C. S., "Nonlinear Panel Response by a Monte Carlo Approach," *AIAA Journal*, Vol. 12, No. 5, May 1974, pp. 685-691.
25. Vaicaitis, R., "Nonlinear Panel Response to Non-stationary Wind Forces," *Journal of the Engineering Mechanics Division*, ASCE, Vol. 101, No. 4, August 1975, pp. 333-347.
26. Mixon, J. S. and Roussos, L. A., "Acoustic Fatigue: Overview of Activities at NASA Langley," NASA TM-89143, 1987.
27. Bruhn, E. F., *Analysis and Design of Flight Vehicle Structures*, Tri-State Offset Co., Ohio, 1965.
28. Vaicaitis, R. and Choi, S. T., "Sonic Fatigue and Nonlinear Response of Stiffened Panels," AIAA 12th Aeronautics Conference, San Antonio, Texas, April 10-12, 1989.
29. Cockburn, J. A. and Jolly, A. C., "Structural-Acoustic Response, Noise Transmission Losses and Interior Noise Levels of an Aircraft Fuselage Excited by Random Pressure Fields," AFFDL-TR-68-2, Air Force Flight Dynamics Laboratory, Wright-Patterson Air Force Base, Ohio, August 1968.
30. Ojalvo, I. U., Levy, A., and Austin, F., "Thermal Stress Analysis of Reusable Insulation for Shuttle," NASA CR-132502, 1974.
31. Vaicaitis, R., "Generalized Random Forces for Rectangular Panels," *AIAA Journal*, Vol. 11, No. 7, July 1973, pp. 984-988.
32. Shinozuka, M. (Editor), *Stochastic Mechanics*, Vol. I and II, Dept. of Civil Engineering and Engineering Mechanics, Columbia University, New York, New York, 1987.
33. Ambartsumyan, S. A., *Theory of Anisotropic Plates*, Progress in Materials Science Series, Volume II, J. E. Ashton, Ed., Technomic Publication Co., Inc., Stamford, Connecticut, 1970.
34. Boley, B. A. and Wiener, J. H., *Theory of Thermal Stresses*, John Wiley and Sons, New York, 1966.

35. Bolotin, V. V., *Nonconservative Problems of the Theory of Elastic Stability*, Pergamon Press, Oxford, 1963.
36. Hong, H. K. and Vaicaitis, R., "Nonlinear Response of Double Wall Sandwich Panels," *Journal of Structural Mechanics*, 12(4), (84-85), pp. 483-503.
37. Vaicaitis, R., "Acoustic Fatigue -- A Monte Carlo Approach," AIAA/ASME/ASCE/AHS 28th SDM Conference, Paper No. 87-0916, Monterey, California, April 6-8, 1987.
38. Vaicaitis, R. and Choi, S., "Response of Stiffened Panels for Application to Acoustic Fatigue," AIAA 11th Aeroacoustics Conference, Paper No. 87-2711, Sunnyvale, California, October 19-21, 1987.
39. Vaicaitis, R. and Choi, S., "Acoustic Fatigue of Stiffened Structures," Proceedings of the Third Conference on Recent Advances in Structural Dynamics, Southampton, England, 1988.
40. Vaicaitis, R. and Choi, S. T., "Sonic Fatigue of Stiffened Structures," 29th AIAA/ASME/ASCE/AHS SDM Conference, Williamsburg, Virginia, 1988.
41. Vaicaitis, R. and Choi, S. T., "Acoustic Fatigue of Stiffened Structures," Proceedings of the Third International Conference on Recent Advances in Structural Dynamics, University of Southampton, England, July 18-22, 1988.
42. Vaicaitis, R. and Choi, S. T., "Nonlinear Response and Fatigue of Stiffened Panels," Symposium on Stochastic Structural Dynamics, University of Illinois at Urbana-Champaign, October 30-November 1, 1988.
43. Lin, Y. K., *Probabilistic Theory of Structural Dynamics*, McGraw-Hill, New York, 1967.
44. Miner, M. A., "Cumulative Damage in Fatigue," *Journal of Applied Mechanics*, Transactions of the ASME, Vol. 12, 1945, pp. A159-A164.
45. Nayfeh, A. H. and Mook, T. D., *Nonlinear Oscillations*, John Wiley and Sons, New York, 1979.
46. Shinozuka, M., Vaicaitis, R., Chang, J. B., Engle, B., and Ishikawa, M., "Equivalent Load Spectra for Fatigue Crack Growth Prediction," 1982 Symposium on Reliability of Structures, ASCE, New Orleans, Louisiana.

## **FIGURES**



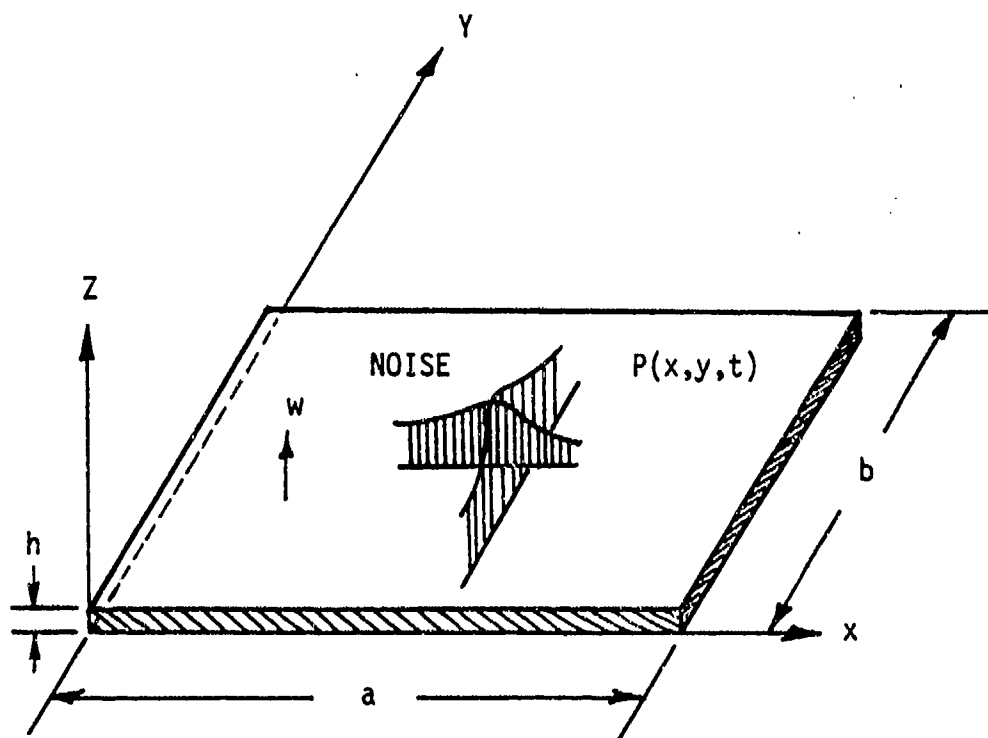


Figure 1 A Rectangular Panel Exposed to Random Pressure

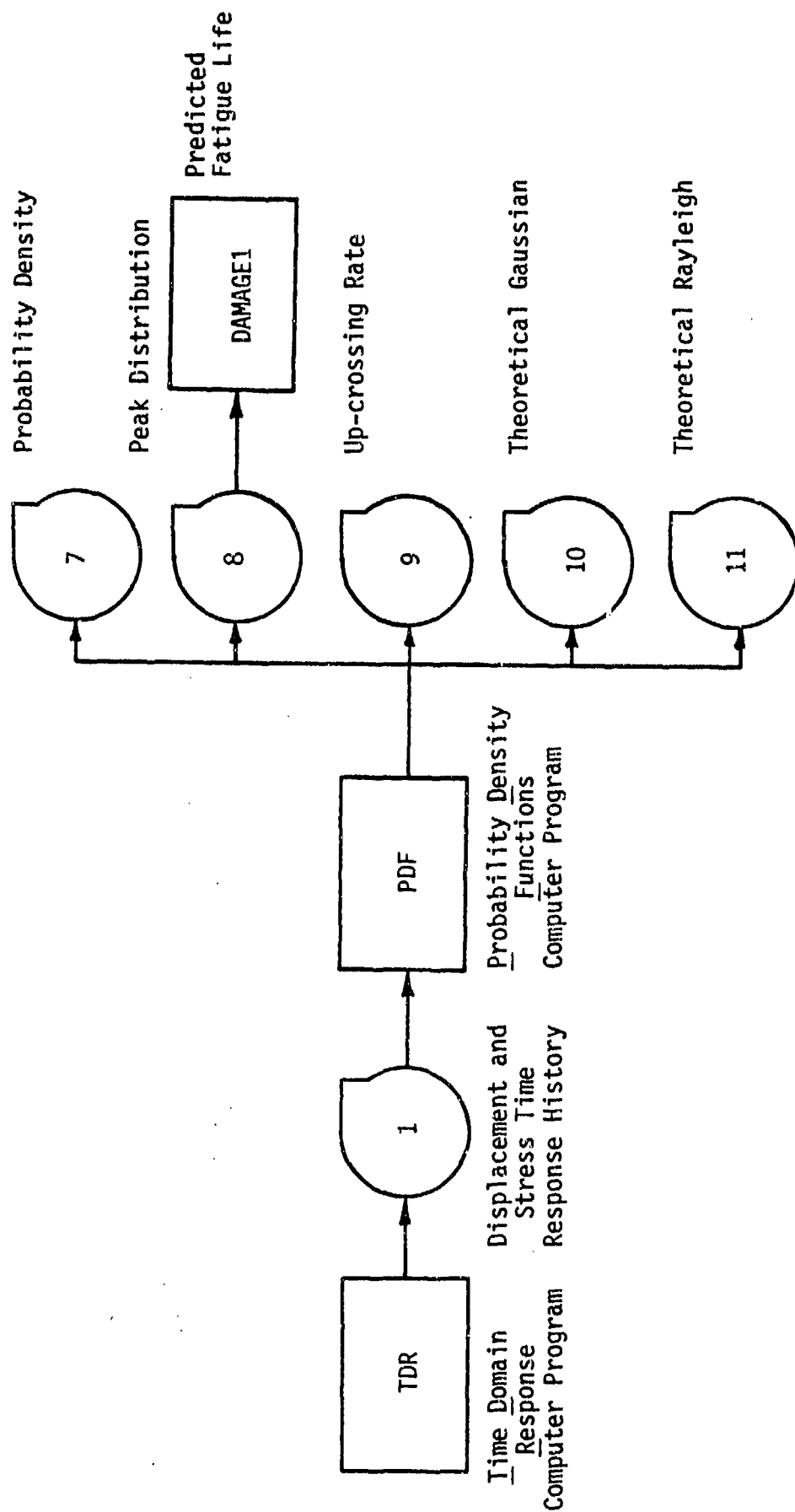


Figure 2 Computer Programs Used to Perform Time Domain Analysis and Predict Fatigue Life

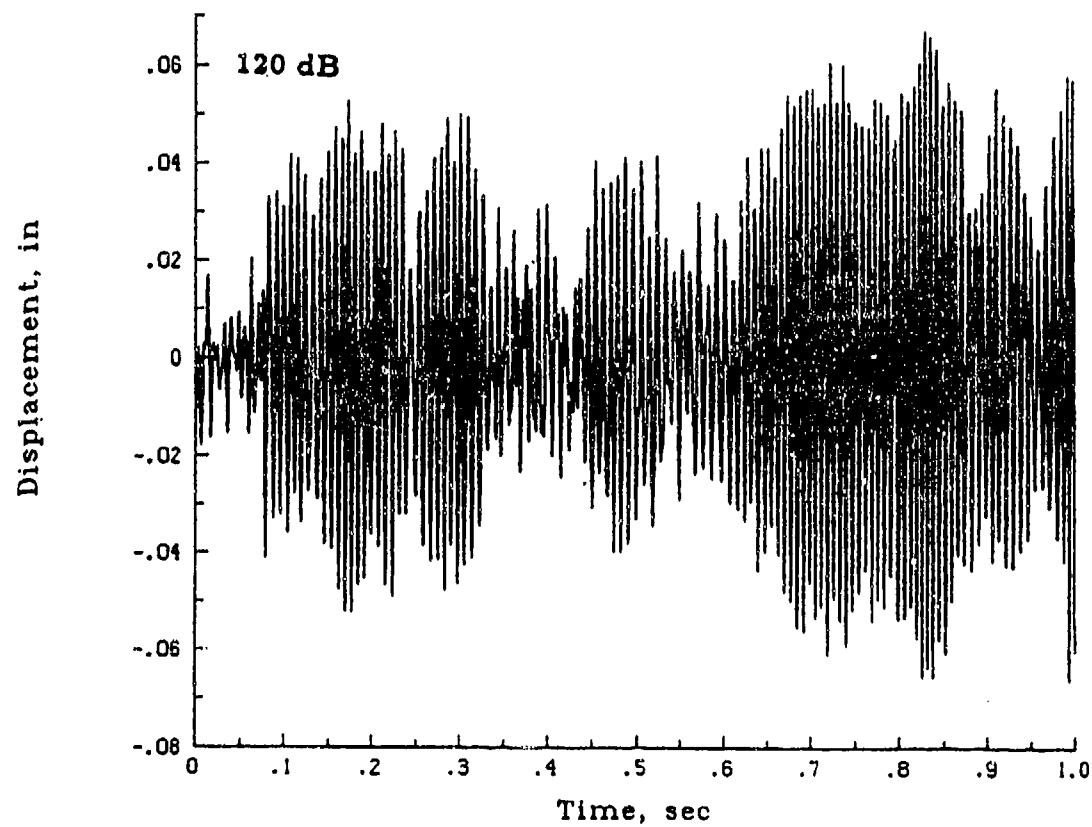
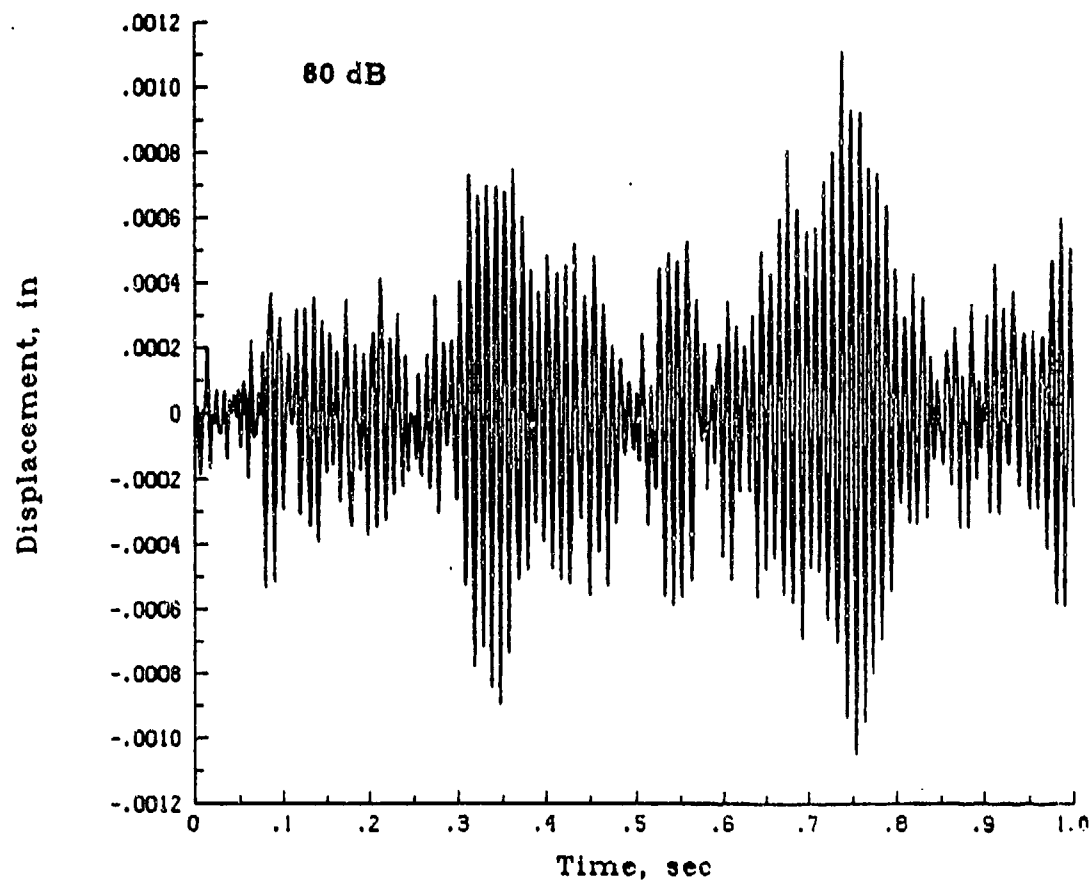


Figure 3 Displacement Response Time Histories for Input Sound Pressure Levels of 80 dB and 120 dB

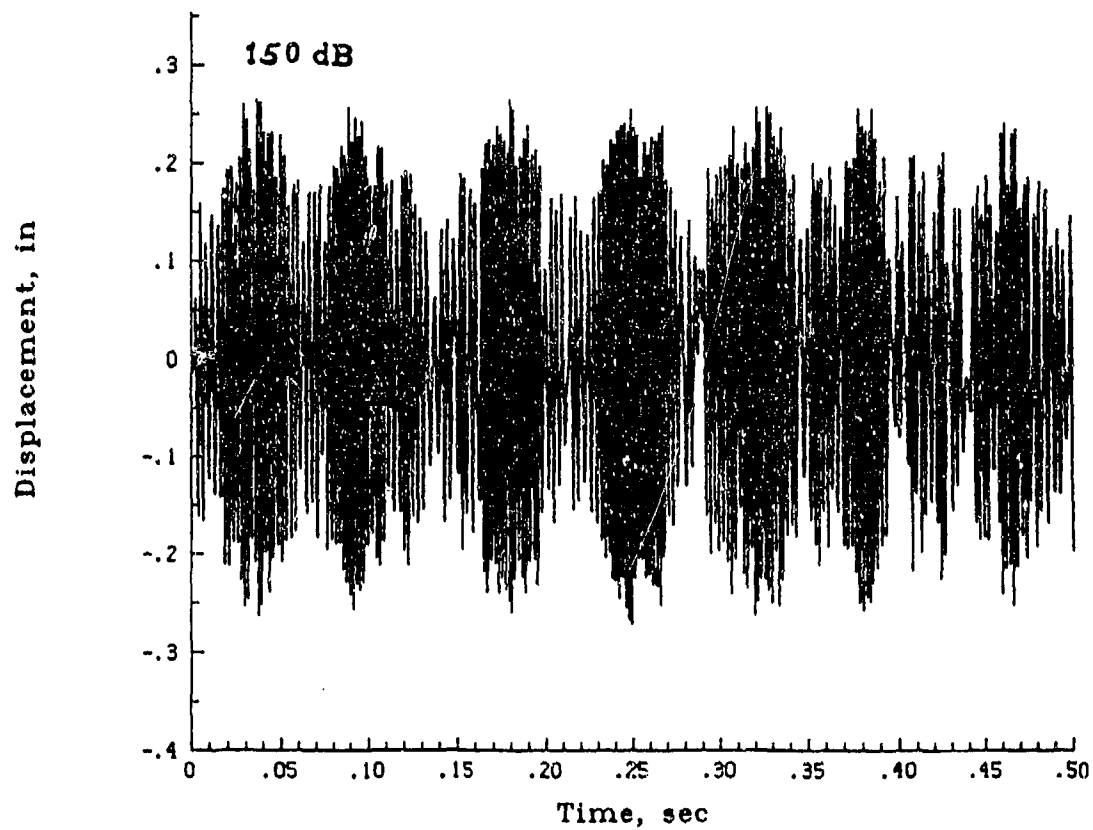
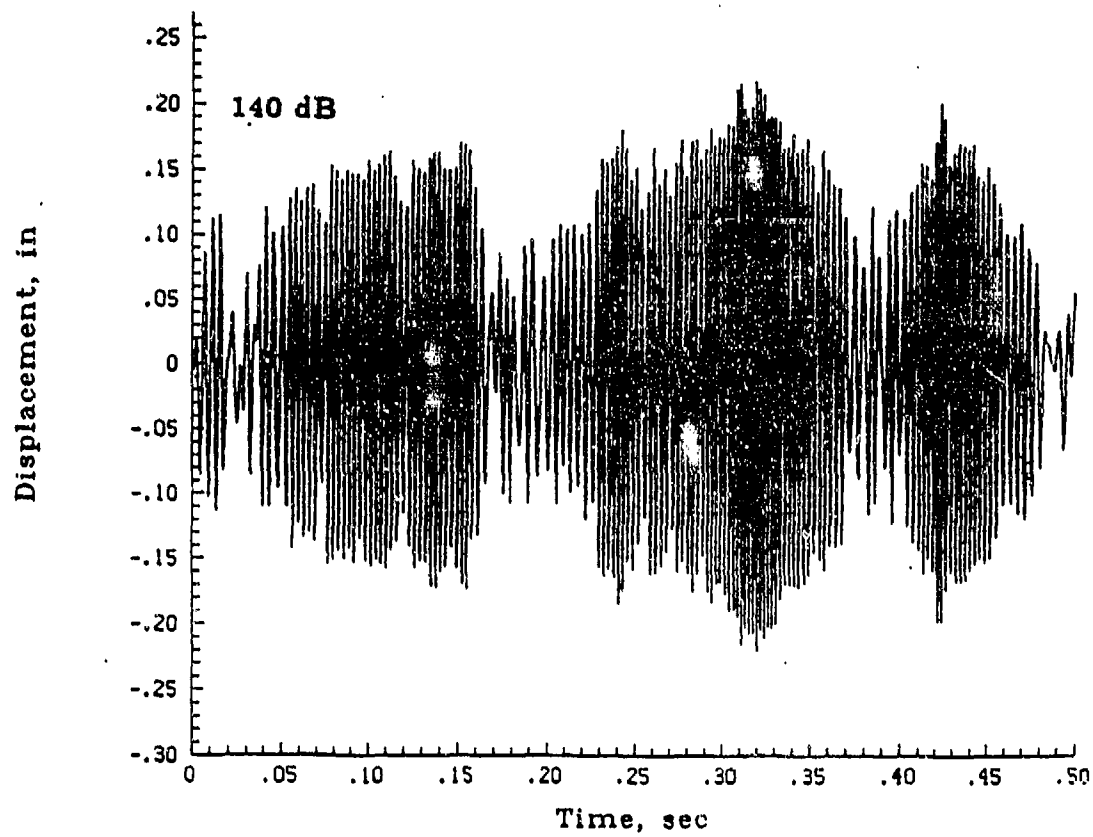


Figure 4 Displacement Response Time Histories for Input Sound Pressure Levels of 140 dB and 150 dB

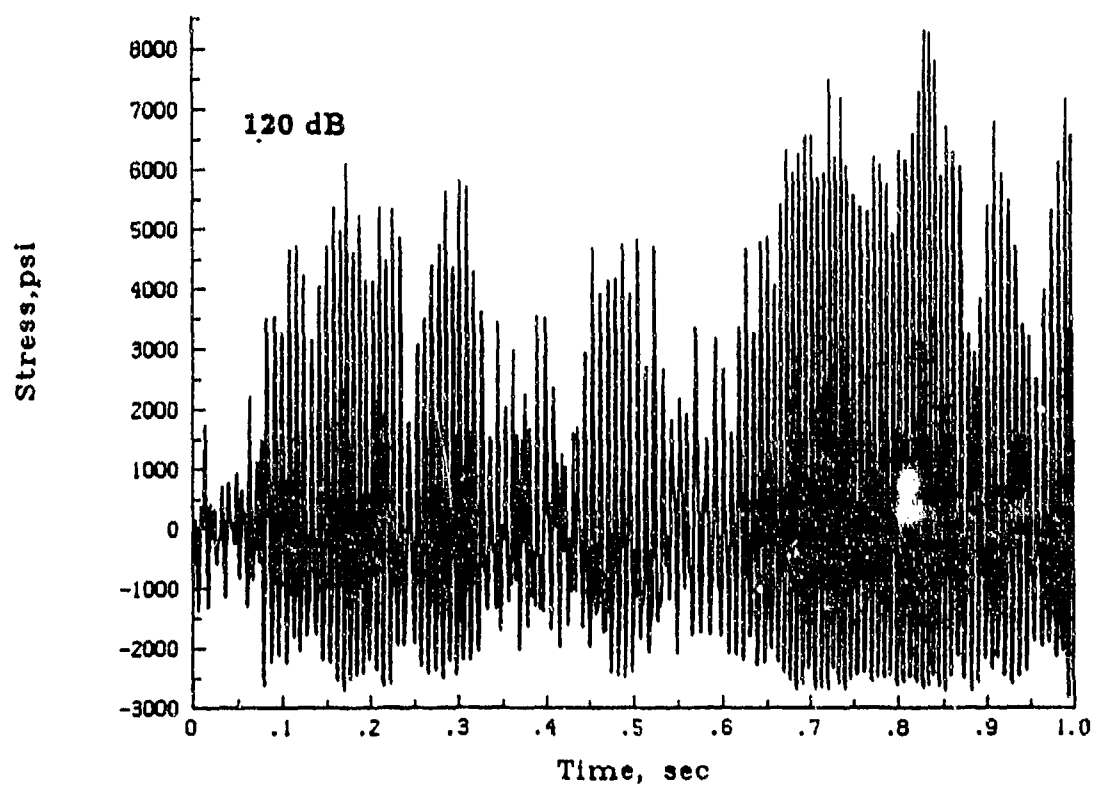
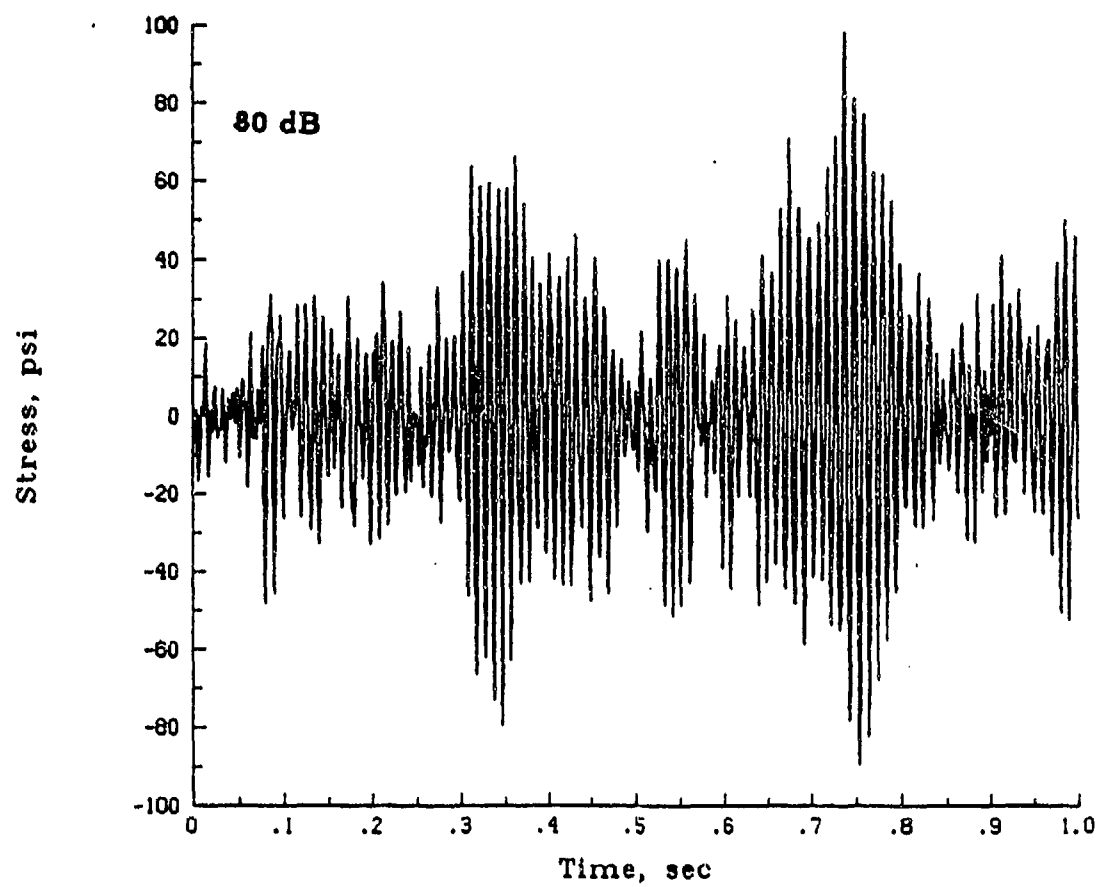


Figure 5 The  $\sigma_y$  Stress Response Time Histories for Input Sound Pressure Levels of 80 dB and 120 dB

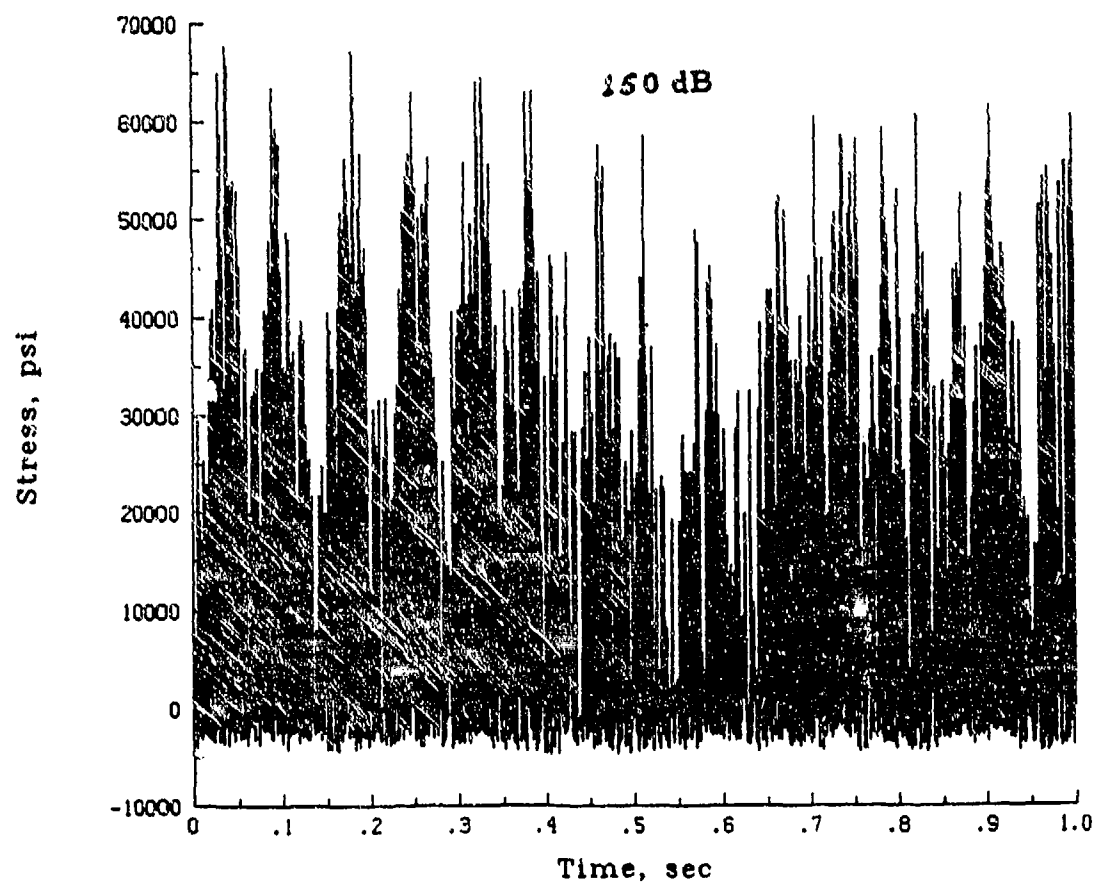
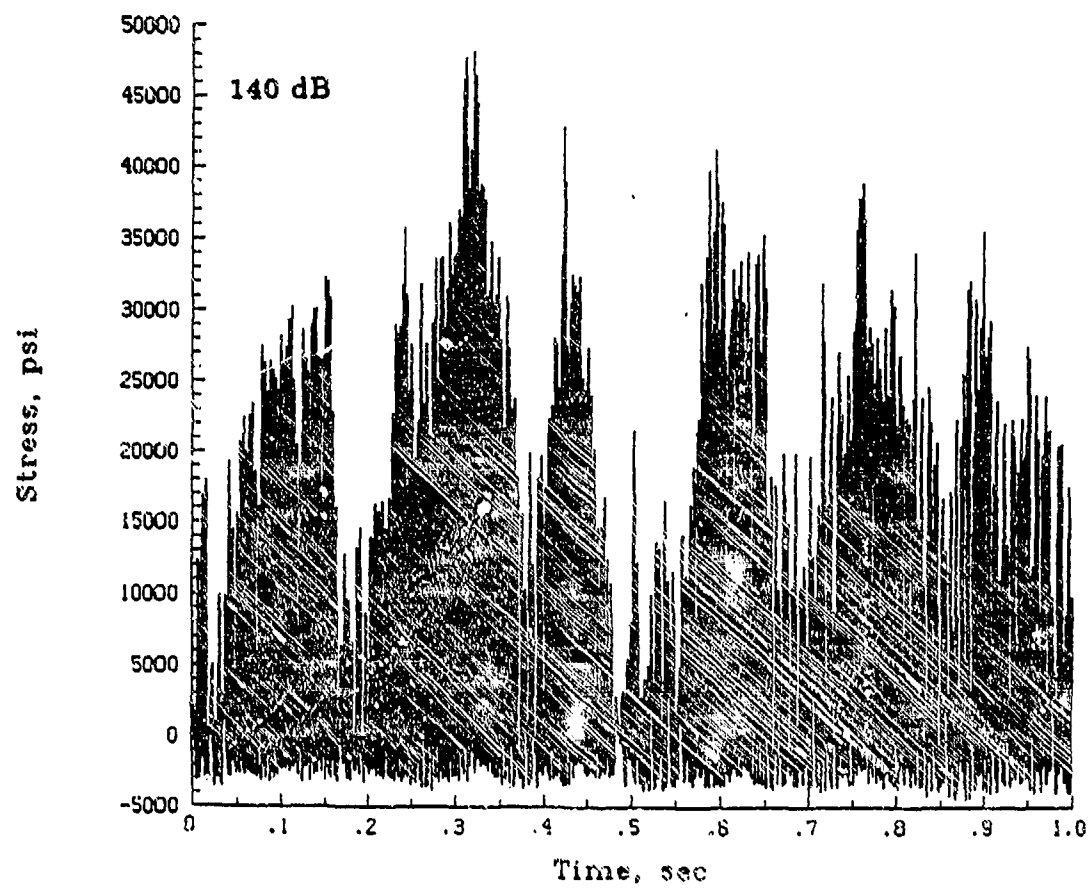


Figure 6 The  $\sigma_y$  Stress Response Time Histories for Input Sound Pressure Levels of 140 dB and 150 dB

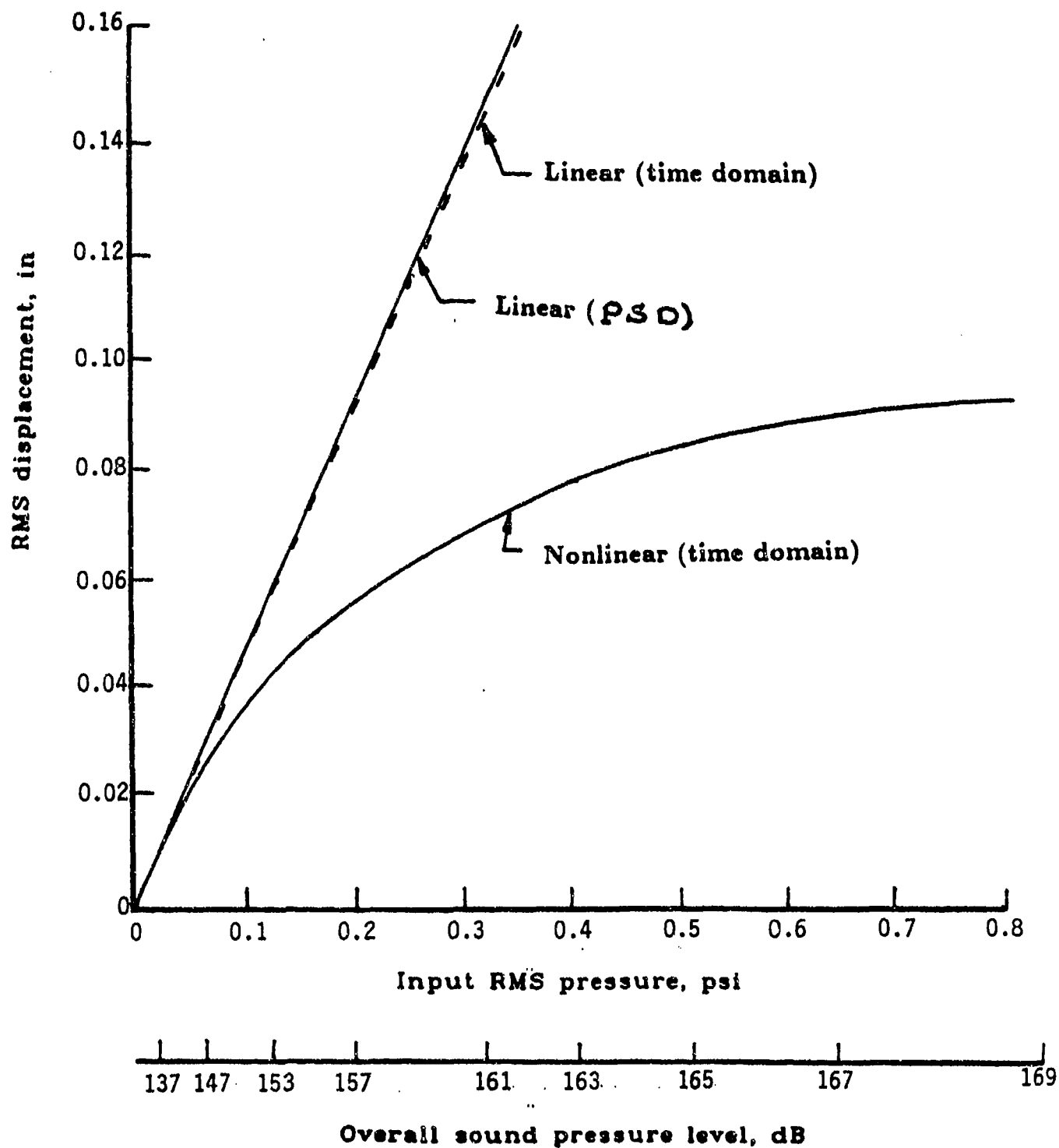


Figure 7 Linear and Nonlinear Root-Mean-Square Displacement Response

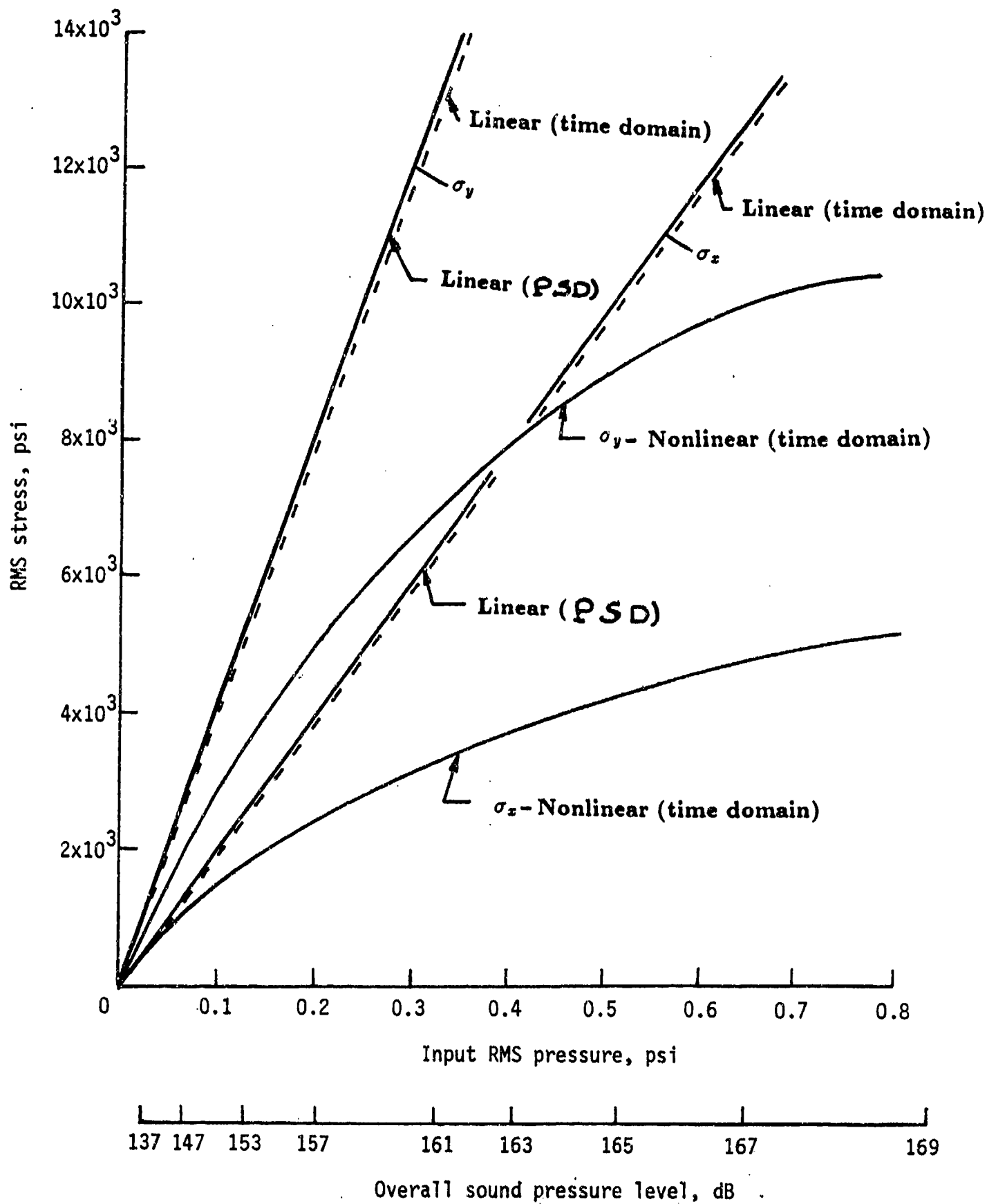


Figure 8 Linear and Nonlinear Root-Mean-Square Stress Response



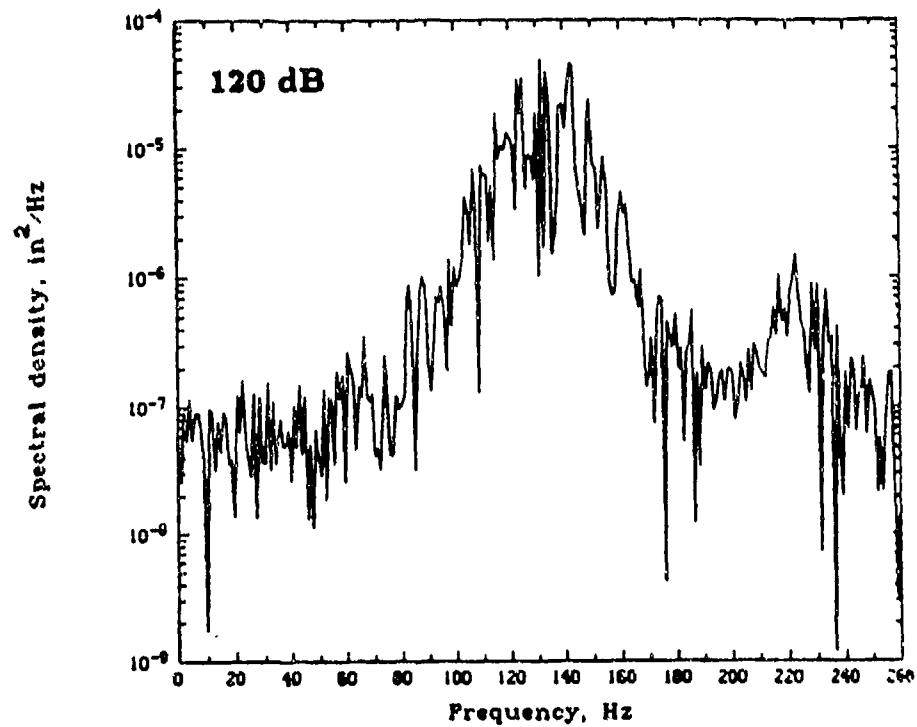
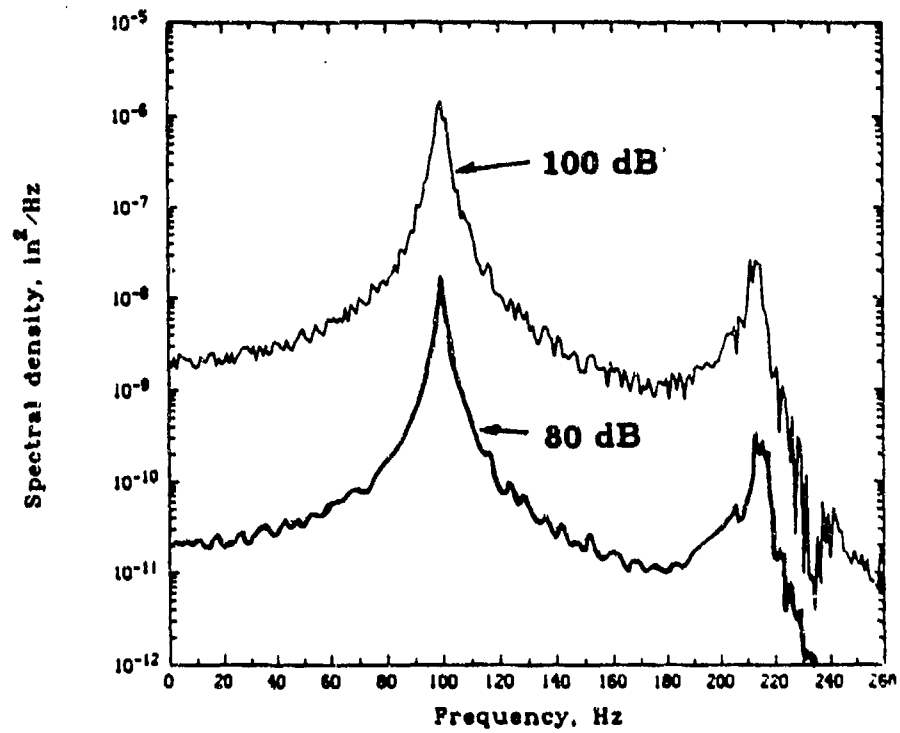


Figure 9 Spectral Density of Displacement Response for Input Sound Pressure Levels of 80 dB, 100 dB, and 120 dB

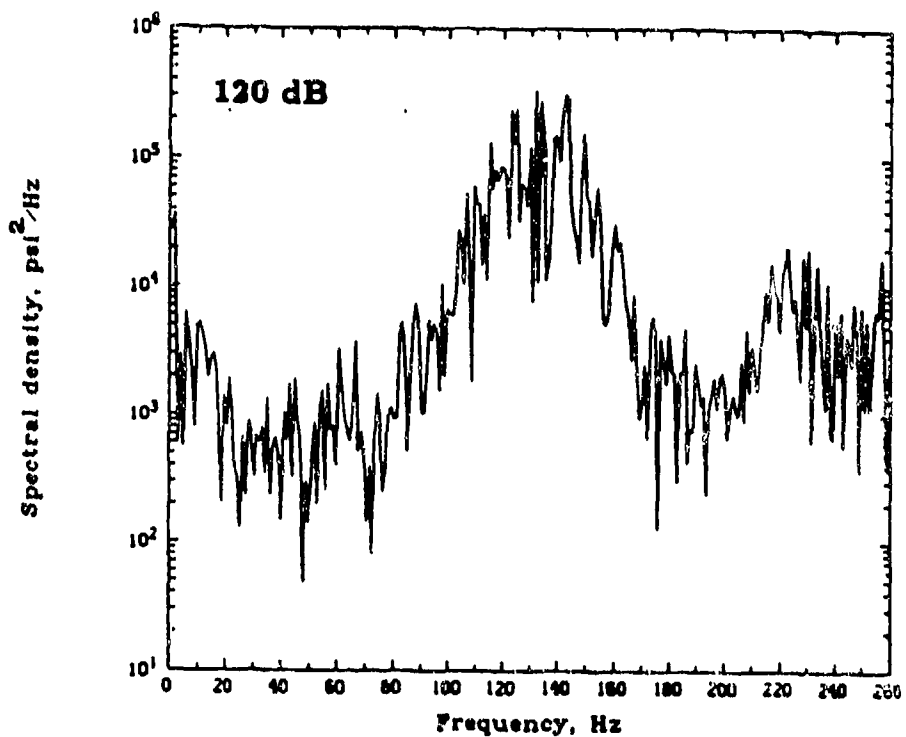
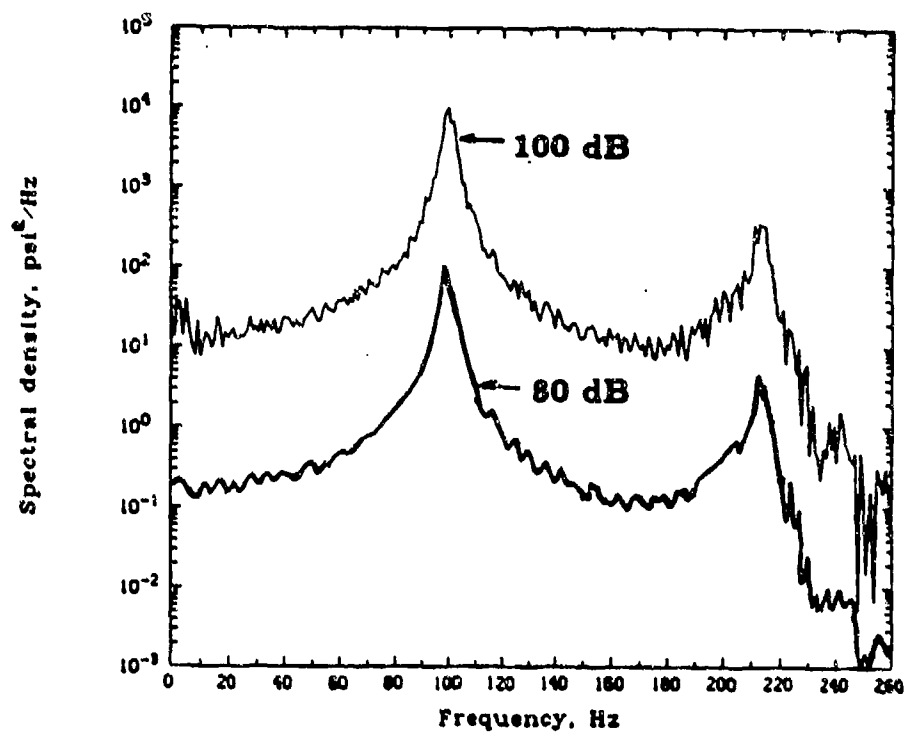


Figure 10 Spectral Densities of Stress  $\sigma_y$  for Input Sound Pressure Levels of 80 dB, 100 dB, and 120 dB

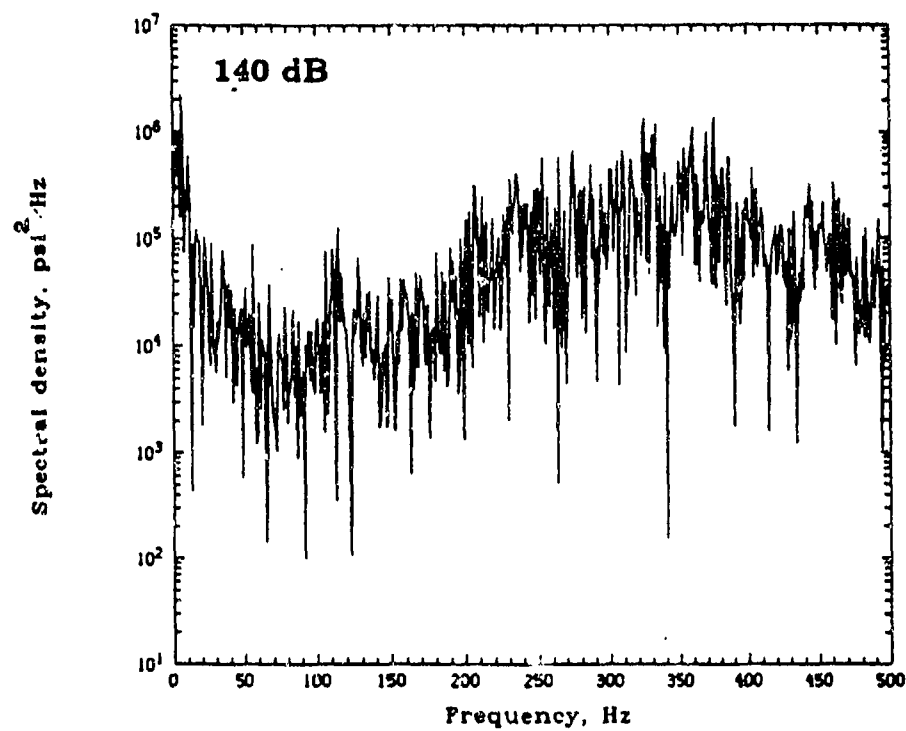
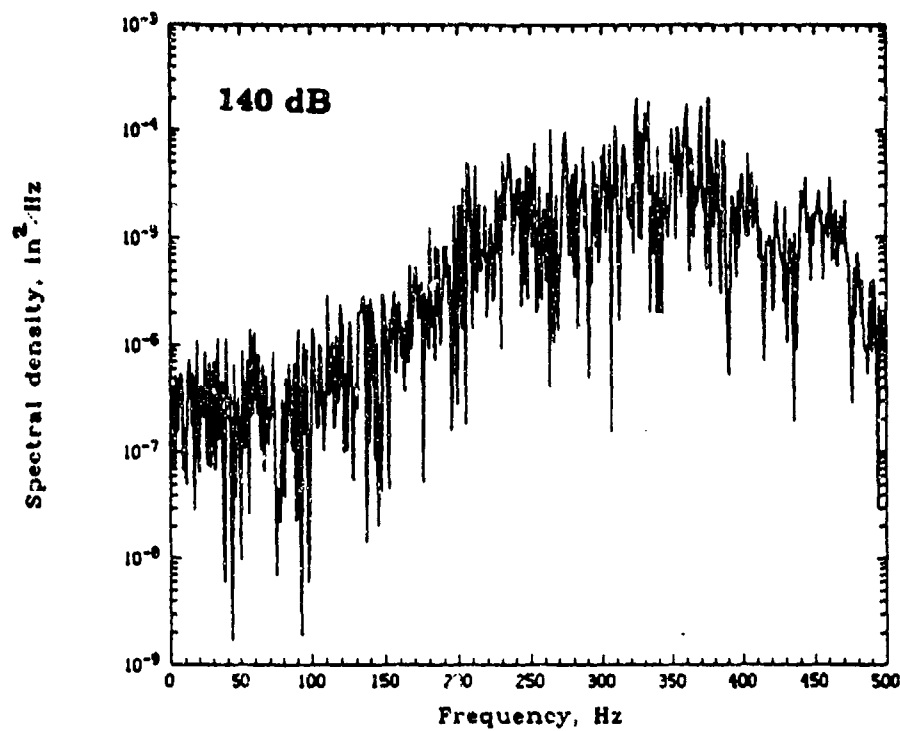


Figure 11 Spectral Densities of Displacement and Stress  $\sigma_y$  for Input Pressure Level of 140 dB

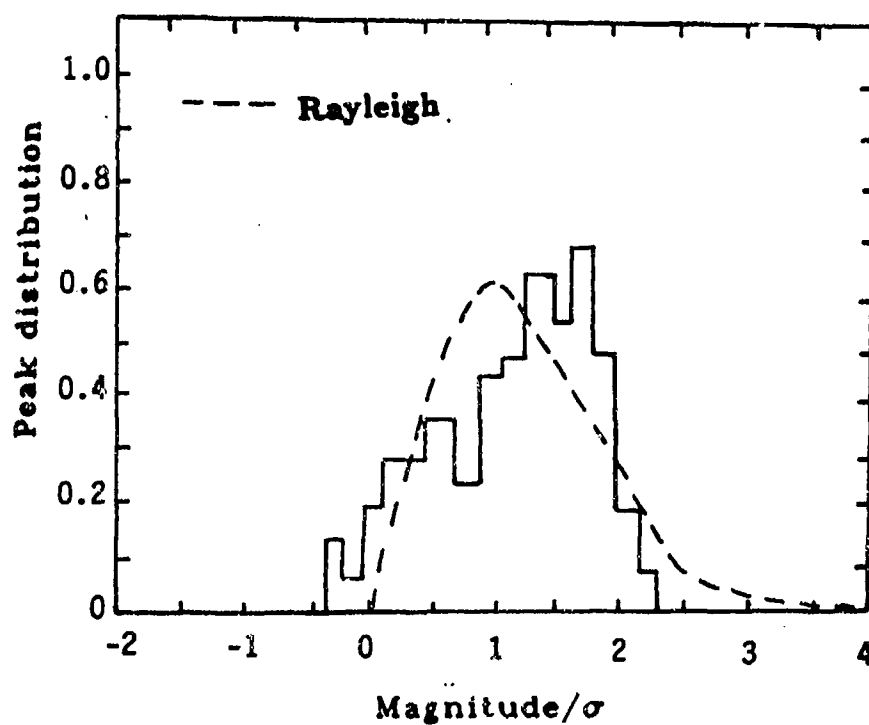
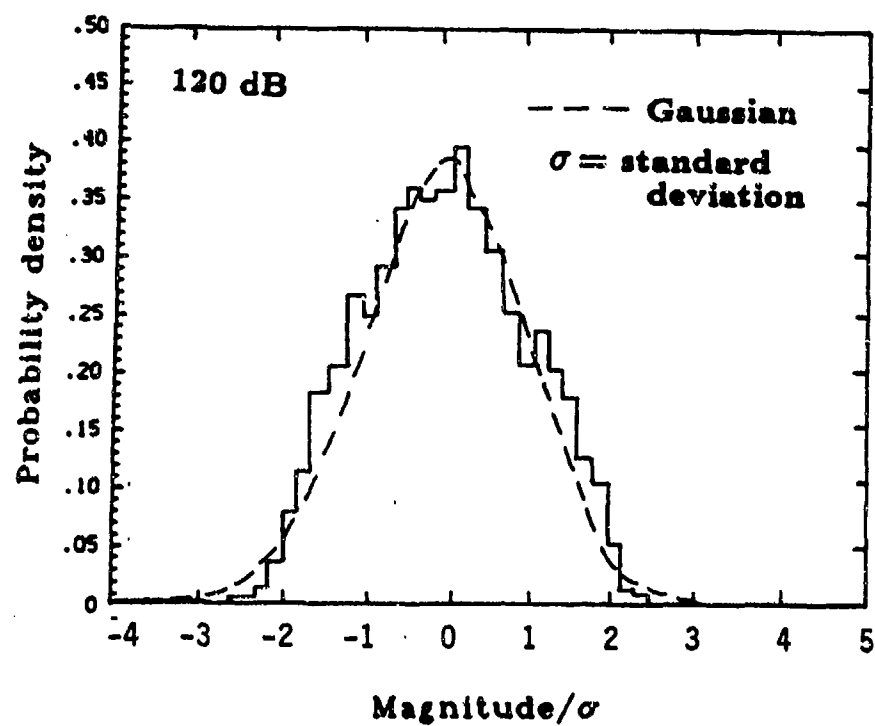


Figure 12 Probability Density and Peak Distribution Histograms of Displacement  $w$  for 120 dB Input

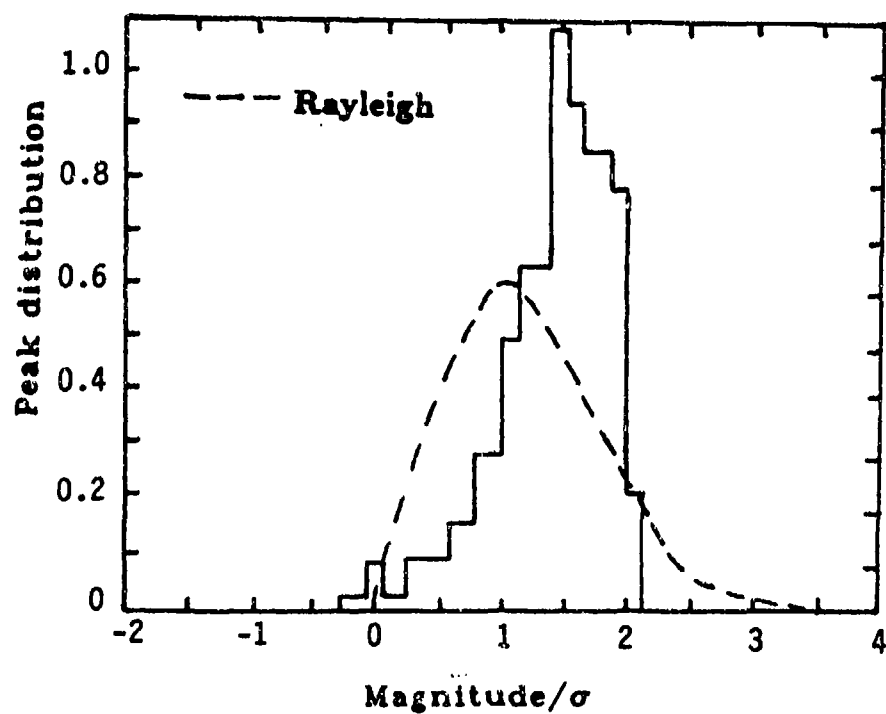
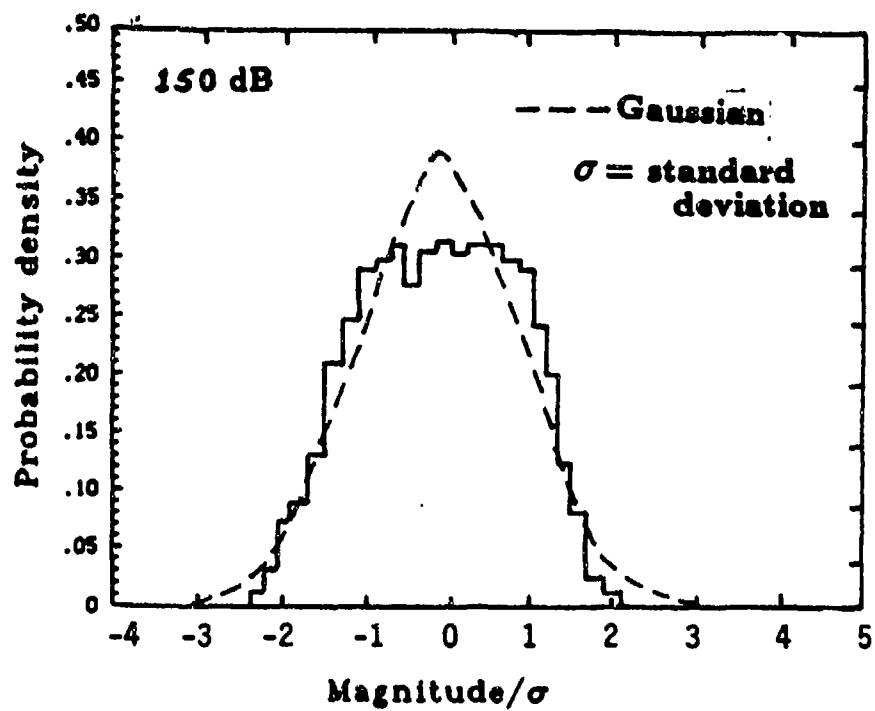


Figure 13 Probability Density and Peak Distribution Histograms of Displacement  $w$  for 150 dB Input

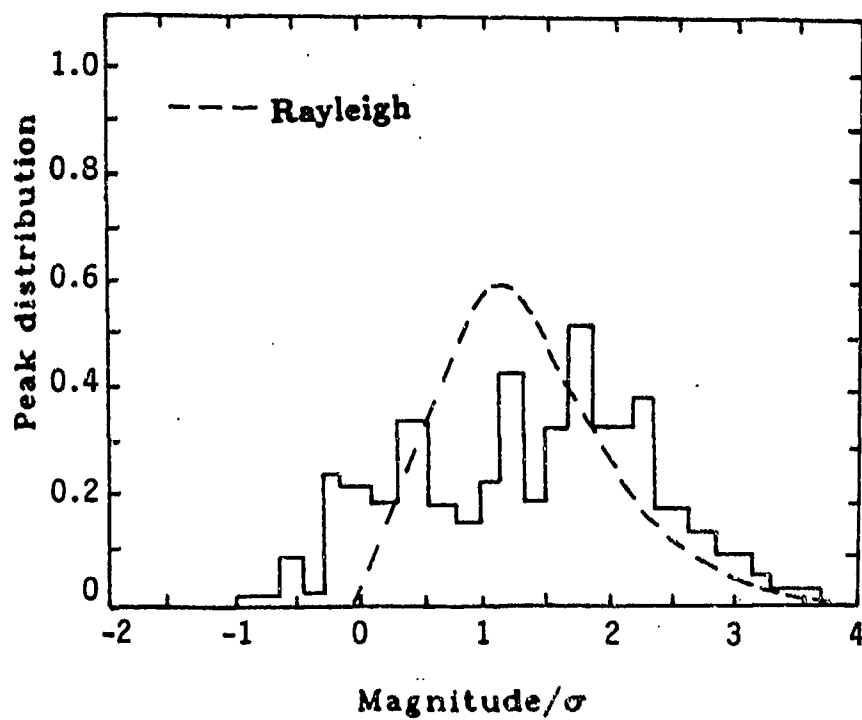
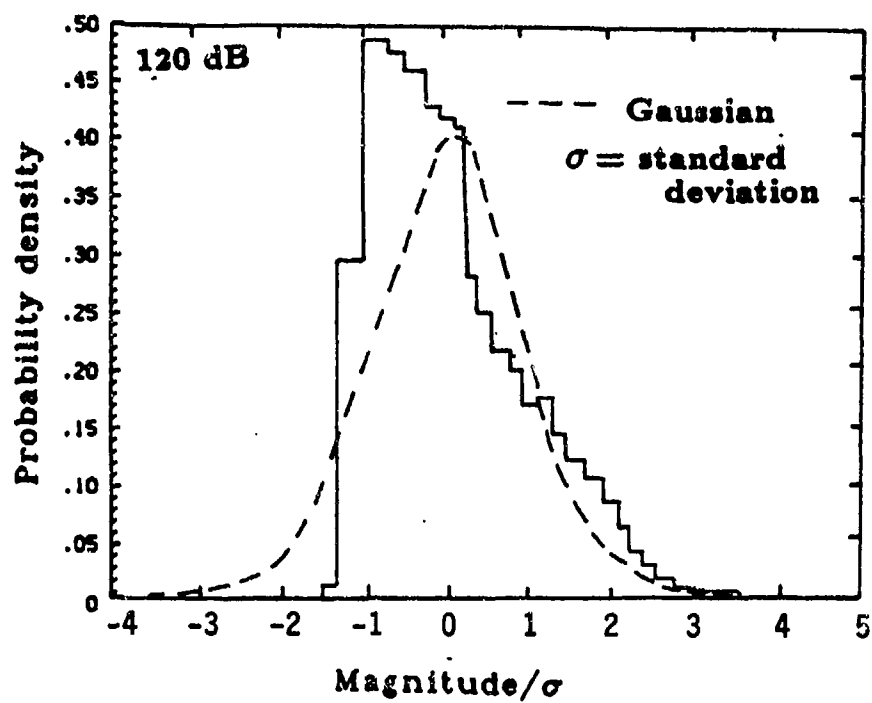


Figure 14 Probability Density and Peak Distribution Histograms of Normal Stress  $\sigma_y$  for 120 dB Input

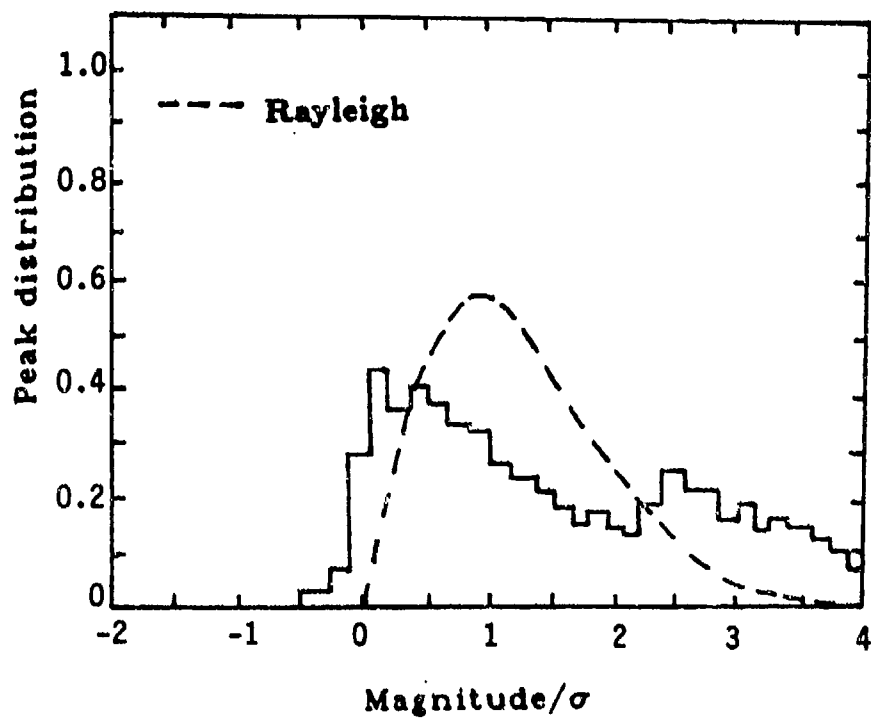
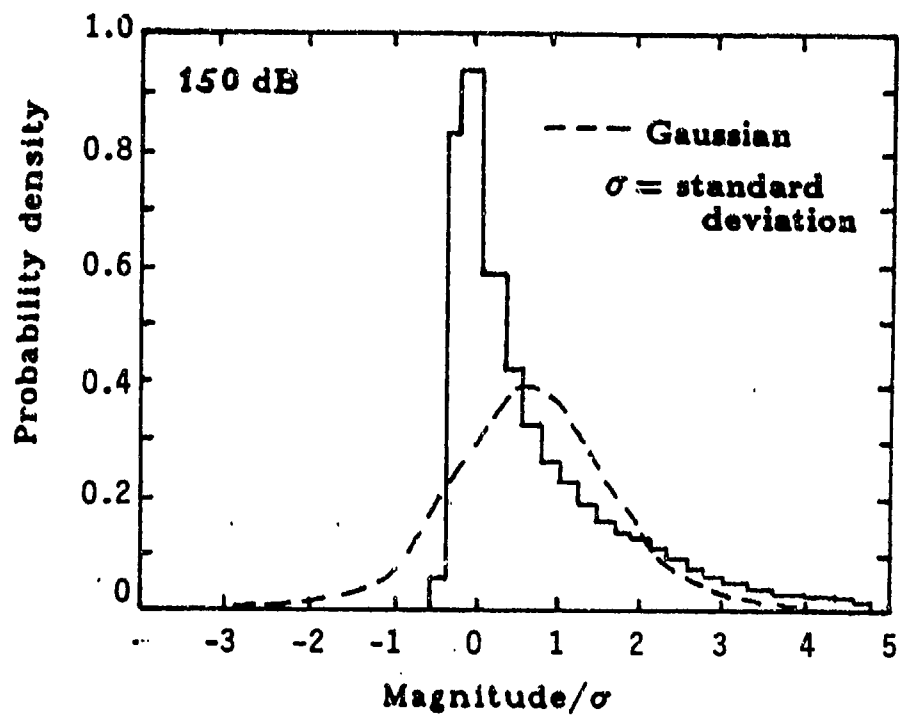


Figure 15 Probability Density and Peak Distribution Histograms of Normal Stress  $\sigma_y$  for 150 dB Input

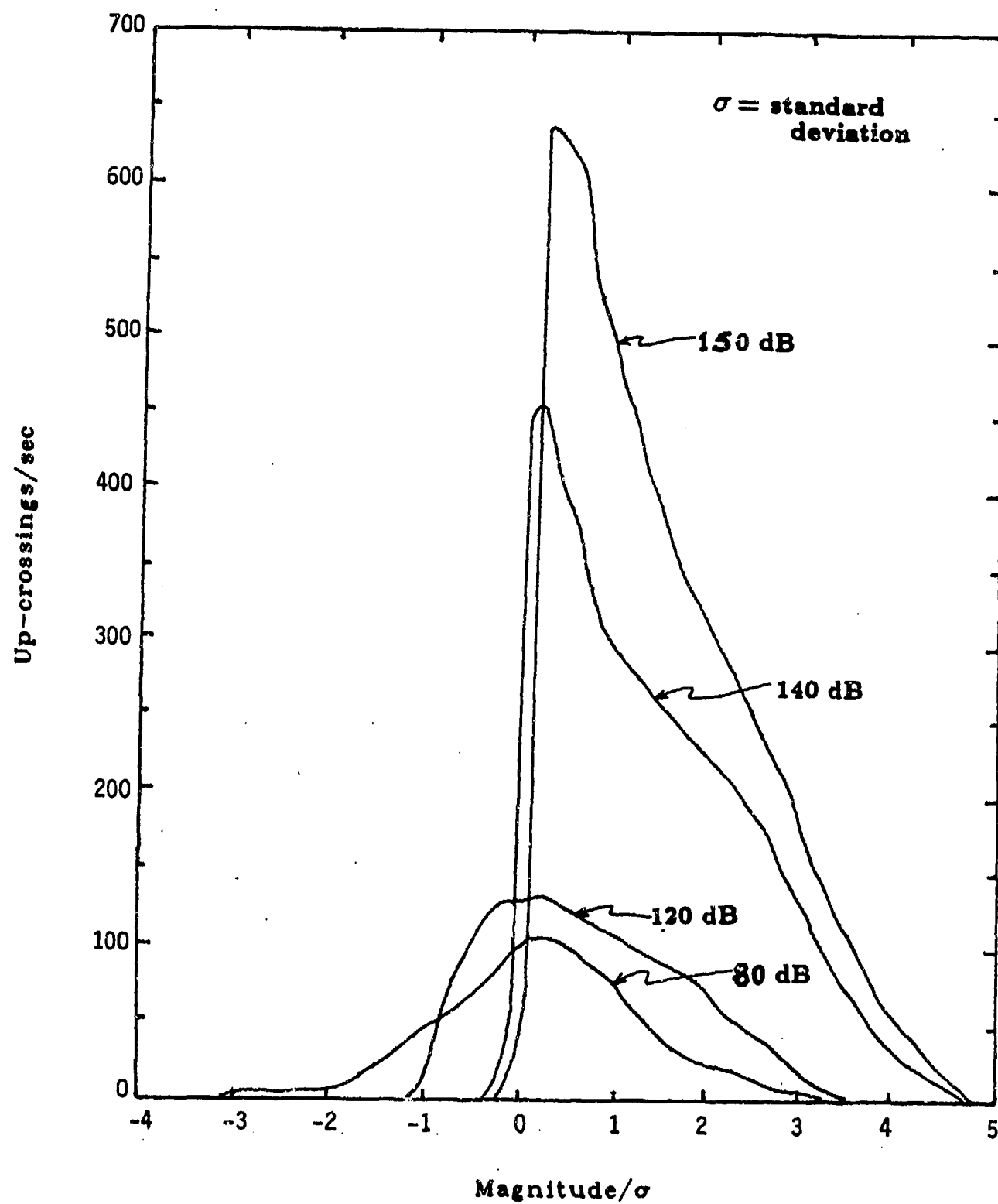


Figure 16 Threshold Up-crossing Rate for Stress  $\sigma_y$



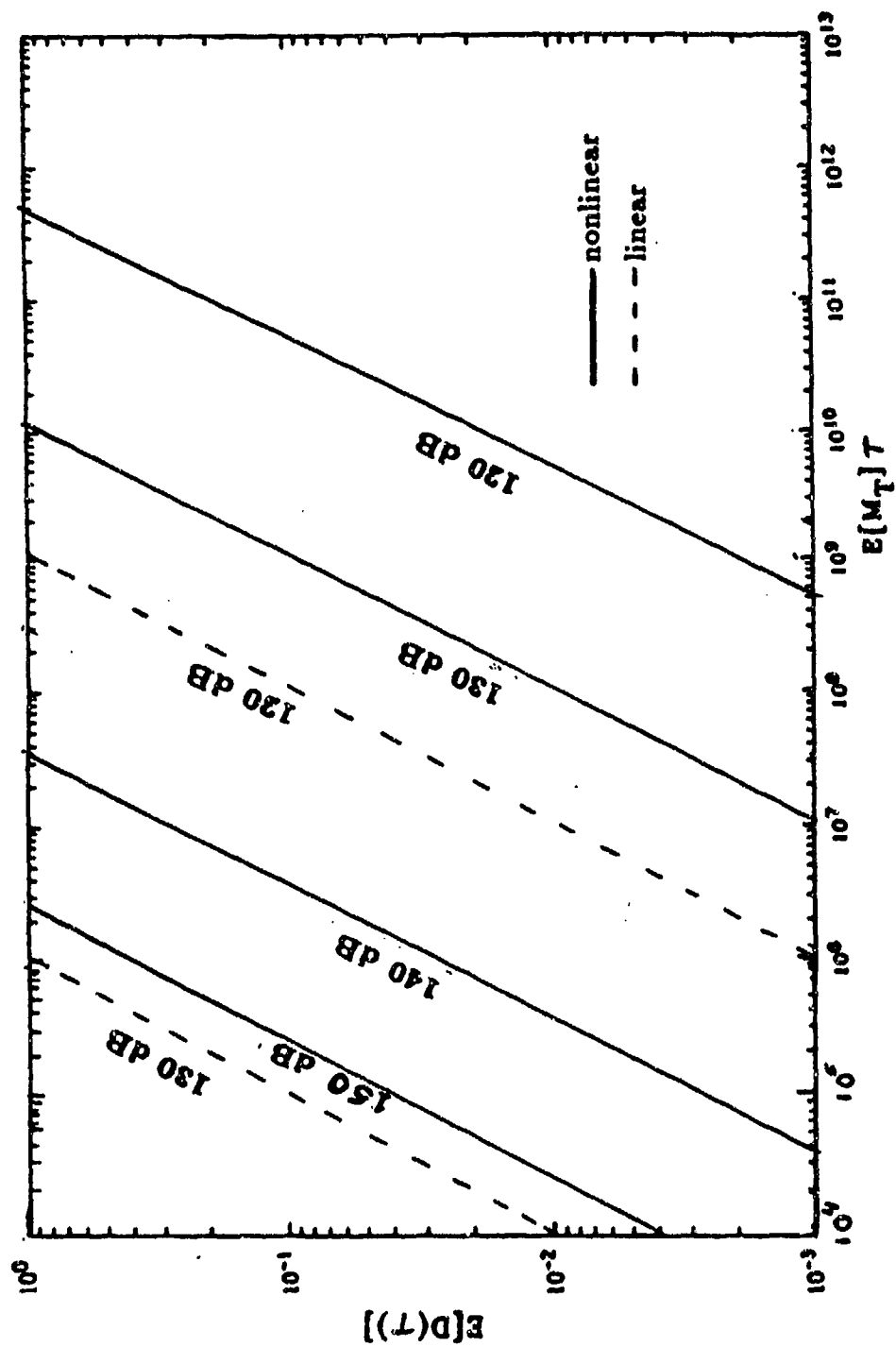


Figure 17 Fatigue Damage for Different Input Pressure Levels

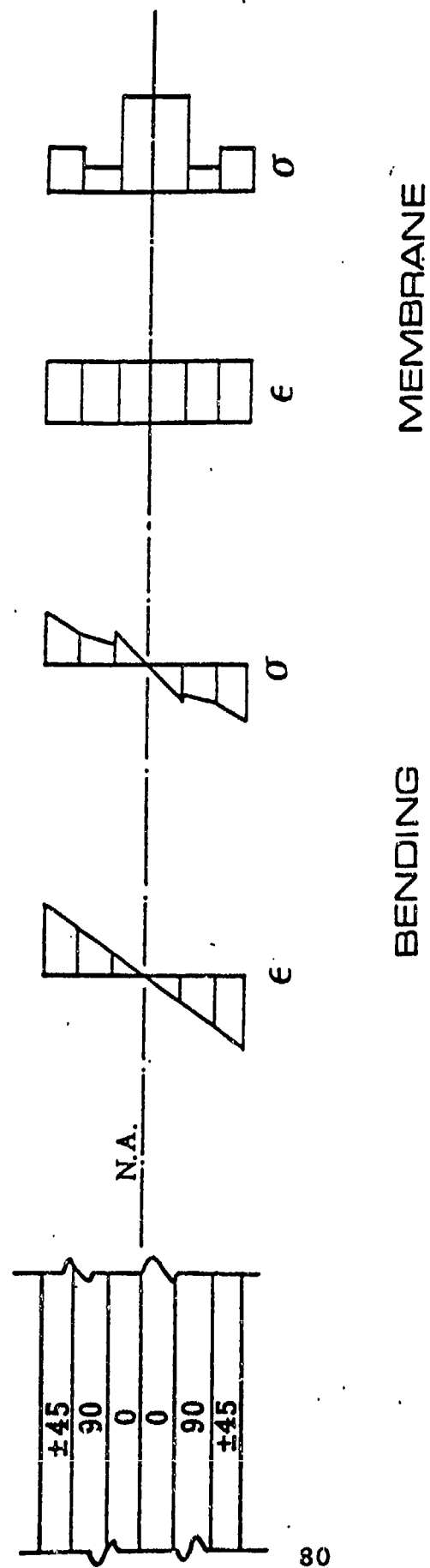


Figure 18 Typical Laminate Stress/Strain Distributions

**DISPLACEMENT RESPONSE TIME HISTORY**  
G/E [0/45/-45/90] SYM.

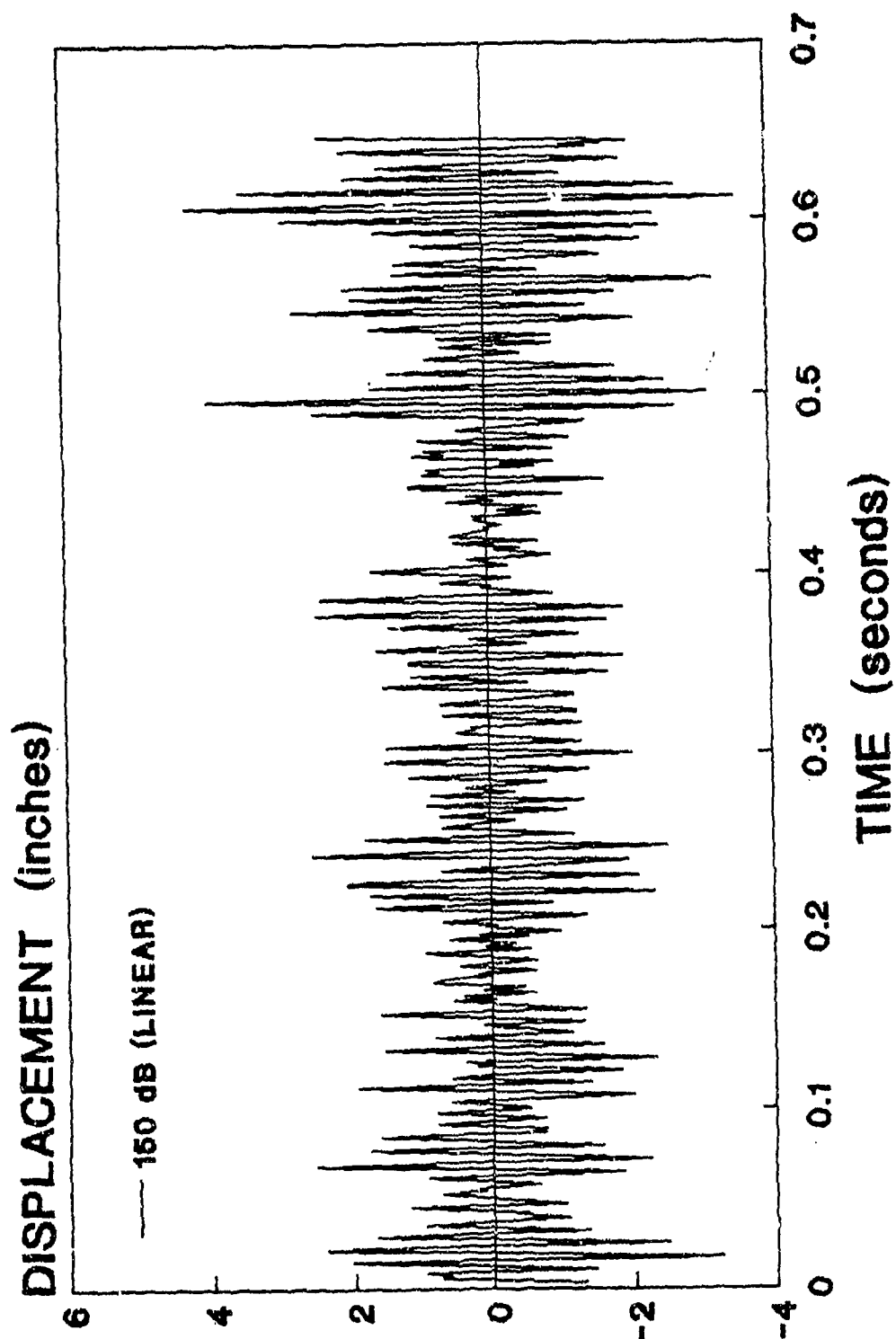


Figure 19 Displacement Response Time History (150 dB Linear)

# DISPLACEMENT RESPONSE TIME HISTORY

G/E [0/45/-45/90] SYM.

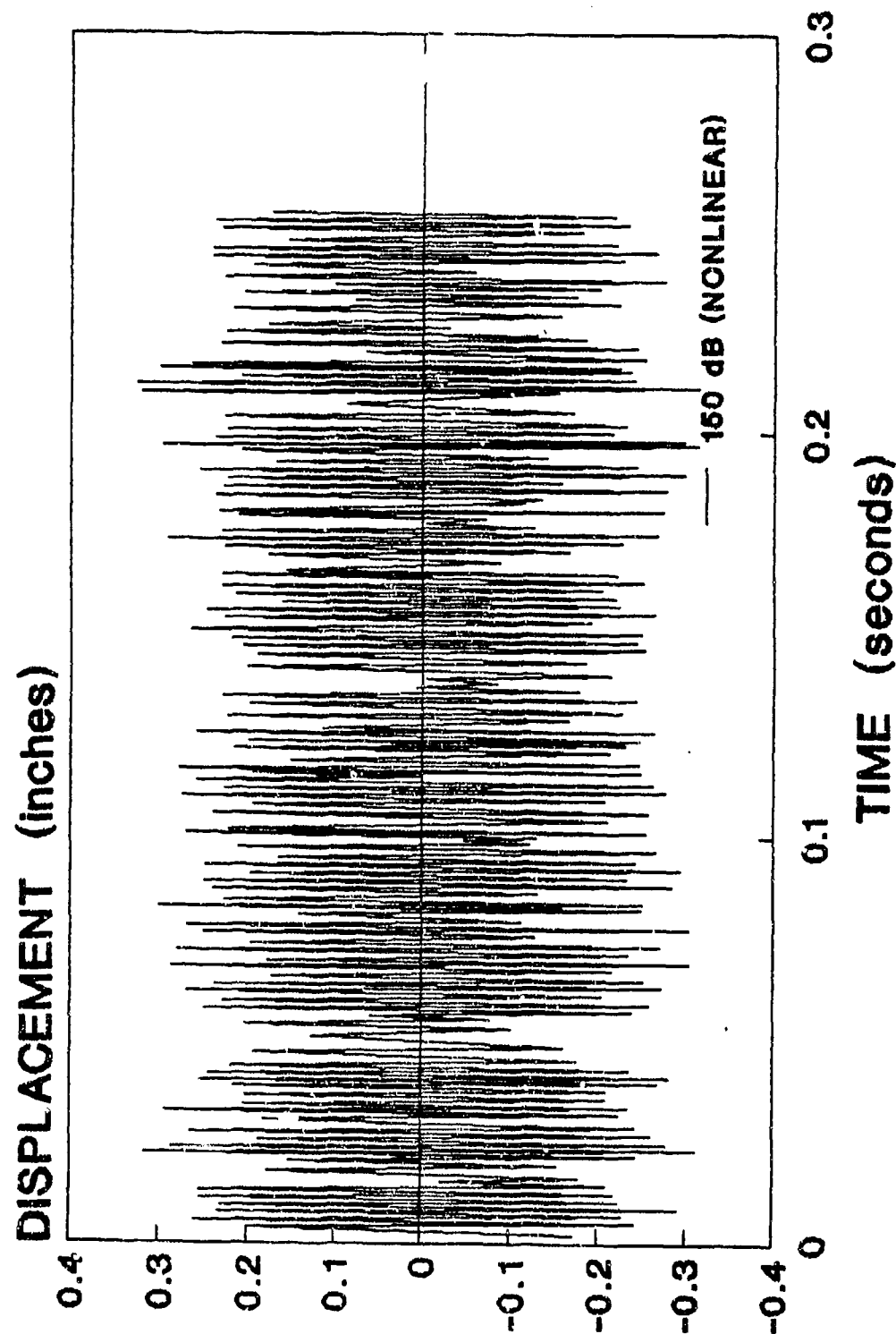


Figure 20 Displacement Response Time History (150 dB Nonlinear)

**STRESS RESPONSE TIME HISTORY**  
G/E [0/45/-45/90] SYM.

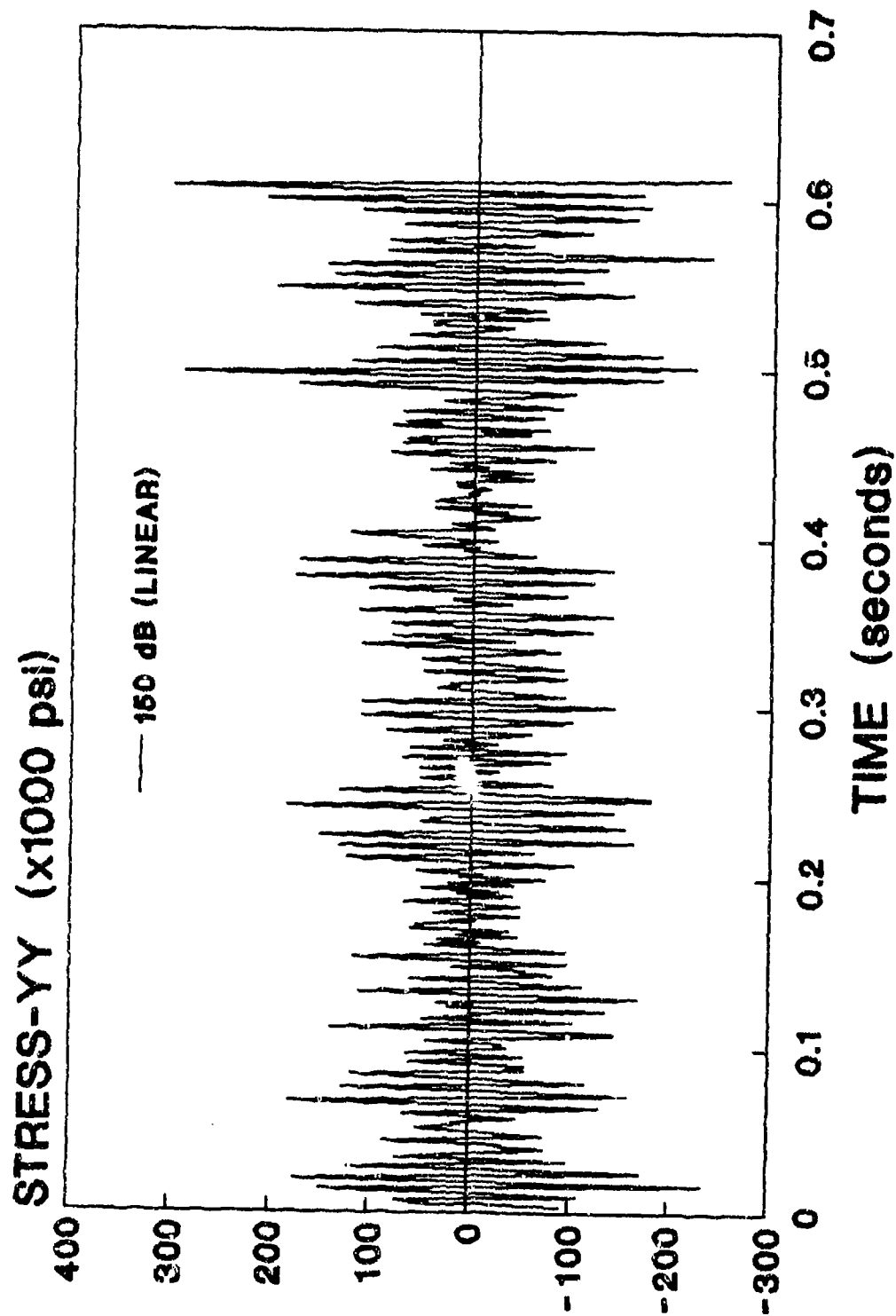


Figure 21  $\sigma_{yy}$  Stress Response Time History (150 dB Linear)

**STRESS RESPONSE TIME HISTORY**  
G/E [0/45/-45/90] SYM.

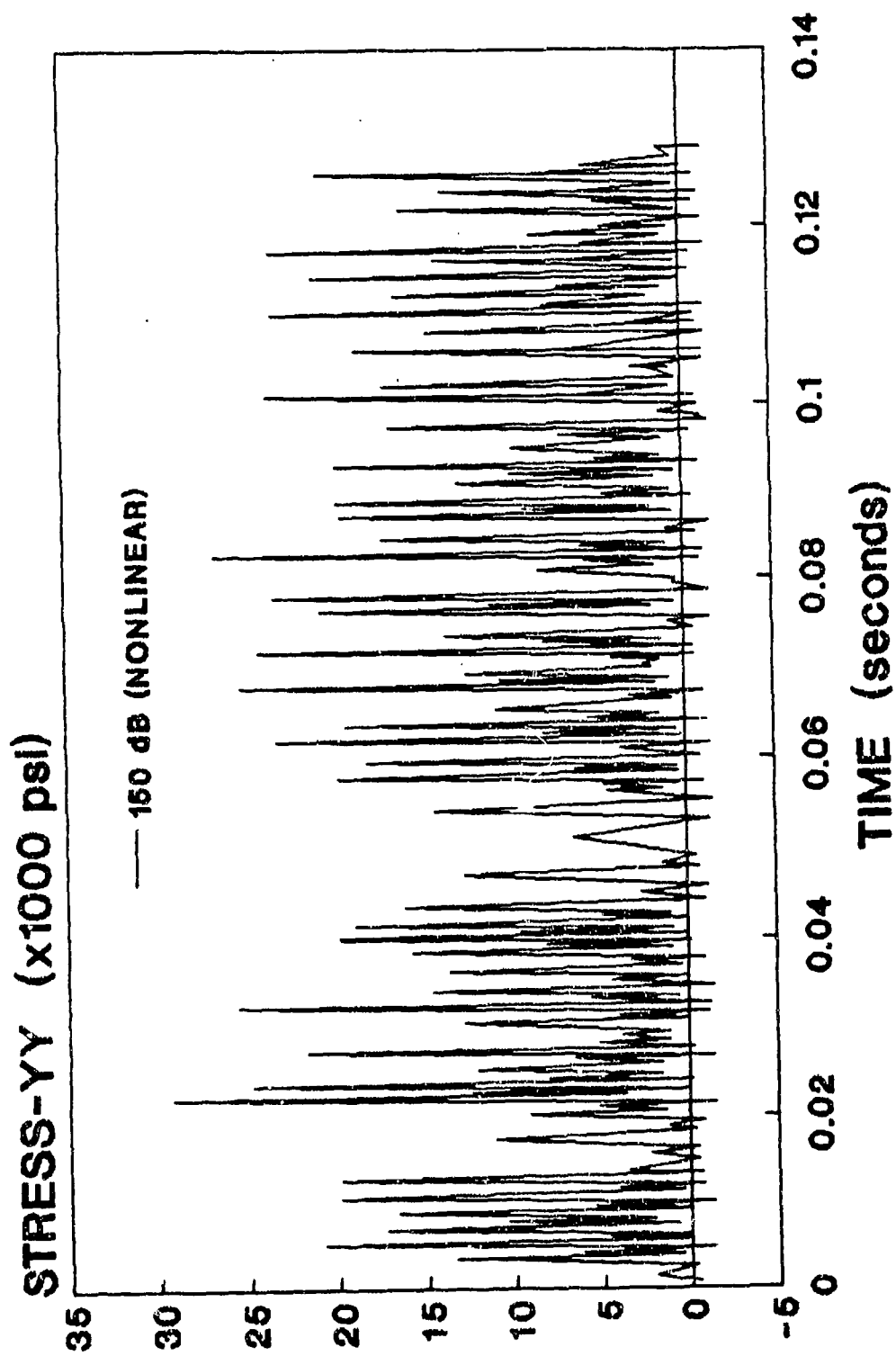


Figure 22  $\sigma_{yy}$  Stress Response Time History (150 dB Nonlinear)

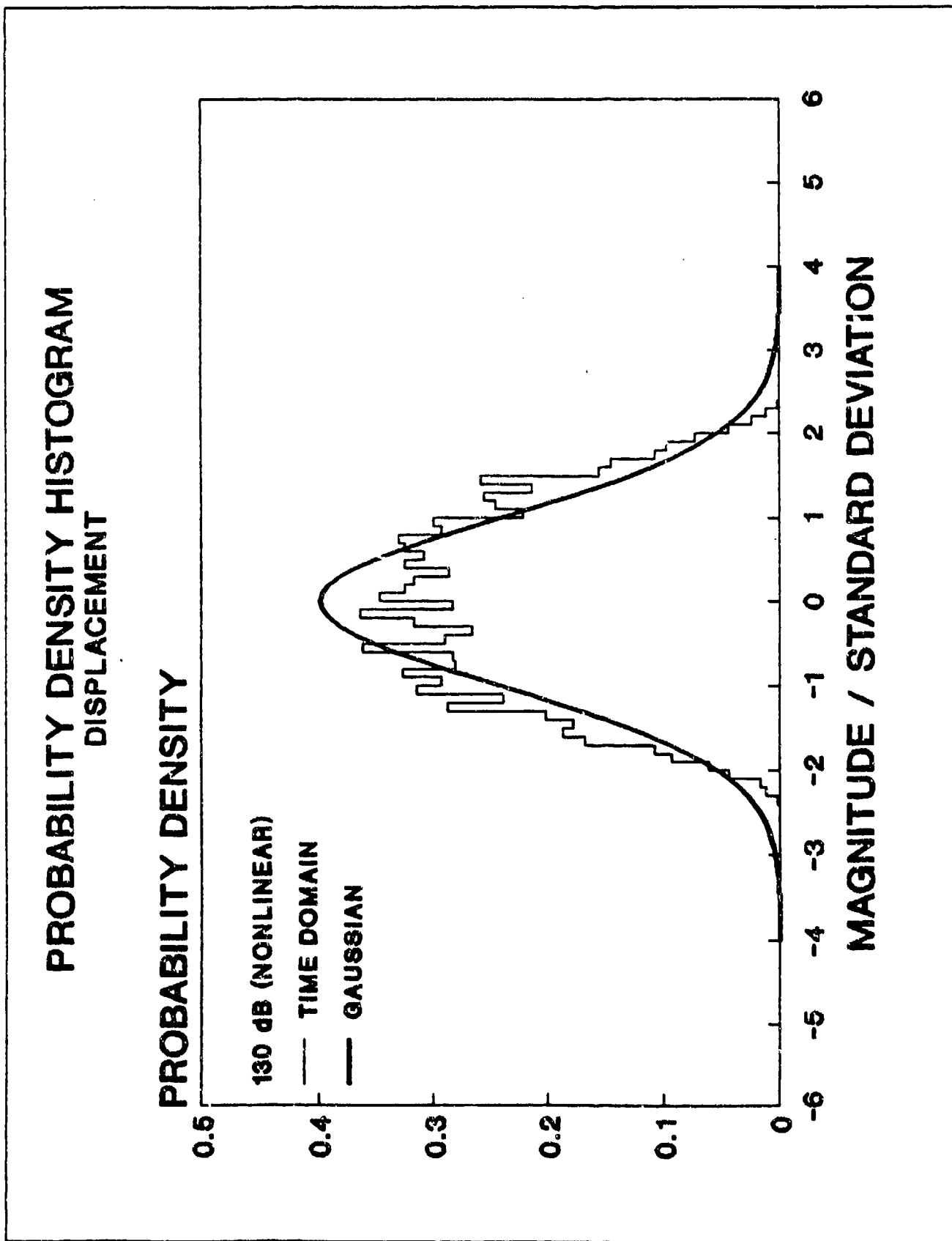


Figure 23 Probability Density Histogram of Displacement (130 dB Nonlinear)

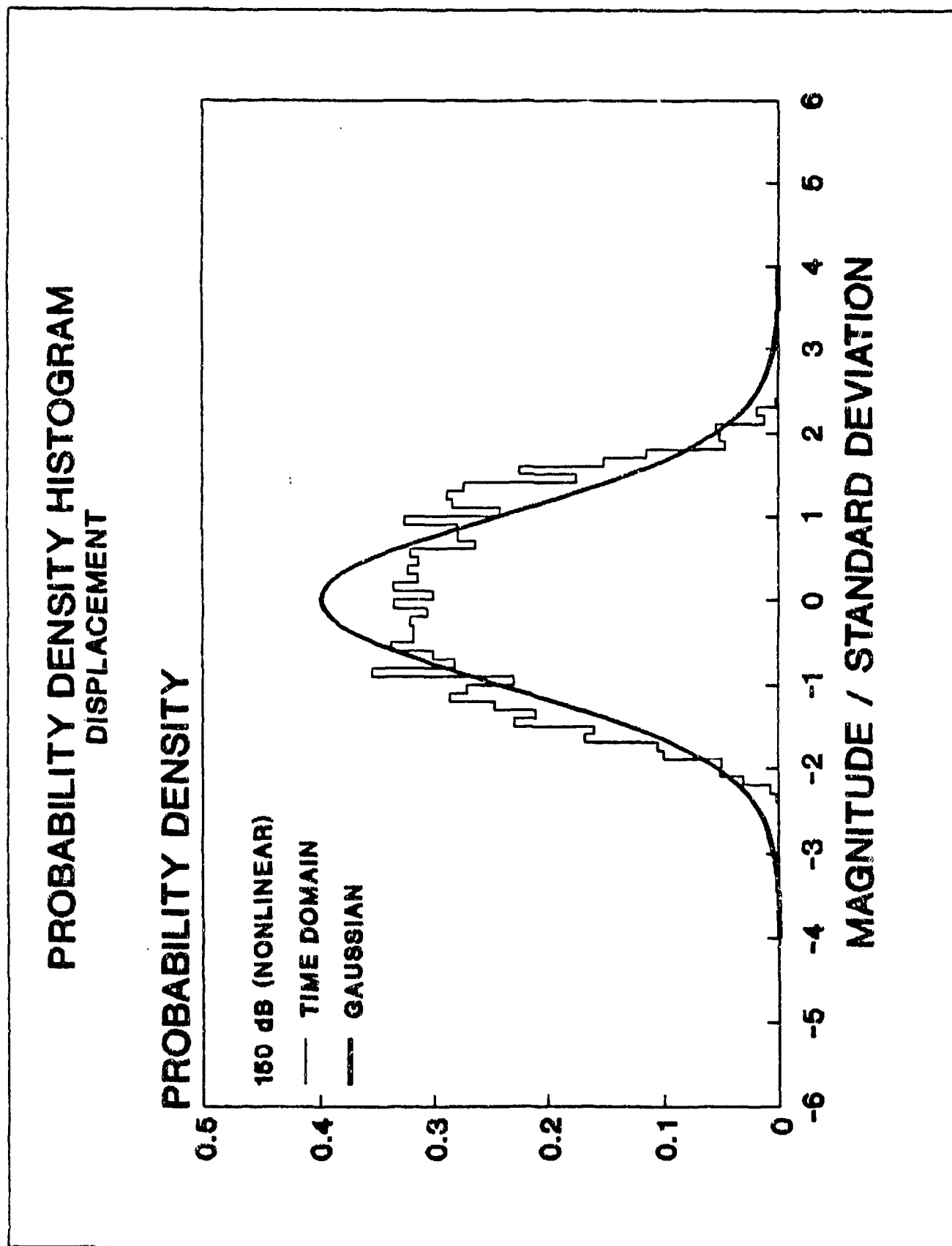


Figure 24 Probability Density Histogram of Displacement (150 dB Nonlinear)



# PEAK DISTRIBUTION HISTOGRAM DISPLACEMENT

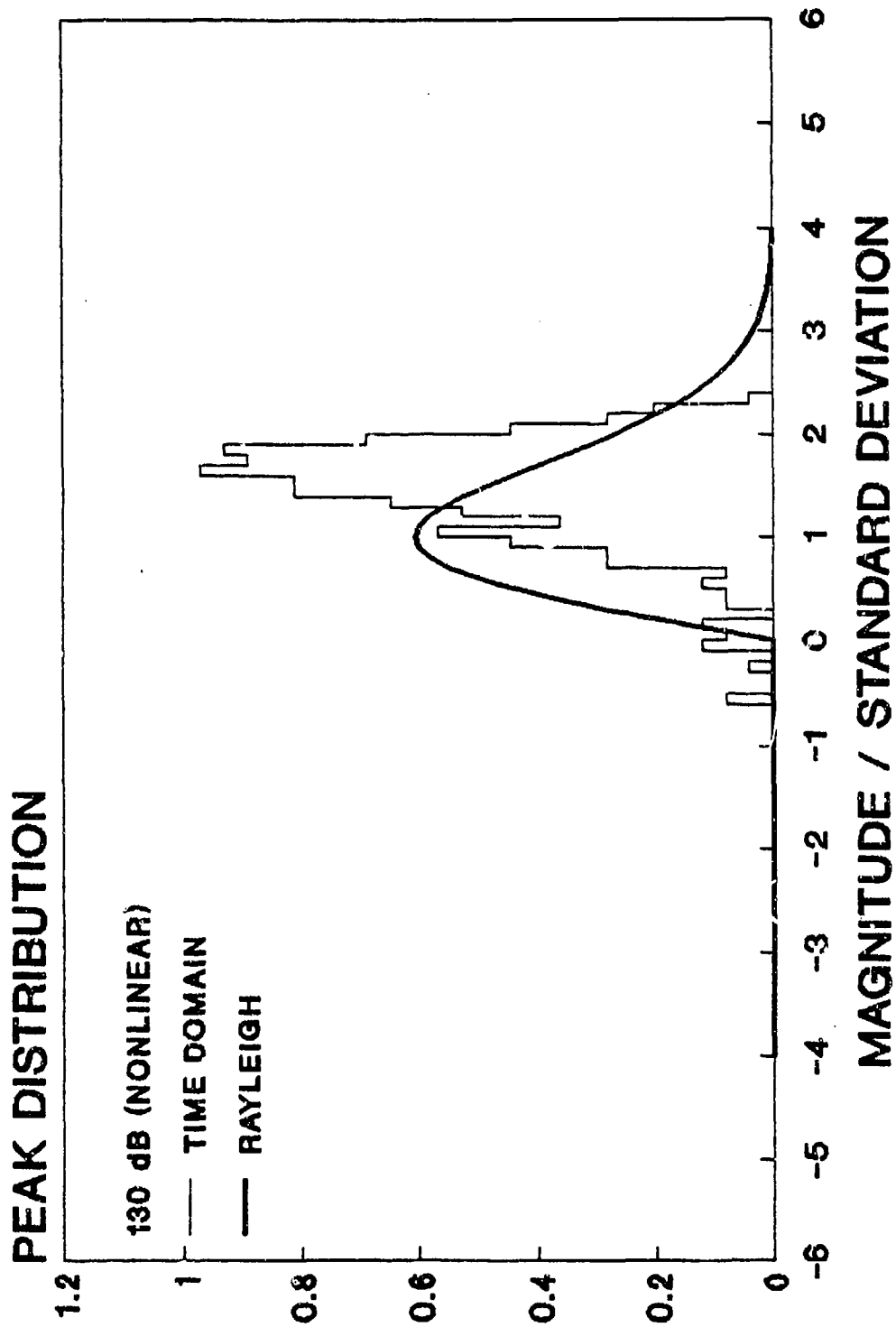


Figure 25 Peak Distribution Histogram of Displacement (130 dB Nonlinear)

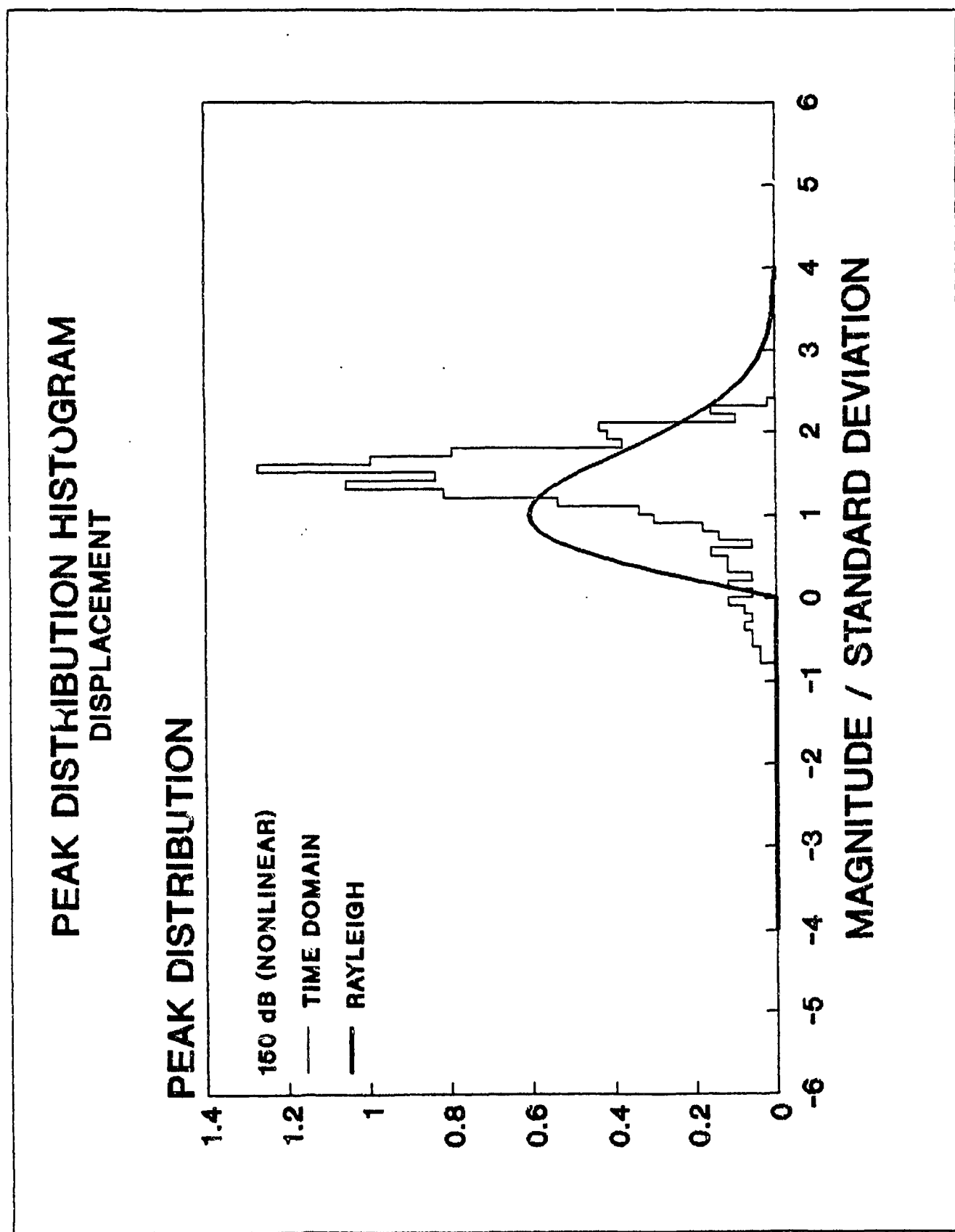


Figure 26 Peak Distribution Histogram of Displacement (150 dB Nonlinear)

# PROBABILITY DENSITY HISTOGRAM STRESS-YY

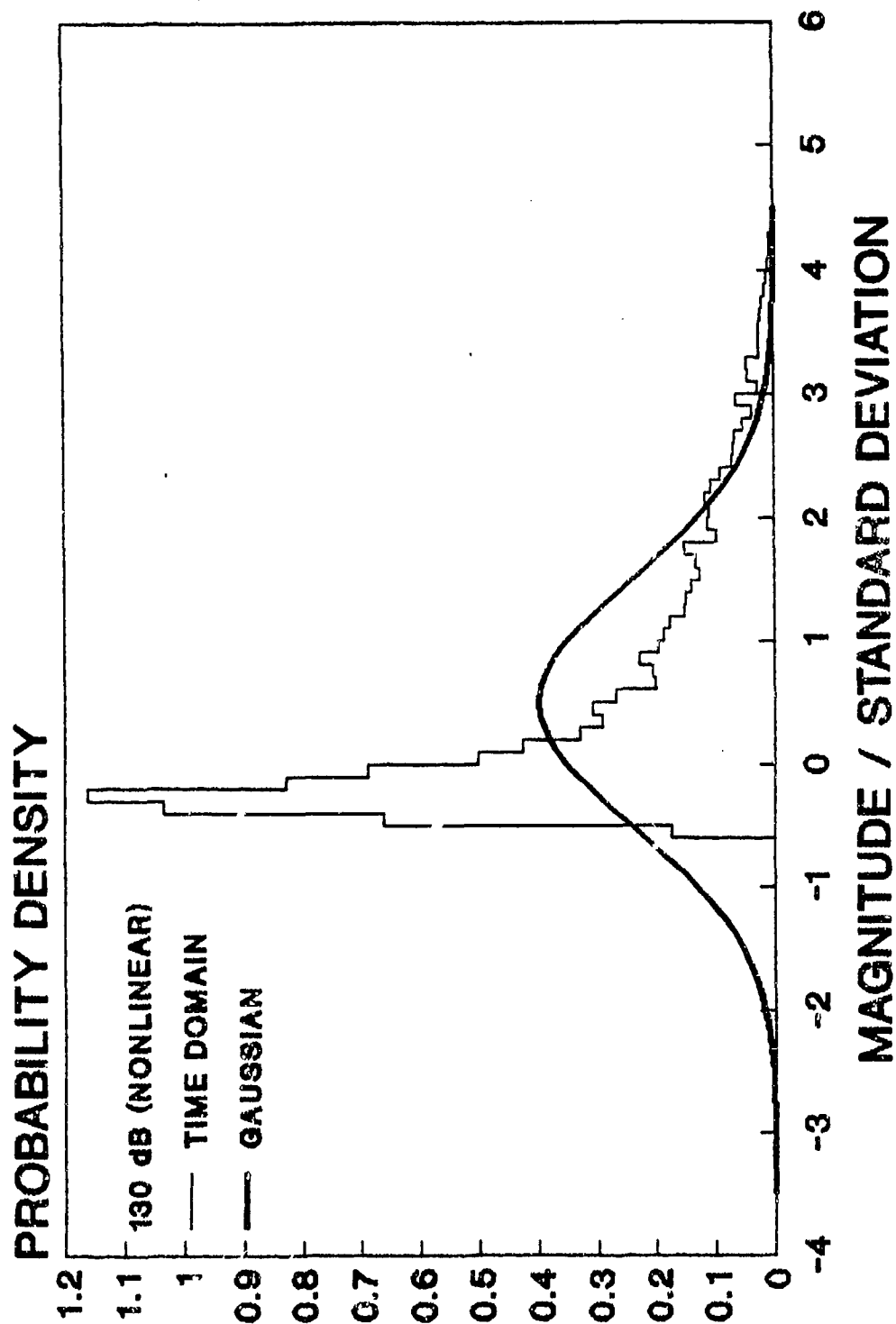


Figure 27 Probability Density Histogram of  $\sigma_{yy}$  (130 dB Nonlinear)

# PROBABILITY DENSITY HISTOGRAM STRESS-YY

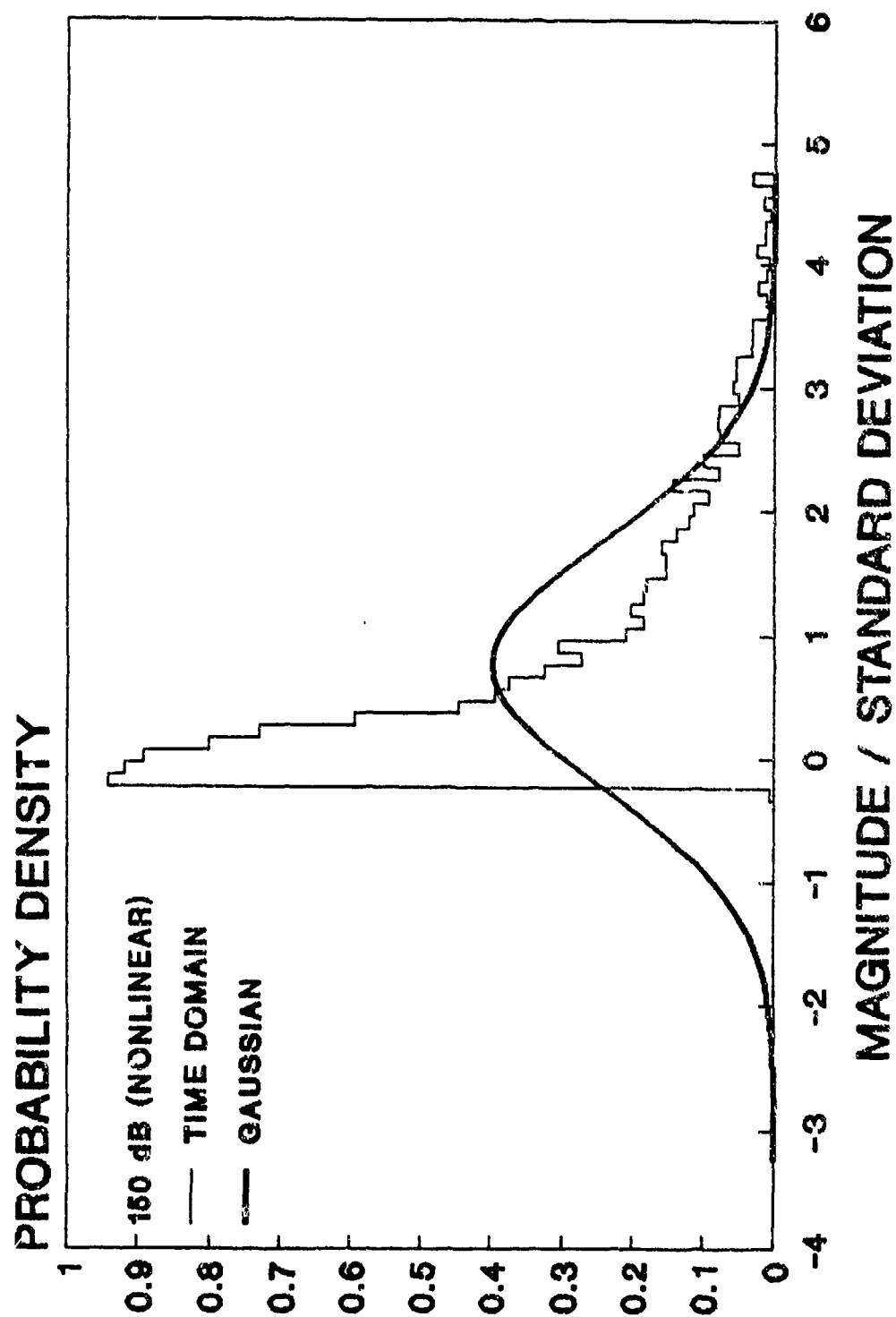


Figure 28 Probability Density Histogram of  $\sigma_{yy}$  (150 dB Nonlinear)

# PEAK DISTRIBUTION HISTOGRAM STRESS-YY

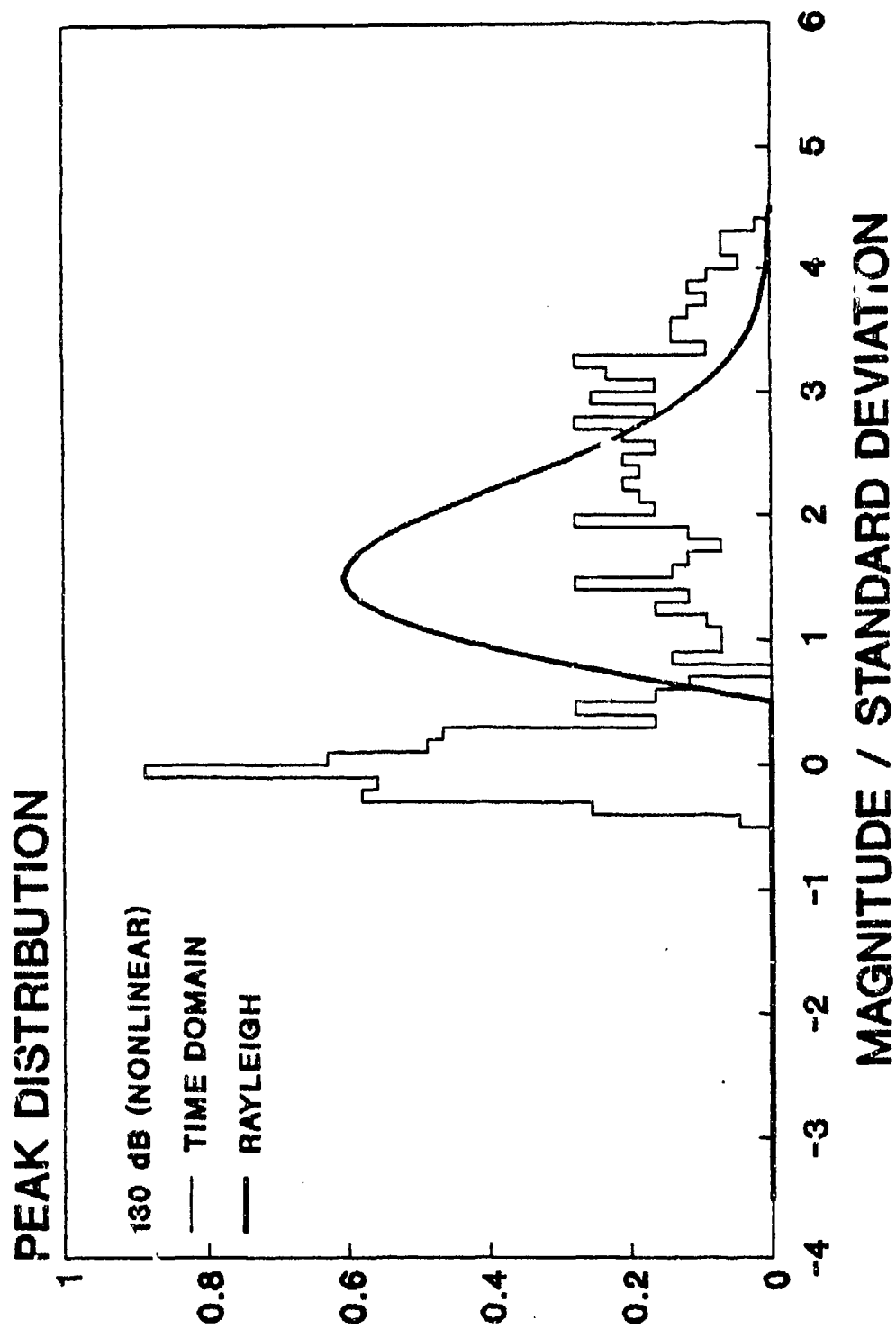


Figure 29 Peak Distribution Histogram of  $\sigma_{yy}$  (130 dB Nonlinear)

# PEAK DISTRIBUTION HISTOGRAM STRESS-YY

## PEAK DISTRIBUTION

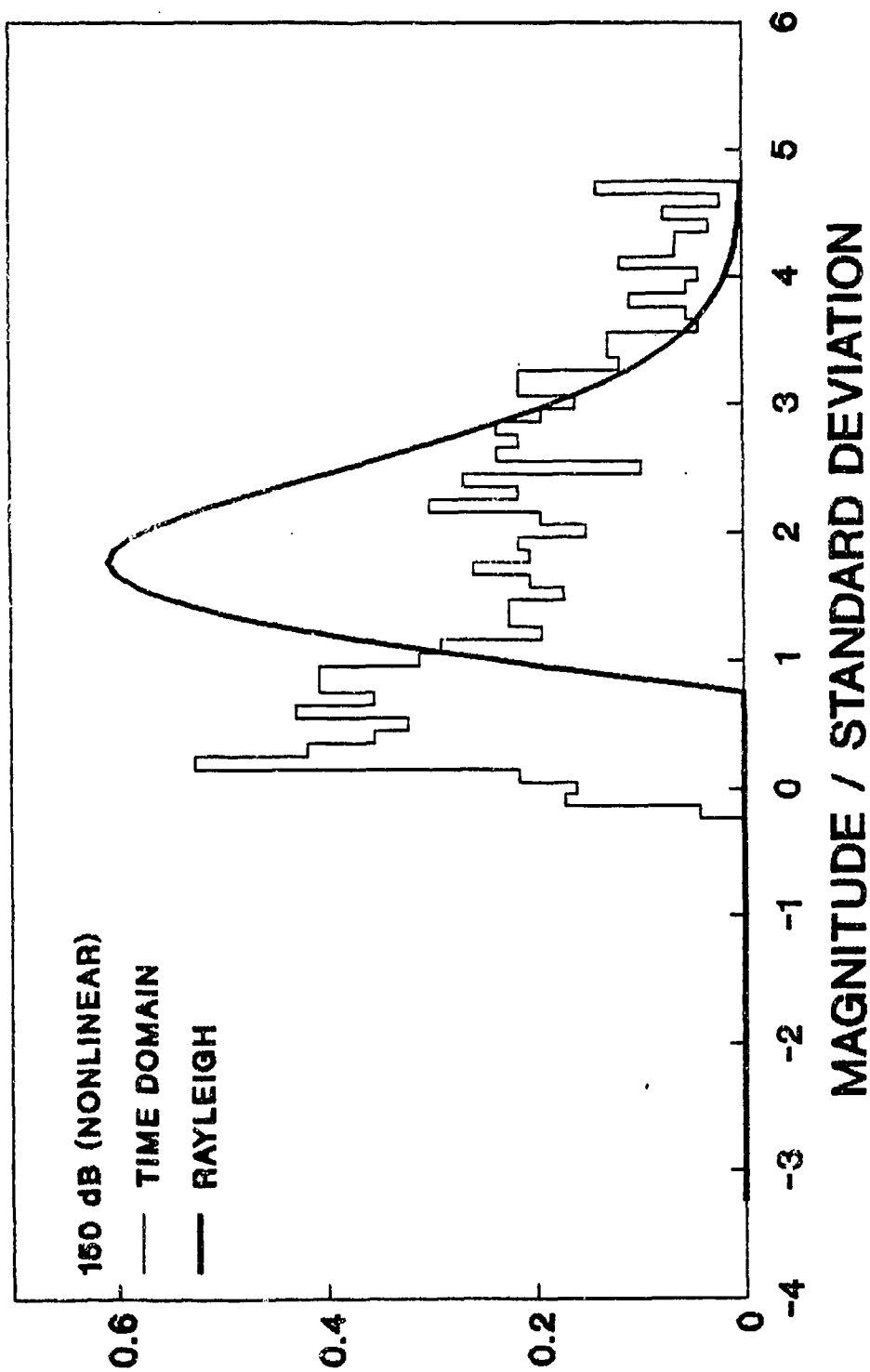


Figure 30 Peak Distribution Histogram of  $\sigma_{yy}$  (150 dB Nonlinear)

# UP-CROSSINGS PER SECOND STRESS-YY

## UP-CROSSINGS PER SECOND

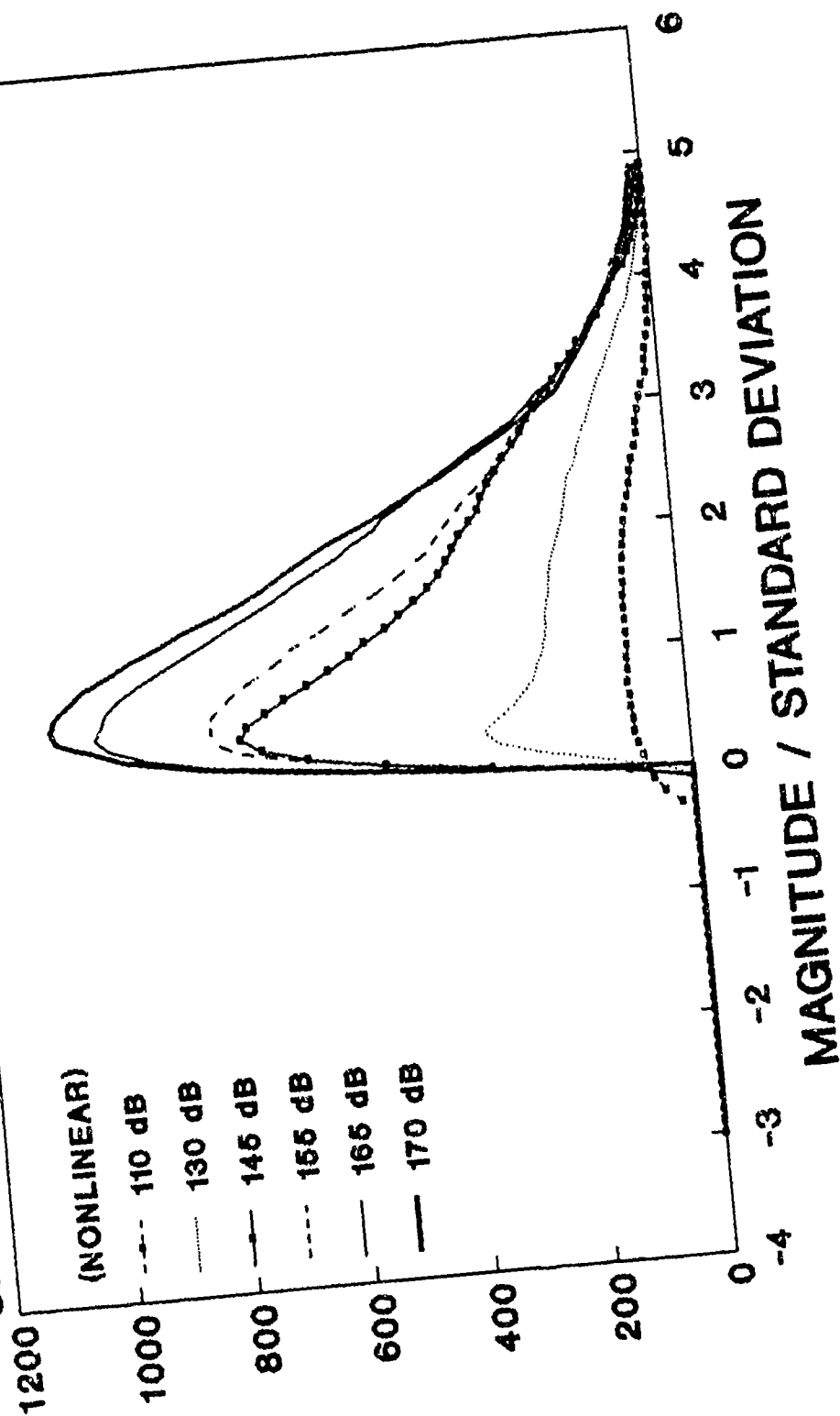


Figure 31 Up-Crossing Rate for  $\sigma_{yy}$  for Various Sound Pressure Levels

# RMS STRESS (YY) AS A FUNCTION OF ANGLE LAMINATE [0/+THETA/-THETA/90] SYMM.

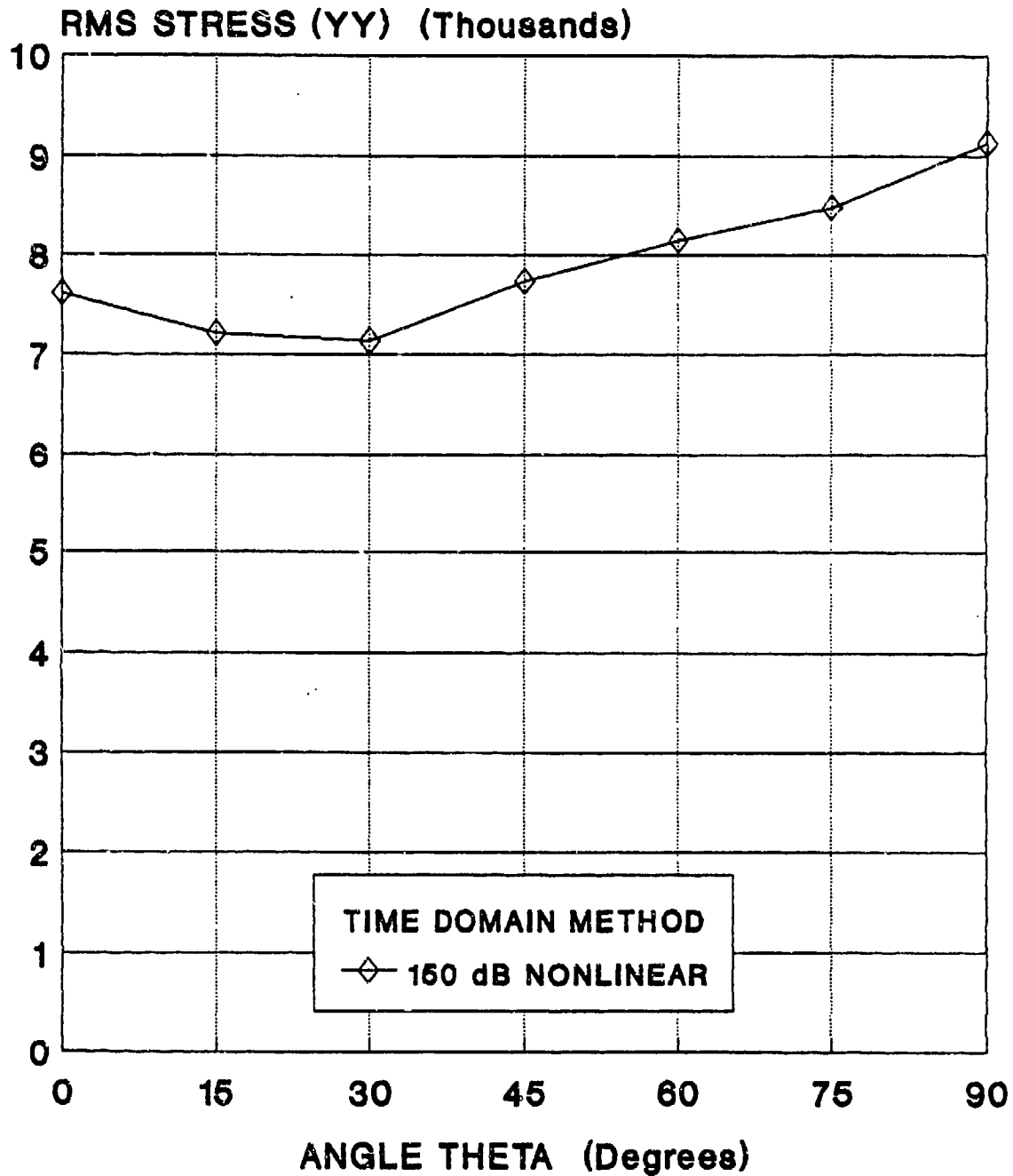


Figure 32 RMS of  $\sigma_{yy}$  as a Function of Lay-Up Angle



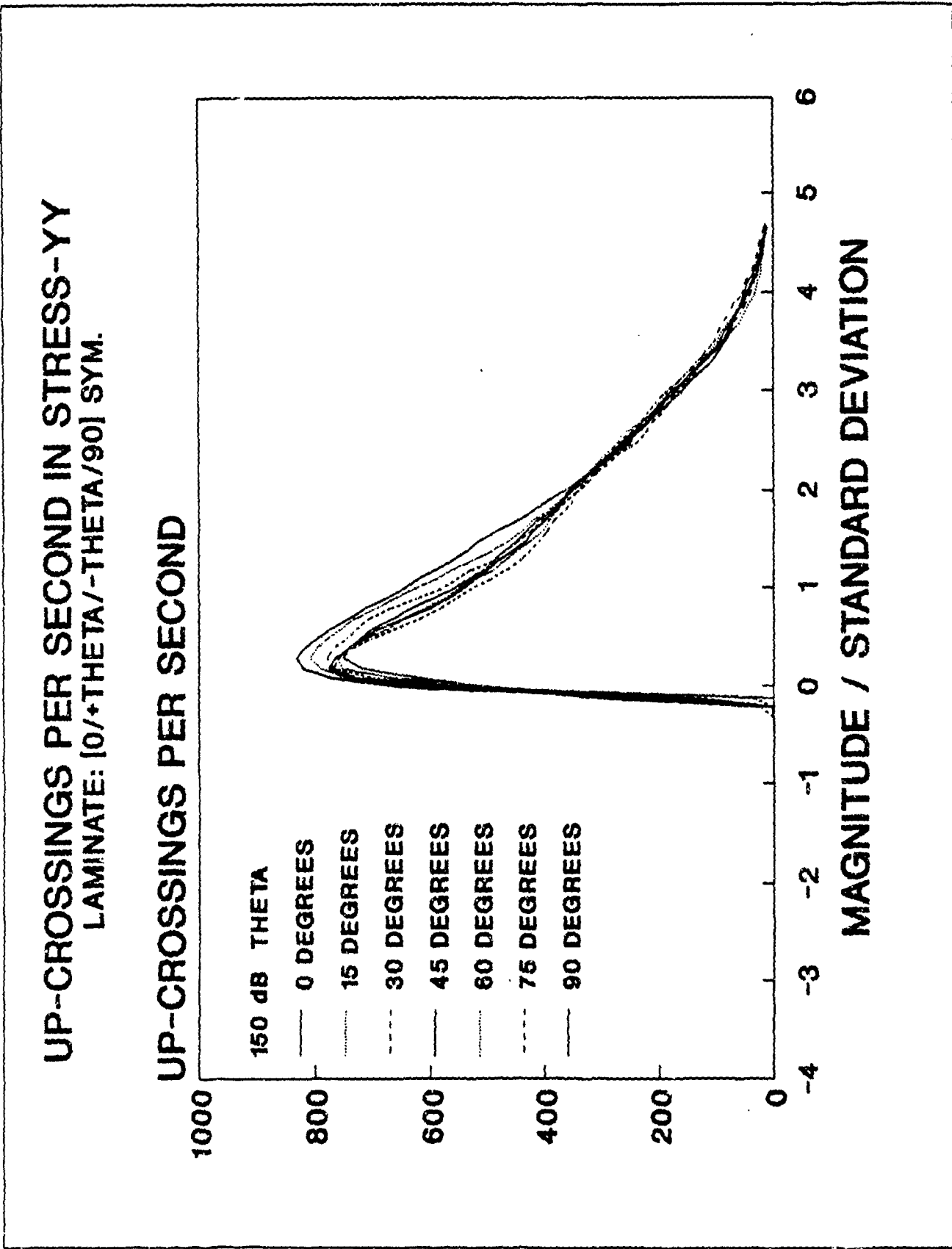


Figure 33 Up-Crossing Rate for  $\sigma_{yy}$  as a Function of Lay-Up Angle

# UP-CROSSINGS PER SECOND IN STRESS-XX LAMINATE: [THETA/ THETA]x2 SYMMETRIC

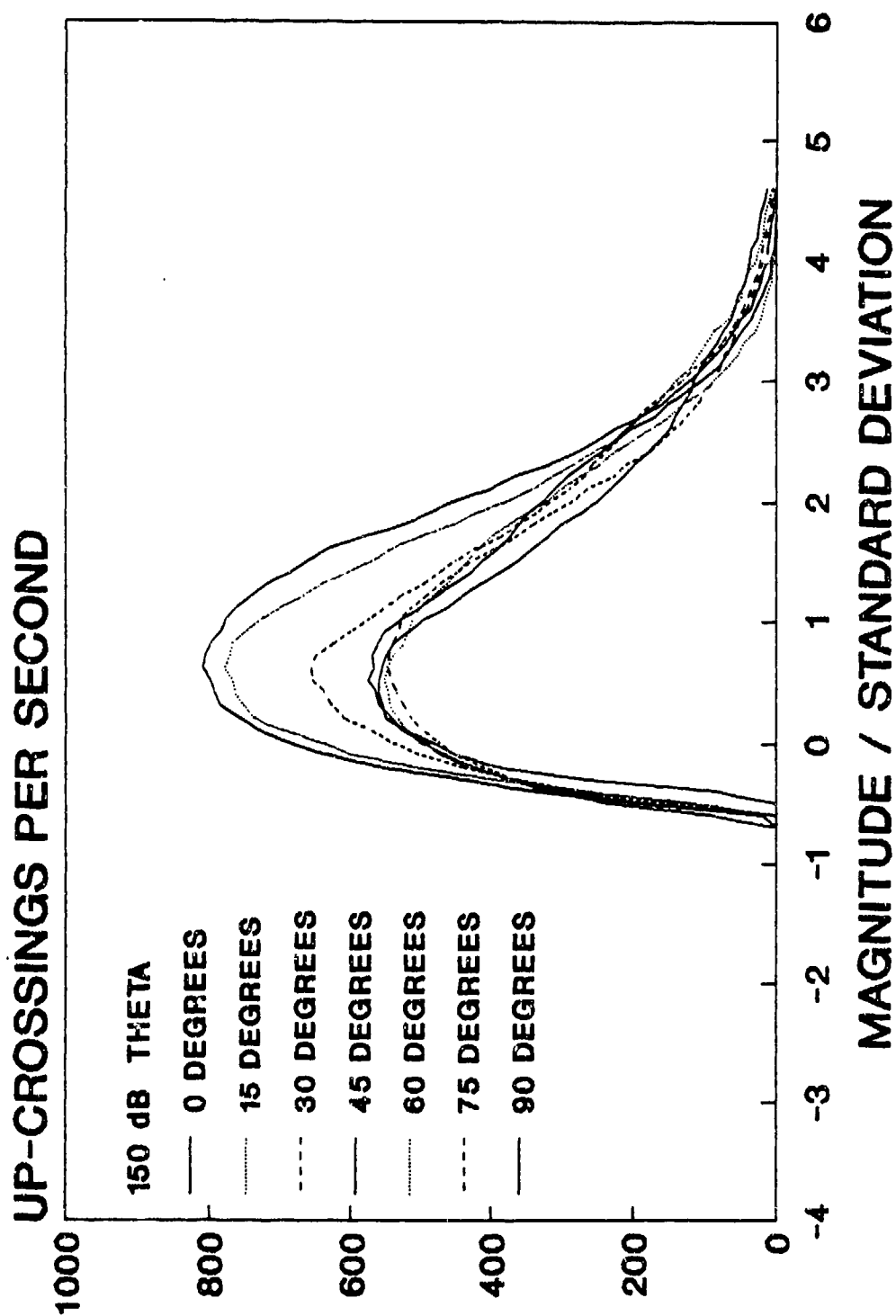


Figure 34 Up-Crossing Rate for  $\sigma_{xx}$  as a Function of Lay-Up Angle

# UP-CROSSINGS PER SECOND IN STRESS-YY LAMINATE: $[\theta/\theta/-\theta/\theta]_2$ SYMMETRIC

UP-CROSSINGS PER SECOND

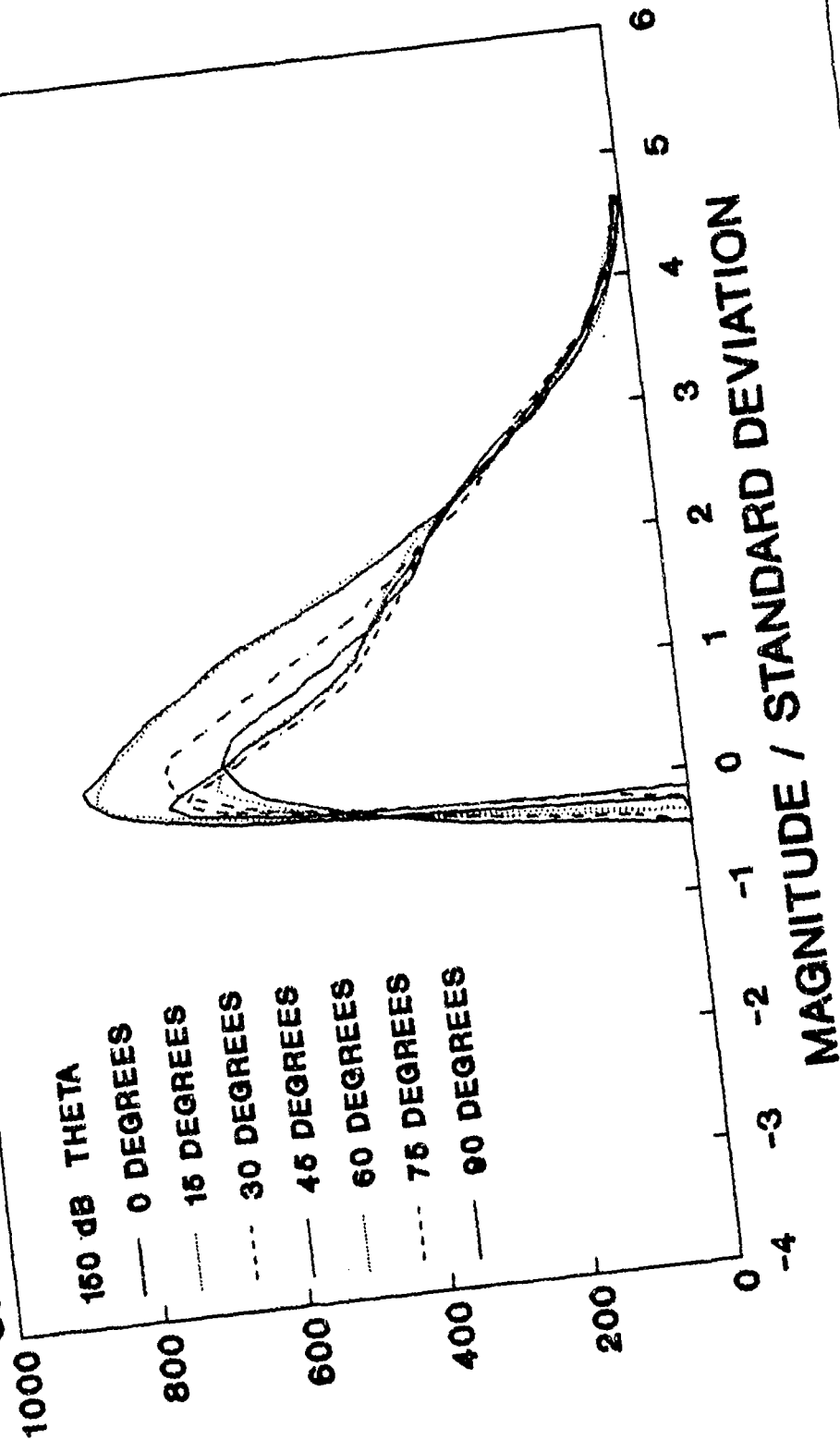


Figure 35 Up-Crossing Rate for  $\sigma_{yy}$  as a Function of Lay-Up Angle,  $[\theta/\theta/-\theta/\theta]_2$

# **RMS STRESSES AS A FUNCTION OF ANGLE LAMINATE [+THETA/-THETA]x2 SYMMETRIC**

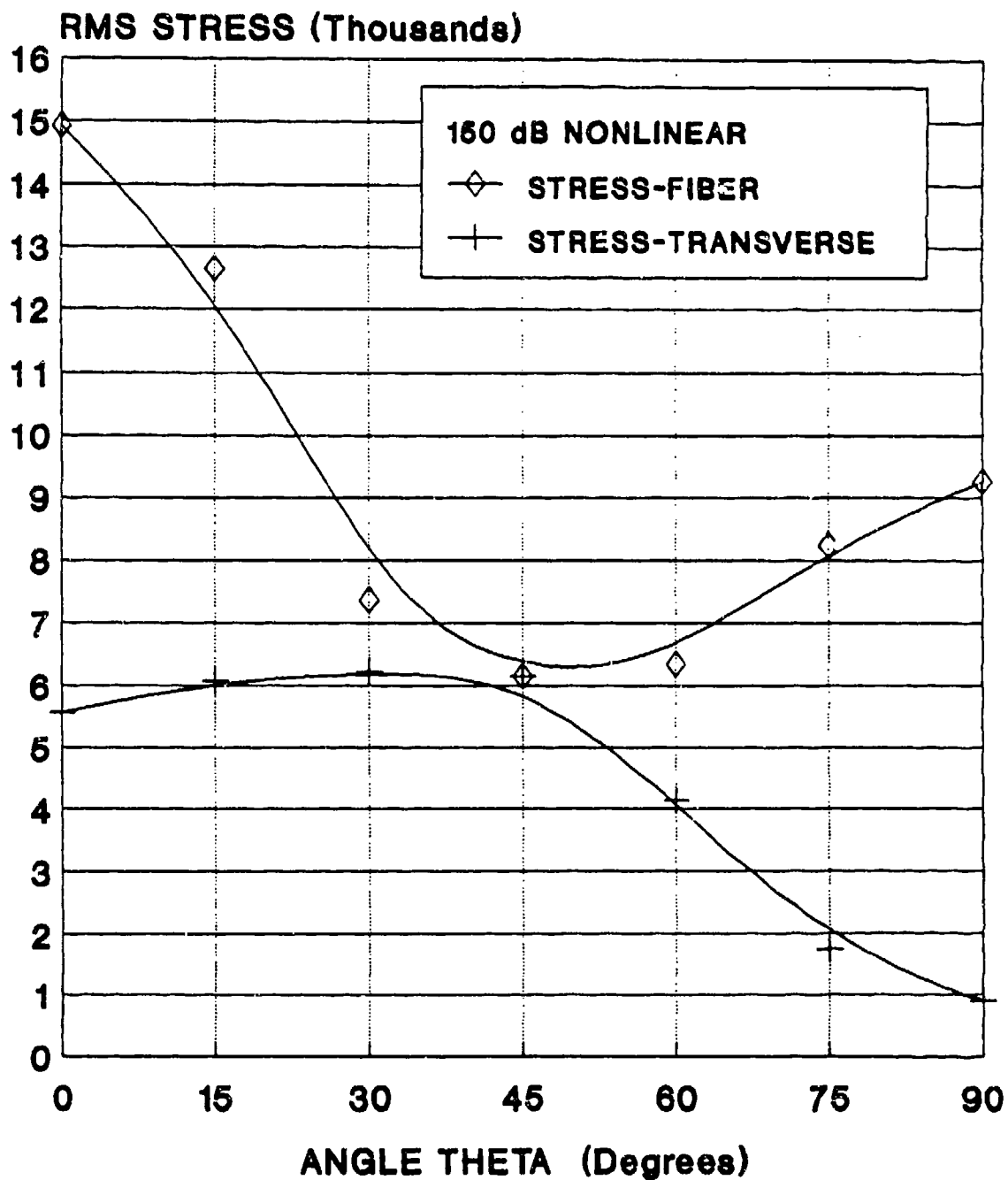


Figure 36 RMS of  $\sigma_1$ ,  $\sigma_t$  as a Function of Lay-Up Angle,  $[+\theta/-\theta]_{x2s}$

## APPENDIX A

## LISTING OF COMPUTER PROGRAM TDR

```
C*****
C****
C****      T D R
C****
C****      TIME DOMAIN RESPONSE ANALYSIS OF A SIMPLY SUPPORTED PLATE
C****      SUBJECTED TO UNIFORM RANDOM PRESSURE AND THERMAL LOAD
C****
C****      BASED ON THE WORK OF RIMAS VAICAITIS OF COLUMBIA UNIVERSITY
C****      AND S. T. CHOI (RESEARCH ASSISTANT), 1988-89
C****
C****      MODIFIED TO INCLUDE ORTHOTROPIC MATERIALS BY ROCKY ARNOLD,
C****      ANAMET LABORATORIES, INC., 1989
C****
C*****
C****
C****      SIMPLY-SUPPORTED SINGLE PANEL SUBJECTED TO UNIFORM RANDOM
C****      PRESSURE AND THERMAL LOADS.
C****
C****      THIS PROGRAM IS USED TO FIND THE DISPLACEMENT AND STRESS
C****      RESPONSE TIME HISTORIES FOR A SIMPLY SUPPORTED PANEL USING
C****      MODAL ANALYSIS IN THE TIME DOMAIN WITH NMODEX MODES IN THE
C****      X-DIRECTION AND NOMODEY MODES IN THE Y-DIRECTION.
C****
C****      LOADING IS UNIFORM AND TEMPERATURE DISTRIBUTION IS ASSUMED
C****      UNIFORM.
C****
C****      PARAMETERS
C****      NX      = MAXIMUM NO. OF MODES IN X-DIRECTION
C****      NY      = MAXIMUM NO. OF MODES IN Y-DIRECTION
C****      NXY     = NX * NY
C****      NTEQ    = MAXIMUM TOTAL NUMBER OF EQUATIONS (=2*NXY)
C****      NSTEPT  = MAXIMUM NO. OF TIME STEPS
C****      NMODEX  = ACTUAL NO. OF MODES IN X-DIRECTION USED IN ANALYSIS
C****      NMODEY  = ACTUAL NO. OF MODES IN Y-DIRECTION USED IN ANALYSIS
C****      RMSD    = ROOT MEAN SQUARE OF DISPLACEMENT RESPONSE
C****      RMSX    = ROOT MEAN SQUARE OF STRESS RESPONSE SIGMA(X)
C****      RMSY    = ROOT MEAN SQUARE OF STRESS RESPONSE SIGMA(Y)
C****      RMSXY   = ROOT MEAN SQUARE OF STRESS RESPONSE SIGMA(XY)
C****      RLOAD   = GAUSSIAN RANDOM PRESSURE
C****
C*****
```

```

REAL*4 TIME(10)
COMMON /COM0/ XL,YL,V,ZETA11
COMMON /COM1/ QIJ,WIJ2,C0
COMMON /COM2/ XYL,I,J,K,L
COMMON /COM3/ NMODEX,NMODEY,NMODEXY,NDIMX,NDIMY,NDIMXY,ILIN
COMMON /COM4/ VIJMN,ZIJKLMNRS
COMMON /COM5/ IHEAT,ZNTIJ
COMMON /RNG/ NR,XR,YR,DYR,HH,JR,JMAX,MR,XOUT,IFREQ,X1R,X2R,X3R,
1      Y1R,Y2R,Y3R,TOL
COMMON /XFER/ ISTEP,DSTEP,DDT,RLOAD(8192)
COMMON/ PROPS/ A11,A12,A22,A66,H,T1,T2,T3
DATA NDIMX,NDIMY,NDIMXY/3,3,9/
C*****
C**** READ IN INPUT DATA ****
C*****
TIME(1)=SECNDS(0.)
CALL READ(X,Y,DSTEP,NSTEP,NEQ,PI,WIJ,PQ1,C1,C2,C3,C4,
1      PX,PY,XYL,XL2,YL2,VIJMN,ZIJKLMNRS,IHEAT,ZNTIJ,
2      STHERX,STHERY,SPL)
TIME(2)=SECNDS(TIME(1))+TIME(1)
NR=NEQ
C*****
C**** CALL ROUTINE TO CALCULATE TIME DOMAIN SIMULATION OF PRESSURE ****
C*****
TIME(3)=SECNDS(TIME(2))+TIME(2)
CALL SIMLOAD(SPL)
TIME(4)=SECNDS(TIME(3))+TIME(3)
C*****
C**** INITIALIZE SUMMING PARAMETERS ****
C*****
SUMD=0.0
SUMD2=0.0
SUMX=0.0
SUMX2=0.0
SUMY=0.0
SUMY2=0.0
SUMXY=0.0
SUMXY2=0.0
T=0.0
XR=T
C*****
C**** COMPUTE DAMPING TERM ****
C*****
DO 5 I=1,NMODEX
DO 5 J=1,NMODEY
ZETAIJ(I,J)=ZETA11*(WIJ(1,1)/WIJ(I,J))
CO(I,J)=2.*ZETAIJ(I,J)*WIJ(I,J)
WIJ2(I,J)=WIJ(I,J)*WIJ(I,J)
5 CONTINUE
C*****
C*** COMPUTE PRESSURE TERM ****
C*****
DO 20 I=1,NMODEX

```

```

      DO 20 J=1,NMODEY
        QIJ(I,J)=PQ1/I/J*(1-(-1)**I)*(1-(-1)**J)
20    CONTINUE
C*****
C**** SOLVE PDEs FOR DISPLACEMENT ****
C*****
      TIME(5)=SECNDS(TIME(4))+TIME(4)
      DO 10 ISTEP=1,NSTEP
        TEND = FLOAT(ISTEP)*DSTEP
        HH=DMIN1(DSTEP,DDT)*0.125
        XOUT=TEND
        CALL RUNGE
        DO 30 I=1,NMODEX
          DO 30 J=1,NMODEY
            K=(I-1)*NMODEY+J
            A(I,J)=YR(K)
30      CONTINUE
C*****
C**** COMPUTE STRESS RESPONSE ****
C*****
      T=XR
      TD=DSTEP
      CALL RESPON(A,XL,YL,ISTEP,TD,C1,C2,C3,C4,PX,PY,XYL,IHEAT,
1          STHRX,STHERY,SUMD,SUMD2,SUMX,SUMX2,SUMY,SUMY2,
2          SUMXY,SUMXY2)
10    CONTINUE
      TIME(6)=SECNDS(TIME(5))+TIME(5)
C*****
C**** COMPUTE MEAN, MEAN SQUARE AND RMS VALUES ****
C*****
      SUMD=SUMD/FLOAT(NSTEP)
      SUMD2=SUMD2/FLOAT(NSTEP)
      RMSD=DSQRT(SUMD2)
      SUMX=SUMX/FLOAT(NSTEP)
      SUMX2=SUMX2/FLOAT(NSTEP)
      RMSX=DSQRT(SUMX2)
      SUMY=SUMY/FLOAT(NSTEP)
      SUMY2=SUMY2/FLOAT(NSTEP)
      RMSY=DSQRT(SUMY2)
      SUMXY=SUMXY/FLOAT(NSTEP)
      SUMXY2=SUMXY2/FLOAT(NSTEP)
      RMSXY=DSQRT(SUMXY2)
C*****
C**** WRITE OUT SIMPLE STATISTICS OF TIME DOMAIN RESPONSE ****
C*****
      WRITE(6,1000) SUMD, SUMD2, RMSD
      WRITE(6,1003) SUMX, SUMX2, RMSX
      WRITE(6,1004) SUMY, SUMY2, RMSY
c    WRITE(6,1005) SUMXY, SUMXY2, RMSXY
1000  FORMAT(' Displ. (in): Mean = ',E11.4,'      M.S. = ',E11.4,
+        '      RMS = ',E11.4)
1003  FORMAT(' sigmaX (psi): Mean = ',E11.4,'      M.S. = ',E11.4,
+        '      RMS = ',E11.4)

```

```

1004 FORMAT(' sigmaY (psi): Mean = ',E11.4,' M.S.= ',E11.4,
+          ' RMS = ',E11.4)
c1005 FORMAT(' tauXY (psi): Mean = ',E11.4,' M.S.= ',E11.4,
c      +          ' RMS = ',E11.4)
C**
      PRINT 1100
1100  FORMAT(/,' Output files FOR008: Response histories',/)
      TIME(7)=SECNDS(TIME(6))+TIME(6)
C*****
C****          PRINT OUT TIME SUMMARY          ****
C*****
      WRITE(6,9999)
9999  FORMAT(///,X,'SUMMARY OF TIME EXPENDITURES',/)
      WRITE(6,9998) TIME(2)-TIME(1)
9998  FORMAT(/,X,'TIME IN READ SUBROUTINE= ',F8.1,' SECONDS')
      WRITE(6,9997) TIME(3)-TIME(2)
9997  FORMAT(/,X,'TIME BETWEEN READ AND SIMLOAD SUBROUTINES= ',F8.1,
1      ' SECONDS')
      WRITE(6,9996) TIME(4)-TIME(3)
9996  FORMAT(/,X,'TIME IN SIMLOAD SUBROUTINE= ',F8.1,' SECONDS')
      WRITE(6,9995) TIME(5)-TIME(4)
9995  FORMAT(/,X,'TIME BETWEEN SIMLOAD AND RUNGE SUBROUTINES= ',F8.1,
1      ' SECONDS')
      WRITE(6,9994) TIME(6)-TIME(5)
9994  FORMAT(/,X,'TIME IN RUNGE SUBROUTINE= ',F8.1,' SECONDS')
      WRITE(6,9993) TIME(7)-TIME(6)
9993  FORMAT(/,X,'TIME BETWEEN RUNGE AND PROGRAM END= ',F8.1,
1      ' SECONDS')
      STOP
      END

```



```

C*****
C****                                     ****
C****                                     ****
C****                                     ****
C*****
SUBROUTINE IJKLMNRS(VIJMN,ZIJKLMNRS,ZNTIJ,P2,P3,P4X,P4Y,
1          XL2,YL2,IHEAT)
IMPLICIT REAL*8 (A-H,O-Z)
COMMON /COM2/ XYL,I,J,K,L
COMMON /COM3/ NMODEX,NMODEY,NMODEXY,NDIMX,NDIMY,NDIMXY,ILIN
COMMON /PROPS/ A11,A12,A22,A66,H,T1,T2,T3
DIMENSION VIJMN(NDIMX,NDIMY,NDIMX,NDIMY),ZNTIJ(NDIMX,NDIMY),
1          ZIJKLMNRS(NDIMXY,NDIMXY,NDIMXY,NDIMXY)
C*****
C**** COMPUTE LINEAR (HOMOGENEOUS) COMPONENT OF AIRY STRESS FUNCTION ****
C*****
DO 10 I=1,NMODEX
  CI2XL2=I*I/XL2
DO 10 J=1,NMODEY
  CJ2YL2=J*J/YL2
DO 10 M=1,NMODEX
  CM2XL2=M*M/XL2
DO 10 N=1,NMODEY
  CN2YL2=N*N/YL2
  VIJMN(I,J,M,N)=P2*(CI2XL2*(T1*CM2XL2+T2*CN2YL2)
1      +CJ2YL2*(T2*CM2XL2+T3*CN2YL2))
10 CONTINUE
IF(ILIN.EQ. 0) GO TO 20
C*****
C**** COMPUTE NONLINEAR (PARTICULAR) COMPONENT OF AIRY STRESS FUNCTION ****
C*****
DO 15 I=1,NMODEX
DO 15 J=1,NMODEY
  IJ=(I-1)*NMODEY+J
DO 15 K=1,NMODEX
DO 15 L=1,NMODEY
  KL=(K-1)*NMODEY+L
DO 15 M=1,NMODEX
DO 15 N=1,NMODEY
  MN=(M-1)*NMODEY+N
DO 15 IR=1,NMODEX
  MPR=M+IR
  MMR=M-IR
DO 15 IS=1,NMODEY
  IRS=(IR-1)*NMODEY+IS
  NPS=N+IS
  NMS=N-IS
  NR=N*IR
  MS=M*IS
  ZIJKLMNRS(IJ,KL,MN,IRS) = P3 *
1      (MS*(NR-MS)*(FIJ(MPR,NPS)+FIJBAR(MMR,NMS)))+
2      MS*(NR+MS)*(FIJ(MMR,NPS)+FIJ(MPR,NMS)))
15 CONTINUE

```

```

C*****
C**** COMPUTE THERMAL COMPONENT OF AIRY STRESS FUNCTION ****
C*****
20  IF (IHEAT .NE. 1) THEN
    ELSE
      DO 30 I=1,NMODEX
        CI2XL2=I*I/XL2
        DO 30 J=1,NMODEY
          ZNTIJ(I,J)=P4X*CI2XL2+P4Y*J*J/YL2
30  CONTINUE
    END IF
    RETURN
    END

```

```

C*****
C****                                     ****
C****          S I M L O A D          ****
C****                                     ****
C*****
C      N      -- NO. OF INTERVALS IN THE SPECTRUM
C              N SHOULD BE AN INTEGER POWER OF TWO
C      NPT     -- NO. OF POINTS FOR THE TIME SERIES
C              NPT SHOULD BE INTEGER POWER OF TWO. NPT>N
C      ISEED   -- RANDOM NUMBER SEED
C-----
      SUBROUTINE SIMLOAD(SPL)
      IMPLICIT REAL*8 (A-H,O-Z)
      COMMON /XFER/ ISTEP,DSTEP,DT,Y(8192)
      DIMENSION X(8192),SP(3500),W(3500),RAND(8192)
      COMPLEX X,ZIMAG
      LOGICAL INVERSE
      DATA FMAX,INVERSE/500.,.TRUE./
      DATA N,NPT /512, 4096/
C*****
C****  INITIALIZE VARIABLES  ****
C*****
      SPP=8.41*10**(-18.+SPL/10.)
      PI  = 3.141592654
      PI2 = PI * 2.0
      NP1 = N + 1
      ZIMAG = CMPLX(0.0,1.0)
      SPPW=SPP/PI2
      WU=FMAX*PI2
      DW  = WU / FLOAT(N)
      DO 119 I=1,NP1
          SP(I)=SPPW
          W(I)=(I-1)*DW
119  CONTINUE
      AREA=SPP*FMAX
      SQ2DW = DSQRT(2.0*DW)
      TTOTAL=PI2/DW
      DT=TTOTAL/FLOAT(NPT)
C*****
C****  SET X(1)=0. IN ORDER TO OBTAIN NEW MEAN ZERO TIME SERIES  ****
C*****
      X(1) = CMPLX(0.0,0.0)
      DO 50 I = N+1,NPT
          X(I) = CMPLX(0.0,0.0)
50  CONTINUE
C*****
C****  GENERATE RANDOM PHASE ANGLES UNIFORMLY DISTRIBUTED BETWEEN  ****
C****  ZERO AND 2.*PI  ****
C*****
      ISEED=12357
      DO 51 I=1,N
51  RAND(I)=RAN(ISEED)
      DO 60 I=2,N+1

```

```

      PHI = RAND(I-1) * PI2
      P1 = SQ2DW * DSQRT(SP(I))
      X(I) = P1 * CDEXP(-ZIMAG*PHI)
60    CONTINUE
C*****
C****  PERFORM FORWARD TRANSFORM                      ****
C*****
      CALL FFT (X,NPT,1)
C*****
C****  GET REAL PART                                  ****
C*****
      DO 70 I=1,NPT
        Y(I) = REAL(X(I))
70    CONTINUE
      RETURN
      END

```

```

C*****
C****                                     ****
C****                                F I J                                ****
C****                                     ****
C*****
      FUNCTION FIJ(IG,IH)
      IMPLICIT REAL*8 (A-H,O-Z)
      COMMON /COM2/ XYL,I,J,K,L
      COMMON /PROPS/ A11,A12,A22,A66,H,T1,T2,T3
      IPK=I+K
      IMK=I-K
      JPL=J+L
      JML=J-L
      KH=K*IH
      LG=L*IG
      FIJ=2.*KH*LG*(BETA(IPK,IG)+BETA(IMK,IG))*(BETA(JPL,IH)+
1      BETA(JML,IH))-(KH**2+LG**2)*(GAMMA(IPK,IG)-
2      GAMMA(IMK,IG))*(GAMMA(JPL,IH)-GAMMA(JML,IH))
      DENOM=A22*IG**4+(A66+2.*A12)*XYL**2*(IH*IG)**2
1      +A11*XYL**4*IH**4
      FIJ=FIJ/(H*DENOM)
      RETURN
      END

```

```

C*****
C****
C****          F I J B A R
C****
C*****
FUNCTION FIJBAR(IG,IH)
IMPLICIT REAL*8 (A-H,O-Z)
COMMON /COM2/ XYL,I,J,K,L
COMMON /PROPS/ A11,A12,A22,A66,H,T1,T2,T3
IF (IG .EQ. IH .AND. IG .EQ. 0) THEN
    FIJBAR=0.0
ELSE
    IPK=I+K
    IMK=I-K
    JPL=J+L
    JML=J-L
    KH=K*IH
    LG=L*IG
    FIJBAR=2.*KH*LG*(BETA(IPK,IG)+BETA(IMK,IG))*(BETA(JPL,IH)+
1      BETA(JML,IH))-(KH**2+LG**2)*(GAMMA(IPK,IG)-
2      GAMMA(IMK,IG))*(GAMMA(JPL,IH)-GAMMA(JML,IH))
    DENOM=A22*IG**4+(A66+2.*A12)*XYL**2*(IH*IG)**2+A11*XYL**4*IH**4
    FIJBAR=FIJBAR/(H*DENOM)
END IF
RETURN
END

```

```

C*****
C****
C****          B E T A
C****
C*****
      FUNCTION BETA(IP,IQ)
      IMPLICIT REAL*8 (A-H,O-Z)
      IF (IP .EQ. IQ .AND. IP .NE. 0) THEN
        BETA = 1.0
      ELSE IF (IP .EQ. -IQ .AND. IP .NE. 0) THEN
        BETA = -1.0
      ELSE
        BETA = 0.0
      END IF
      RETURN
      END

```

```

C*****
C****                                     ****
C****           G A M M A               ****
C****                                     ****
C*****
      FUNCTION GAMMA(IP,IQ)
      IMPLICIT REAL*8 (A-H,O-Z)
      IF (IP**2+IQ**2 .EQ. 0) THEN
        GAMMA = 2.0
      ELSE IF (IABS(IP) .EQ. IABS(IQ) .AND. IP .NE. 0) THEN
        GAMMA = 1.0
      ELSE
        GAMMA = 0.0
      END IF
      RETURN
      END

```



```

C*****
C****
C****          D I F F E Q
C****
C*****
      SUBROUTINE DIFFEQ
      IMPLICIT REAL*8 (A-H,O-Z)
      COMMON /RNG/ N,X,Z,ZPRIME,HH,JR,JMAX,MR,XOUT,IFREQ,
1      X1,X2,X3,Y1,Y2,Y3,TOL
      COMMON /XFER/ ISTEP,DSTEP,DT,RLOAD(8192)
      DIMENSION Z(18),ZPRIME(18),Y1(18),Y2(18),Y3(18)
      DIMENSION QIJ(3,3),WIJ2(3,3),CO(3,3),ZNTIJ(3,3),
1      VIJMN(3,3,3,3),ZIJKLMNRS(9,9,9,9)
      COMMON /COM1/ QIJ, WIJ2, CO
      COMMON /COM3/ NMODEX,NMODEY,NMODEXY,NDIMX,NDIMY,NDIMXY,ILIN
      COMMON /COM4/ VIJMN, ZIJKLMNRS
      COMMON /COM5/ IHEAT, ZNTIJ
      DATA ICNT/0/
C*****
C**** INTERPOLATE TO DETERMINE LOAD TERM
C*****
      NEQ=N
      IF(ICNT.GT.0)GO TO 2
      ICNT=1
      IPLUS=1
      PRM=0.0
      PRP=0.0
      T1=0.0
      T0=-DT
      SLOPE=0.0
      PR=0.0
2      IF(X.GT.T1) GO TO 1
      IF(X.LT.T0) GO TO 2
      PR=PRM+(X-T0)*SLOPE
      GO TO 20
3      IPLUS=-1
1      ICNT=ICNT+IPLUS
      PRM=RLOAD(ICNT-1)
      PRP=RLOAD(ICNT)
      SLOPE=(PRP-PRM)/DT
      T0=T0+DT*IPLUS
      T1=T1+DT*IPLUS
      IPLUS=1
      GO TO 2
20     CONTINUE
C*****
C**** SPECIFY DIFFERENTIAL EQUATIONS
C*****
      DO 5 K=1,NMODEXY
      ZPRIME(K)=Z(K+NMODEXY)
5      CONTINUE
      DO 10 I=1,NMODEX
      DO 10 J=1,NMODEY

```

```

      K=(I-1)*NMODEY+J
      KK=NMODEXY+K
      CALL VZIJ(VIJ,ZIJ,Z,NEQ,I,J)
      ZPRIME(KK) = PR*QIJ(I,J)-CO(I,J)*Z(KK)-WIJ2(I,J)*Z(K)
10      -VIJ*Z(K)-ZIJ+ZNTIJ(I,J)*Z(K)
      CONTINUE
      RETURN
      END

```

```

C*****
C****
C****
C****
C*****
SUBROUTINE VZIJ(VIJ,ZIJ,Z,NEQ,I,J)
IMPLICIT REAL*8 (A-H,O-Z)
DIMENSION Z(NEQ), VIJMN(3,3,3,3),
+      ZIJKLMNRS(9,9,9,9)
COMMON /COM3/ NMODEX,NMODEY,NMODEXY,NDIMX,NDIMY,NDIMXY,ILIN
COMMON /COM4/ VIJMN,ZIJKLMNRS
C**
VIJ=0.0
ZIJ=0.0
IJ=(I-1)*NMODEY+J
C**
DO 10 M=1,NMODEX
DO 10 N=1,NMODEY
MN=(M-1)*NMODEY+N
IF(ILIN.EQ. 0) GO TO 10
VIJ=VIJ+Z(MN)*Z(MN)*VIJMN(I,J,M,N)
ZKLRS=0.0
DO 20 K=1,NMODEX
DO 20 L=1,NMODEY
KL=(K-1)*NMODEY+L
ZRS=0.0
DO 30 IR=1,NMODEX
DO 30 IS=1,NMODEY
IRS=(IR-1)*NMODEY+IS
ZRS=ZRS+Z(IRS)*ZIJKLMNRS(IJ,KL,MN,IRS)
30 CONTINUE
ZKLRS=ZKLRS+Z(KL)*ZRS
20 CONTINUE
ZIJ=ZIJ+Z(MN)*ZKLRS
10 CONTINUE
RETURN
END

```

```

C*****
C****
C****      R E S P O N      ****
C****
C*****
SUBROUTINE RESPON(A,XL,YL,ISTEP,DT,C1,C2,C3,C4,PX,PY,XYL,IHEAT,
1          STHERX,STHERY,SUMD,SUMD2,SUMX,SUMX2,SUMY,SUMY2,
2          SUMXY,SUMXY2)
IMPLICIT REAL*8 (A-H,O-Z)
DIMENSION A(NDIMX,NDIMY)
COMMON /COM3/ NMODEX,NMODEY,NMODEXY,NDIMX,NDIMY,NDIMXY,ILIN
COMMON /PROPS/ A11,A12,A22,A66,H,T1,T2,T3
C*****
C**** INITIALIZE      ****
C*****
DISPL=0.0
SIGMAX=0.0
SIGMAY=0.0
TAUXY=0.0
C*****
C**** COMPUTE STRESSES BY SUMMING LINEAR AND NONLINEAR TERMS      ****
C*****
DO 10 M=1,NMODEX
  SINMX=DSIN(M*PX)
  COSMX=DCOS(M*PX)
  XLM=M/XL
  DO 10 N=1,NMODEY
    YLN=N/YL
    SINNY=DSIN(N*PY)
    COSNY=DCOS(N*PY)
    DISPL=DISPL+A(M,N)*SINMX*SINNY
C*****
C**** CALCULATE STRESSES FROM NONLINEAR PART OF AIRY STRESS FUNCTION      ****
C*****
CALL SUMRS(RSX1,RSX2,RSY1,RSY2,RSXY1,RSXY2,M,N,
1          A,PX,PY,XL,YL,XYL)
  CC1=C2*A(M,N)
  IF(ILIN.EQ. 0) CC1=0.
C*****
C**** ADD LINEAR AND NONLINEAR CONTRIBUTIONS      ****
C*****
  CC0=A(M,N)*(C1*SINMX*SINNY+CC1)
  SIGMAX=SIGMAX+CC0*(T1*XLM**2+T2*YLN**2)-C3*A(M,N)*(RSX1+RSX2)
  SIGMAY=SIGMAY+CC0*(T2*XLM**2+T3*YLN**2)-C3*A(M,N)*(RSY1+RSY2)
  TAUXY=TAUXY+(C4/A66)*A(M,N)*COSMX*COSNY-C3*A(M,N)*(RSXY1+RSXY2)
10 CONTINUE
C*****
C**** ADD IN THERMAL COMPONENT      ****
C*****
  IF (IHEAT.NE. 1) THEN
    ELSE
      SIGMAX=SIGMAX-STHERX
      SIGMAY=SIGMAY-STHERY

```

```

      END IF
C*****
C****  PRINT OUT TIME DOMAIN RESPONSE      ****
C*****
      T=DT*ISTEP
      WRITE(6,100) T, DISPL, SIGMAX, SIGMAY
100   FORMAT(2X,F8.6,3(2X,E14.6))
      WRITE(1,1000) T,DISPL,SIGMAX,SIGMAY,TAUXY
1000  FORMAT(5E10.3)
C*****
C****  SUM DISPLACEMENT/STRESSES AND SQUARES      ****
C*****
      SUMD=SUMD+DISPL
      SUMD2=SUMD2+DISPL*DISPL
      SUMX=SUMX+SIGMAX
      SUMX2=SUMX2+SIGMAX*SIGMAX
      SUMY=SUMY+SIGMAY
      SUMY2=SUMY2+SIGMAY*SIGMAY
      SUMXY=SUMXY+TAUXY
      SUMXY2=SUMXY2+TAUXY*TAUXY
      RETURN
      END

```

```

C*****
C****                                     ****
C****                                S U M R S                                ****
C****                                     ****
C*****
SUBROUTINE SUMRS(RSX1,RSX2,RSY1,RSY2,RSXY1,RSXY2,M,N,
1          A,PX,PY,XL,YL,XYL)
IMPLICIT REAL*8 (A-H,O-Z)
COMMON /COM3/ NMODEX,NMODEY,NMODEXY,NDIMX,NDIMY,NDIMXY,ILIN
COMMON /PROPS/ A11,A12,A22,A66,H,T1,T2,T3
DIMENSION A(NDIMX,NDIMY)
C*****
C**** INITIALIZE                                     ****
C*****
S1=A22*H
S2=(2.*A12+A66)*H
S3=A11*H
RSX1=0.0
RSX2=0.0
RSY1=0.0
RSY2=0.0
RSXY1=0.0
RSXY2=0.0
IF(ILIN.EQ. 0) RETURN
C*****
C**** COMPUTE NONLINEAR STRESSES (FROM PARTICULAR SOLUTION) ****
C*****
DO 10 IR=1,NMODEX
  MPR=M+IR
  MMR=M-IR
  MPR2=MPR*MPR
  MMR2=MMR*MMR
  XLMPR=MPR/XL
  XLMMR=MMR/XL
  XLMPR2=XLMPR**2
  XLMMR2=XLMMR**2
  CMPRX=DCOS(MPR*PX)
  CMMRX=DCOS(MMR*PX)
  SMPRX=DSIN(MPR*PX)
  SMMRX=DSIN(MMR*PX)
DO 10 IS=1,NMODEY
  NPS=N+IS
  NMS=N-IS
  NPS2=NPS*NPS
  NMS2=NMS*NMS
  YLNPS=NPS/YL
  YLNMS=NMS/YL
  YLNPS2=YLNPS**2
  YLNMS2=YLNMS**2
  CNPSY=DCOS(NPS*PY)
  CNMSY=DCOS(NMS*PY)
  SNPSY=DSIN(NPS*PY)
  SNMSY=DSIN(NMS*PY)

```

```

XYNPS=XYL*NPS
XYNMS=XYL*NMS
XYNPS2=XYNPS**2
XYNM32=XYNMS**2
C*****
C**** TERMS FOR WHICH "KR .NE. ML" ****
C*****
IF (N*IR .EQ. M*IS) THEN
ELSE
PP1=CMPRX*CNPS/(S1*MPR2**2+S2*MPR2*XYNPS2+S3*XYNPS2**2)
PP2=CMMRX*CNM/Y/(S1*MMR2**2+S2*MMR2*XYNMS2+S3*XYNMS2**2)
PP5=SMPRX*SNPSY/(S1*MPR2**2+S2*MPR2*XYNPS2+S3*XYNPS2**2)
PP6=SMMRX*SNMSY/(S1*MMR2**2+S2*MMR2*XYNMS2+S3*XYNMS2**2)
Q1=A(IR,IS)*M*IS*(N*IR-M*IS)
RSX1=RSX1+Q1*(YLNPS2*PP1+YLNMS2*PP2)
RSY1=RSY1+Q1*(XLMPR2*PP1+XLMMR2*PP2)
RSXY1=RSXY1+Q1*(XLMPR*YLNPS*PP5+XLMMR*YLNMS*PP6)
END IF
C*****
C**** TERMS FOR WHICH "KR .EQ. ML" ****
C*****
PP3=CMPRX*CNMSY/(S1*MPR2**2+S2*MPR2*XYNMS2+S3*XYNMS2**2)
PP4=CMMRX*CNPSY/(S1*MMR2**2+S2*MMR2*XYNPS2+S3*XYNPS2**2)
PP7=SMPRX*SNMSY/(S1*MPR2**2+S2*MPR2*XYNMS2+S3*XYNMS2**2)
PP8=SMMRX*SNPSY/(S1*MMR2**2+S2*MMR2*XYNPS2+S3*XYNPS2**2)
Q2=A(IR,IS)*M*IS*(N*IR+M*IS)
RSX2=RSX2+Q2*(YLNMS2*PP3+YLNPS2*PP4)
RSY2=RSY2+Q2*(XLMPR2*PP3+XLMMR2*PP4)
RSXY2=RSXY2+Q2*(XLMPR*YLNMS*PP7+XLMMR*YLNPS*PP8)
10 CONTINUE
RETURN
END

```

```

C*****
C****                                     ****
C****                                R U N G E                                ****
C****                                     ****
C*****
SUBROUTINE RUNGE
  IMPLICIT REAL*8 (A-H,O-Z)
  COMMON /RNG/N,X,Y,DY,HH,J,JMAX,M, XOUT,IFREQ,X1,X2,X3,Y1,Y2,Y3,TOL
  DIMENSION Y(18),DY(18),Y1(18),Y2(18),Y3(18)
  J=1
  JMAX=1
  IFREQ=3
  M=1
  CALL EUNKUT
  RETURN
  END

```



```

C*****
C****
C****
C****
C*****

SUBROUTINE RUNKU1
  IMPLICIT REAL*8 (A-H,O-Z)
  COMMON/RNG/N, X,Y,DY,HH,J,JMAX,M, XOUT,IFREQ,X1,X2,X3,Y1,Y2,Y3,TOL
  DIMENSION Y(18),DY(18),Y1(18),Y2(18),Y3(18)
  INDE9 = 0
  CALL ADJSTP
  IF(J-JMAX) 10,10,50
10 INDE9 = INDE9 + 1
  CALL INTPOL
  IF(J-JMAX) 20,20,50
20 CALL STEP
  X1 = X2
  X2 = X3
  X3 = X
  DO 30 I = 1, N
    Y1(I) = Y2(I)
    Y2(I) = Y3(I)
30 Y3(I) = Y(I)
  IF (INDE9 - IFREQ) 10,40,40
40 INDE9 = 0
  CALL ADJSTP
  IF(J-JMAX) 10,10,50
50 RETURN
  END

```

```

C*****
C****                                     ****
C****                                A D J S T P                                ****
C****                                     ****
C*****

```

```

SUBROUTINE ADJSTP
IMPLICIT REAL*8 (A-H,O-Z)
COMMON/RNG/N,X,Y,DY,HH,J,JMAX,M,XOUT,IFREQ,X1,X2,X3,Y1,Y2,Y3,TOL
DIMENSION Y(18),DY(18),Y1(18),Y2(18),Y3(18)
KSL=0
HFACT      = 1.0 D+31
HFACT1     = 1.0D+30
GO TO (30,10), M
10 H1      = HH
   HH      = 2.0 * HH
   X       = X1
   DO 20 I = 1, N
20 Y(I)    = Y1(I)
   GO TO 100
30 KSL=1
40 H1      = HH
   XXX     = X
   DO 50 I = 1, N
50 Y1(I)   = Y(I)
   X1      = X
   CALL INTPOL
   IF(J-JMAX) 60,60,250
60 CALL STEP
   DO 70 I = 1, N
70 Y2(I)   = Y(I)
   X2      = X
   CALL INTPOL
   IF(J-JMAX) 80,80,250
80 CALL STEP
   DO 90 I = 1, N
   Y3(I)    = Y(I)
90 Y(I)    = Y1(I)
   X3      = X
   X       = XXX
   HH      = 2.0 * HH
100 CALL STEP
   DO 150 I = 1, N
   DELY    = DABS ( Y(I)-Y3(I))/30.0
   IF(DELY -DABS (Y2(I))*TOL )120,110,110
110 IF( DABS (Y2(I))-TOL) 120,130,130
120 HFIRST = 1.0D+30
   GO TO 140
130 HFIRST= (DABS (Y2(I))* TOL/DELY ) **0.2
140 CONTINUE
150 HFACT=DMIN1 (HFACT, HFIRST )
   IF (HFACT1 - HFACT) 160,160,170
160 HH     = 2.0 * H1
   GO TO (40,230), M

```

```
170 HH      = H1 * HFACT
    GO TO (180,230), M
180 IF(KSL) 220,220,190
190 KSL=0
    IF(DABS (HH)-DABS (H1)) 200,220,220
200 DO 210 I = 1, N
210 Y(I)     = Y1(I)
    X       = XXX
    GO TO 40
220 KSL=0
    M       = 2
230 DO 240 I = 1, N
240 Y(I)     = Y3(I)
250 RETURN
    END
```

```

C*****
C****
C****
C****
C****
C*****
SUBROUTINE STEP
  IMPLICIT REAL*8 (A-H,O-Z)
  COMMON /RNG/N,X,Y,DY,HH,J,JMAX,M,XOUT,IFREQ,X1,X2,X3,Y1,Y2,Y3,TOL
  DIMENSION Y(18),DY(18),Y1(18),Y2(18),Y3(18)
  DIMENSION Y0(18),P1(18)
  DO 10 I = 1, N
10 Y0(I) = Y(I)
   X0 = X
   CALL DIFFEQ
   DO 20 I = 1, N
   P1(I) = DY(I) * HH
20 Y(I) = Y0(I) + P1(I)*0.5
   X = X0 + HH*0.5
   CALL DIFFEQ
   DO 30 I = 1, N
   P1(I) = P1(I) + 2.0*HH*DY(I)
30 Y(I) = Y0(I) + 0.5*HH*DY(I)
   CALL DIFFEQ
   DO 40 I = 1, N
   P1(I) = P1(I) + 2.0*HH*DY(I)
40 Y(I) = Y0(I) + HH*DY(I)
   X = X0 + HH
   CALL DIFFEQ
   DO 50 I = 1, N
50 Y(I) = Y0(I) + (P1(I) + HH*DY(I))*0.1666667
   RETURN
  END

```

```

C*****
C****                                     ****
C****                                I N T P O L                                ****
C****                                     ****
C*****
SUBROUTINE INTPOL
  IMPLICIT REAL*8 (A-H,O-Z)
  COMMON /RNG/N,X,Y,DY,HH,J,JMAX,M,XOUT,IFREQ,X1,X2,X3,Y1,Y2,Y3,TOL
  DIMENSION Y(18),DY(18),Y1(18),Y2(18),Y3(18)
  IF(DABS (XOUT - X)-DABS (HH)) 10,10,20
10 HH=XOUT-X
  CALL STEP
  J = J + 1
20 RETURN
  END

```

```

C*****
C****                                     ****
C****                                     ****
C****                                     ****
C*****
SUBROUTINE FFT(X,N,K)
IMPLICIT INTEGER (A-Z)
REAL*4 GAIN,PI2,ANG,RE,IM
COMPLEX X(N),XTEMP,T,U(16),V,W
LOGICAL NEW
DATA PI2,GAIN,NO,KO/6.283185307,1.0,0,0/
NEW=NO.NE.N
IF(.NOT.NEW)GO TO 2
L2N=0
NO=1
1  L2N=L2N+1
   NO=NO+NO
   IF(NO.LT.N) GO TO 1
   GAIN=1.0/N
   ANG=PI2*GAIN
   RE=COS(ANG)
   IM=SIN(ANG)
2  IF(.NOT.NEW.AND.K*KO.GE.1) GO TO 4
   U(1)=CMPLX(RE,-SIGN(IM,FLOAT(K)))
   DO 3 I=2,L2N
3  U(I)=U(I-1)*U(I-1)
   KO=K
4  SBY2=N
   DO 7 STAGE=1,L2N
   V=U(STAGE)
   W=(1.0,0.0)
   S=SBY2
   SBY2=S/2
   DO 6 L=1,SBY2
   DO 5 I=1,N,S
   P=I+L-1
   Q=P+SBY2
   T=X(P)+X(Q)
   X(Q)=(X(P)-X(Q))*W
5  X(P)=T
6  W=W*V
7  CONTINUE
   DO 9 I=1,N
   INDEX=1-1
   JNDEX=0
   DO 8 J=1,L2N
   JNDEX=JNDEX+JNDEX
   ITEMP=INDEX/2
   IF(ITEMP+ITEMP.NE.INDEX)JNDEX=JNDEX+1
   INDEX=ITEMP
8  CONTINUE
   J=JNDEX+1
   IF(J.LT.I)GO TO 9

```

```
      XTEMP=X(J)
      X(J)=X(I)
      X(I)=XTEMP
9     CONTINUE
      IF(K.GT.0)RETURN
      DO 10 I=1,N
10    X(I)=X(I)*GAIN
      RETURN
      END
```

# PROGRAM PDF

```

C*****
C****
C**** THIS PROGRAM IS USED TO CALCULATE THE PROBABILITY DENSITY *****
C**** FUNCTION, PEAK DISTRIBUTION, AND UP-CROSSING RATE OF A RANDOM *****
C**** PROCESS. *****
C****
C**** THE CALCULATION IS DONE FROM -4*SD TO 4*SD WITH NDIV INTERVALS *****
C**** IN EACH STANDARD DEVIATION (SD). THE TOTAL NUMBER OF INTERVALS *****
C**** IS 8*NDIV WITH THE FIRST INTERVAL BEING -INFINITY TO *****
C**** -(4,-(4-1/NDIV)SD) AND THE LAST INTERVAL BEING (4-1/NDIV)SD) TO *****
C**** INFINITY. *****
C****
C**** THE INPUT DATA FILE IS FOR001.DAT WHICH CONTAINS THE RESPONSE *****
C**** TIME HISTORY PRODUCED BY PROGRAM TDR. *****
C****
C*****
COMMON/TITLES/ TITLE(20),SUBTIT(20)
DIMENSION F(13000), XDENS(200), XNPK(200), XCROSS(200)
CALL READDATA(F,NPT,SD,DSD,NHALF,NHALF1,
1 NDIV,NDIVT,DX,TTOTAL,SHIFT)
CALL DENSITY(F,XDENS,NPT,SD,DSD,NHALF,NHALF1,
1 NDIVT,DX,SHIFT)
CALL PEAKDIS(F,XNPK,NPT,SD,DSD,NHALF,NHALF1,
1 NDIVT,DX,TTOTAL,SHIFT)
CALL UPCROSSR(F,XCROSS,NPT,SD,DSD,NHALF,NHALF1,
1 NDIVT,DX,TTOTAL,SHIFT)
C*****
C****
C**** INFORM USER OF OUTPUT FILES AND CONTENTS *****
C****
C*****
TYPE *, '
TYPE *, ' Output files: FOR007 -- Probability density and'
TYPE *, ' theoretical Gaussian'
TYPE *, ' Output files: FOR008 -- Peak distribution'
TYPE *, ' Output files: FOR009 -- Upcrossing rate'
TYPE *, ' Output files: FOR010 -- Theoretical Gaussian'
TYPE *, ' Output files: FOR011 -- Theoretical Rayleigh'
STOP
END
C*****
C****
C**** SUBROUTINE READDATA *****
C****
C**** READS DATA, COMPUTES THE MEAN, RMS, STANDARD DEVIATION, *****
C**** COEFFICIENTS OF SKEWNESS, KURTOSIS OF THE PROCESS *****
C****
C*****
SUBROUTINE READDATA(F,NPT,SD,DSD,NHALF,NHALF1,NDIV,NDIVT,DX,
1 TTOTAL,SHIFT)
DIMENSION F(1)
COMMON/TITLES/ TITLE(20),SUBTIT(20)

```



```

CHARACTER*80 DUMP
C*****
C**** READ IN DATA FROM TDR (FOR001.DAT) AND SCREEN (UNIT 5) ****
C*****
      READ(1,10000) TITLE
10000 FORMAT(X,20A4)
      READ(1,10000) SUBTIT
      READ(1,10001) NPT,DT
10001 FORMAT(I5,E10.3)
      READ (5,111) ICOL,NDIV,IMEAN
111 FORMAT(3I5)
      TTOTAL=DT*(NPT-1)
      DX=1./NDIV          ! DX = nondimensional increment.
      NDIVT=NDIV*8        ! Total # of divisions from -4SD to +4SD
      NHALF=4*NDIV
      NHALF1=NHALF+1
      IF (ICOL .EQ. 2) THEN
      DO 81 I=1,NPT
81      READ (1,99) ZJUNK, F(I)
99      FORMAT(5E10.3)
      ELSE IF (ICOL .EQ. 3) THEN
      DO 82 I=1,NPT
82      READ (1,99) ZJUNK, ZJUNK, F(I)
      ELSE IF (ICOL .EQ. 4) THEN
      DO 83 I=1,NPT
83      READ (1,99) ZJUNK, ZJUNK, ZJUNK, F(I)
      ELSE
      DO 84 I=1,NPT
84      READ (1,99) ZJUNK, ZJUNK, ZJUNK, ZJUNK, F(I)
      END IF
C*****
C**** FIND MEAN AND RMS FOR PROCESS ****
C*****
      SUM=0.0
      SUM2=0.0
      DO 10 I=1,NPT
      SUM=SUM+F(I)
      SUM2=SUM2+F(I)**2
10      CONTINUE
      XMEAN=SUM/NPT
      SUM2=SUM2/NPT
      RMS=SQRT(SUM2)
C*****
C**** FIND STANDARD DEVIATION (SD), COEFFICIENTS OF SKEWNESS, KURTOSIS ****
C*****
      SUMV=0.0
      SUMS=0.0
      SUMK=0.0
      DO 20 I=1,NPT
      DIFF=F(I)-XMEAN
      DIFF2=DIFF*DIFF
      SUMV=SUMV+DIFF2
      SUM3=SUMS+DIFF*DIFF2

```

```

SUMK=SUMK+DIFF2*DIFF2
20  CONTINUE
    SD=SQRT(SUMV/NPT)
    COSKEW=SUMS/SD**3/NPT
    COKURT=SUMK/SD**4/NPT-3.
C*****
C**** WRITE OUT CALCULATIONS ****
C*****
    WRITE(6,1111)
1111  FORMAT(1H1,/,/,10X,'          PDF          ',/,
1      10X,'          FOR AFSC/ASD/PMRNA      ',/,
2      10X,'          WPAFB, OHIO             ',/,
3      10X,' BY ANAMET LABORATORIES, INC. ',/,
4      10X,'          HAYWARD, CALIFORNIA      ',/,
5      10X,' CONTRACT NO. F33615-89-C-3210',/)
    WRITE(6,1234) (TITLE(KK),KK=1,20)
1234  FORMAT(/,X,20A4)
    WRITE(6,1234) (SUBTIT(KK),KK=1,20)
    WRITE (6,30) XMEAN, RMS, SD, COSKEW, COKURT
30    FORMAT(10X,'          MEAN = ',E13.5,/,
+      10X,'          RMS = ',E13.5,/,
+      10X,'          STANDARD DEVIATION = ',E13.5,/,
+      10X,' COEFFICIENT OF SKEWNESS = ',E13.5,/,
+      10X,' COEFFICIENT OF KURTOSIS = ',E13.5,/)
C*****
C**** DIAGNOSTIC MESSAGE ****
C*****
    SHIFT=XMEAN/SD
    IF (SHIFT .GT. 0.05) THEN
        WRITE (6,100) XMEAN,SD,SHIFT
100    FORMAT (/,' MEAN VALUE OF THE PROCESS IS NOT ZERO!!!! ',/,
1      ' MEAN = ',E13.5,' SD = ',E13.5,' RATIO = ',F7.4,/)
    ELSE
        END IF
C*****
C**** RECOMPUTE F(I) WHEN MEAN IS EXCLUDED ****
C*****
    DO 98 I=1,NPT
        F(I)=F(I)-XMEAN
98    CONTINUE
        IF (IMEAN .EQ. 1) THEN
            SHIFT=0.0
        ELSE
            END IF
        DSD=SD/NDIV      ! Increment in actual value
C*****
C**** WRITE RESULTS ON OUTPUT FILES ****
C*****
    WRITE (7,310)
310    FORMAT(' PROBABILITY DENSITY',/)
        WRITE (7,313) XMEAN,SD,RMS,NPT,DT,NDIVT
        WRITE (7,314) IMEAN
        WRITE (8,311)

```

```

311  FORMAT(' PEAK DISTRIBUTION')
      WRITE (8,313) XMEAN,SD,RMS,NPT,DT,NDIVT
      WRITE (8,314) IMEAN
      WRITE (9,312)
312  FORMAT(' UP-CROSSING RATE',/)
      WRITE (9,313) XMEAN,SD,RMS,NPT,DT,NDIVT
      WRITE (9,314) IMEAN
      WRITE (10,315) SD
      WRITE (11,316) SD
313  FORMAT (' MEAN = ',E13.5,' SD = ',E13.5,' RMS = ',E13.5,/,
1      ' NO. OF PTS = ',I5,' DT = ',E13.5,' TOTAL DIV. = ',I3)
314  FORMAT(/,2X,' IMEAN = ',I2,' NOTE: IF IMEAN=1 THEN MEAN EXCLUDED')
315  FORMAT(' THEORETICAL GAUSSIAN WITH MEAN = 0. AND ',
1      ' SD = ',E13.5,/////)
316  FORMAT(' THEORETICAL RAYLEIGH WITH ',
1      ' SD = ',E13.5,/////)
      RETURN
      END
C*****
C****  SUBROUTINE DENSITY ****
C****  THIS SUBROUTINE CALCULATES THE PROBABILITY DENSITY, THEORETICAL ****
C****  GAUSSIAN DESNTIY WITH ZERO MEAN AND STANDARD DEVIATION OF THE ****
C****  RANDOM PROCESS ****
C*****
      SUBROUTINE DENSITY(F,XDENS,NPT,SD,DSD,NHALF,NHALF1,NDIVT,DX,SHIFT)
      COMMON/TITLES/ TITLE(20),SUBTIT(20)
      DIMENSION F(1), XDENS(1)
      PI=3.1415926
      SQ2PI=SQRT(2.*PI)
      DO 10 I=1,NDIVT
      XDENS(I)=0.
10     CONTINUE
      DO 20 I=1,NPT
      TEMP=F(I)/DSD
      ITEMP=IINT(TEMP)      ! Locate the data belongs to which interval
      IF (TEMP .GE. 0.) THEN
      IF (ITEMP .GT. NHALF) ITEMP=NHALF-1
      XDENS(NHALF1+ITEMP)=XDENS(NHALF1+ITEMP)+1.
      ELSE
      IF (ITEMP .LT. -NHALF) ITEMP=-NHALF+1
      XDENS(NHALF+ITEMP)=XDENS(NHALF+ITEMP)+1.
      END IF
20     CONTINUE
C*****
C****  WRITE RESULTS ****
C*****
      WRITE(7,1234) (TITLE(KK),KK=1,20)
1234  FORMAT(X,20A4)
      WRITE(7,1234) (SUBTIT(KK),KK=1,20)
      WRITE (7,210)
210  FORMAT(' MAGNITUDE/SD   PROBA. DENS.   NO.OF OCCUR.   GAUSSIAN',
1      '/',
      (NORMALIZED)')
      WRITE (10,211)

```

```

211  FORMAT('  MAGNITUDE/SD  PROBA. DENSITY',
1      /,'              (GAUSSIAN)')
      AREA=0.0
      X=-4.0
      DO 40 I=1,NDIVT
      XDX=X+DX
      XDENS1=XDENS(I)/NPT/DX
      AREA=AREA+XDENS1
C*****
C****  CALCULATE THE THEORETICAL GAUSSIAN WITH ZERO MEAN      ****
C*****
      GAUSS=EXP(-X*X/2.)/SQ2PI
      GAUDX=EXP(-XDX*XDX/2.)/SQ2PI
      Y=X+SHIFT
      YDX=Y+DX
      IF (I .EQ. 1) WRITE (7,220) Y,ZERO,ZERO,GAUSS
      WRITE (7,220) Y, XDENS1,XDENS(I),GAUSS
      WRITE (7,220) YDX,XDENS1,XDENS(I),GAUDX
220  FORMAT (2(3X,F11.5),3X,F8.1,3X,F11.5)
      IF (I .EQ. NDIVT) WRITE (7,220) YDX,ZERO,ZERO,GAUDX
      IF (I .EQ. 1) WRITE (10,220) Y, GAUSS
      WRITE (10,220) Y, GAUSS
      WRITE (10,220) YDX, GAUDX
      IF (I .EQ. NDIVT) WRITE (10,220) YDX, GAUDX
      X=X+DX
40  CONTINUE
      AREA=AREA*DX
      WRITE (6,700) SD, AREA
700  FORMAT ('  SD = ',E12.5,'  AREA OF DENSITY CURVE = ',F8.4,/)
      RETURN
      END
C*****
C****
C****  SUBROUTINE PEAKDIS      ****
C****  THIS SUBROUTINE CALCULATES THE PEAK DISTRIBUTION AND      ****
C****  THE THEORETICAL RAYLEIGH DISTRIBUTION      ****
C****
C*****
      SUBROUTINE PEAKDIS(F,XNPK,NPT,SD,DSD,NHALF,NHALF1,NDIVT,DX,
1          TTOTAL,SHIFT)
      COMMON/TITLES/ TITLE(20),SUBTIT(20)
      DIMENSION F(1),XNPK(1)
      DO 15 I=1,NDIVT
      XNPK(I)=0.
15  CONTINUE
      DO 20 I=1,NPT
      IF (I .EQ. 1 .OR. I .EQ. NPT) GO TO 2
      DF1=F(I)-F(I-1)
      DF2=F(I+1)-F(I)
      DSIGN=DF1*DF2
      IF (DSIGN .GT. 0.) GO TO 20
      IF (DF2 .GT. DF1) GO TO 20
      TEMP=F(I)/DSD

```

```

ITEMP=IINT(TEMP)
IF (TEMP .GT. 0.) THEN
IF (ITEMP .GT. NHALF) ITEMPE=NHALF-1
XNPK(NHALF1+ITEMP)=XNPK(NHALF1+ITEMP)+1.
ELSE
IF (ITEMP .LT. -NHALF) ITEMPE=-NHALF+1
XNPK(NHALF+ITEMP)=XNPK(NHALF+ITEMP)+1.
END IF
20 CONTINUE
XNPEAK=0.
DO 30 I=1,NDIVT
XNPEAK=XNPEAK+XNPK(I)
30 CONTINUE ! XNPEAK IS THE TOTAL NO. OF PEAKS
PEAKT=XNPEAK/TTOTAL ! NO. OF PEAKS PER UNIT TIME
WRITE (6,210) XNPEAK, PEAKT
WRITE(8,1234) (TITLE(KK),KK=1,20)
1234 FORMAT(X,20A4)
WRITE(8,1234) (SUBTIT(KK),KK=1,20)
WRITE (8,210) XNPEAK, PEAKT
210 FORMAT(' TOTAL NO. OF PEAKS = ',F10.1,
1 ' NO. OF PEAKS PER SEC. = ',F10.1)
WRITE (8,211)
211 FORMAT(' MAGNITUDE/SD PEAK DISTR. NO. OF PEAKS RAYLEIGH',
1 ' /, ' (NORMALIZED)')
WRITE (11,212)
212 FORMAT(' MAGNITUDE/SD PROBA. DENSITY'
1 ' /, ' (RAYLEIGH)')
X=-4.0
DO 40 I=1,NDIVT
XDX=X+DX
XNPK1=XNPK(I)/XNPEAK/DX
IF (XDX .LT. 0.0) THEN
RAY=0.0
RAYDX=0.0
ELSE
RAY=X*EXP(-X*X/2.)
RAYDX=XDX*EXP(-XDX*XDX/2.)
END IF
Y=X+SHIFT
YDX=Y+DX
IF (I .EQ. 1) WRITE (8,220) Y,ZERO,ZERO,RAY
WRITE (8,220) Y, XNPK1,XNPK(I),RAY
WRITE (8,220) YDX,XNPK1,XNPK(I),RAYDX
220 FORMAT (2(3X,F11.5),3X,F8.1,3X,F11.5)
IF (I .EQ. NDIVT) WRITE (8,220) YDX,ZERO,ZERO,RAYDX
IF (I .EQ. 1) WRITE (11,220) X, RAY
WRITE (11,220) X, RAY
WRITE (11,220) XDX, RAYDX
IF (I .EQ. NDIVT) WRITE (11,220) XDX, RAYDX
X=X+DX
40 CONTINUE
RETURN
END

```

```

*****
SUBROUTINE UPCROSSE
*****
*****
THIS SUBROUTINE CALCULATES THE UPCROSSING RATE AT DIFFERENT
*****
THRESHOLD LEVELS.
*****
*****
SUBROUTINE UPCROSSR(F,XCROSS,NPT,SD,DSD,NHALF,NHALF1,NDIVT,DX,
TTOTAL,SHIFT)
COMMON/TITLES/ TITLE(20),SUBTIT(20)
DIMENSION F(1), XCROSS(1)
WRITE(9,1234) (TITLE(KK),KK=1,20)
FORMAT(X,20A4)
WRITE(9,1234) (SUBTIT(KK),KK=1,20)
WRITE (9,210)
FORMAT(/,3X,'THRESHOLD LEVEL/SD          UPCROSSING RATE (#/SEC.)')
DO 10 I=1,NDIVT
XCROSS(I)=0.
CONTINUE
DO 20 I=1,NPT
IF (F(I) .GT. F(I+1)) GO TO 20      ! Only up-crossing is counted.
TEMP1=F(I)/DSD
TEMP2=F(I+1)/DSD
ITEMP1=IINT(TEMP1)
ITEMP2=IINT(TEMP2)
IF (TEMP1 .GT. 0.) THEN
DO 30 K=ITEMP1,ITEMP2-1
XCROSS(NHALF1+1+K)=XCROSS(NHALF1+1+K)+1.0
CONTINUE
ELSE
END IF
IF (TEMP2 .LT. 0.) THEN
DO 40 K=ITEMP1,ITEMP2-1
XCROSS(NHALF+1+K)=XCROSS(NHALF+1+K)+1.0
CONTINUE
ELSE
END IF
IF (TEMP1*TEMP2 .LT. 0.) THEN
DO 50 K=ITEMP1,0
XCROSS(NHALF+1+K)=XCROSS(NHALF+1+K)+1.0
CONTINUE
DO 60 K=0,ITEMP2-1
XCROSS(NHALF1+1+K)=XCROSS(NHALF1+1+K)+1.0
CONTINUE
ELSE
END IF
CONTINUE
K=-4.0+DX      ! the lowest level for crossing is -(4-DX)SD
DO 70 I=1,NDIVT
X=X+SHIFT
XCROSS(I)=XCROSS(I)/TTOTAL
WRITE (9,200) Y, XCROSS(I)

```

200   FORMAT (10X,F11.5,10X,F9.3)  
      X=X+DX  
70   CONTINUE  
      RETURN  
      END

```

C*****
C****                                     ****
C****   This program calculates the damage from a given peak      ****
C****   distribution. Input the standard deviation of the stress  ****
C****   process, SD (in ksi) and the total # of peaks per second, ****
C****   TPEAK, and the material fatigue constants ZLAMDA and B.   ****
C****   The peak distribution histogram is found on FOR008 created ****
C****   from the program PDF run earlier (10 divisions per s.d. in ****
C****   the histogram). Output is E[Mt]*tau and time to failure in ****
C****   seconds..                                                ****
C****                                     ****
C*****
      WRITE(6,1010)
1010  FORMAT(1H1,/,10X,'          DAMAGE          ',/,
      1      10X,'      FOR AFSC/ASD/PMRNA      ',/,
      2      10X,'      WPAFB,OHIO              ',/,
      3      10X,'      BY ANAMET LABORATORIES, INC.',/,
      4      10X,'      HAYWARD, CALIFORNIA      ',/,
      5      10X,'      CONTRACT NO. F33615-89-C-3210',/)
      READ(5,100) SD,TPEAK,ZLAMDA,B
100   FORMAT(4F10.0)
      WRITE(6,1009) SD,TPEAK,ZLAMDA,B
1009  FORMAT(10X,' STANDARD DEVIATION OF STRESS PROCESS= ',F10.1,/,
      1      10X,'      TOTAL NUMBER OF PEAKS PER SECOND= ',F10.1,/,
      2      10X,'      FATIGUE PARAMETER, LAMDA= ',F10.2,/,
      3      10X,'      FATIGUE PARAMETER, B= ',E10.3,/)
      DX=0.1*SD
      SUM=0.0
      READ (8,1100)
1100  FORMAT(/////////)
C**
      DO 10 I=1,80
      READ (8,1200) X,Y
1200  FORMAT(2G,/)
      IF (Y .EQ. 0.0) GO TO 10
      X=(X+0.05)*SD
      PROB=Y/SD
      SLAMDA=ABS(X)**ZLAMDA
      SUM=SUM+PROB*SLAMDA
10    CONTINUE
      SUM=SUM*DX
      EMT=B/SUM
      TFAIL=B/SUM/TPEAK
      WRITE (6,1300) SUM, EMT, TFAIL
1300  FORMAT(10X,'      INTEGRATION = ',E14.6,/,
      1      10X,'      E[Mt]*tau = ',E14.6,/,
      2      10X,'      TIME TO FAILURE= ',E14.6,' SEC',/)
      STOP
      END

```





DEPARTMENT OF THE AIR FORCE  
AIR FORCE RESEARCH LABORATORY  
WRIGHT-PATTERSON AIR FORCE BASE OHIO 45433

9-14-99

MEMORANDUM FOR: Defense Technical Information Center/OMI  
8725 John J. Kingman Rd, Suite 0944  
Ft Belvoir, VA 22060-6218

FROM: Det 1 AFRL/WST  
Bldg 640 Rm 60  
2331 12th Street  
Wright-Patterson AFB OH 45433-7950

SUBJECT: Notice of Changes in Technical Report(s) (see below)

Please change subject report(s) as follows:

*The following have all been approved for public release; distribution is unlimited:*

AFWAL-TR-83-3072,	AD B955 265 ✓
WRDC-TR-90-3081,	AD B 166 585 ✓
WL-TR-96-3043,	AD B212 813 - OK ST-A
WL-TR-96-3094,	<del>AD B 212 361</del> ✓ ST-A
WL-TR-97-3059,	AD B 232 172 ✓ <del>ST-A</del>
	↓
	B212361

*Joseph A. Burke*  
JOSEPH A. BURKE, Team Leader  
STINFO and Technical Editing  
Technical Information Division